

Topological order in condensed matter physics

Topological order in condensed matter physics

ACADEMISCH PROEFSCHRIFT

ter verkrijging van de graad van doctor
aan de Universiteit van Amsterdam
op gezag van de Rector Magnificus
prof. dr. D.C. van den Boom
ten overstaan van een door het college voor promoties
ingestelde
commissie, in het openbaar te verdedigen in de Agnietenkapel

door

Jesper Christian Romers

geboren te Delft.

Promotores: Prof. dr. C.J.M. Schoutens
Prof. dr. ir. F.A. Bais

Overige Leden: Prof. dr. J.-S. Caux
Prof. dr. S.H. Simon
Prof. dr. E.P. Verlinde
Dr. B.D.A. Estienne
Dr. V. Vitelli
Dr. A.M. Turner

Faculteit der Natuurwetenschappen, Wiskunde en Informatica

This work is part of the research program of the "Stichting voor Fundamenteel Onderzoek der Materie (FOM)", which is financially supported by the "Nederlandse Organisatie voor Wetenschappelijk Onderzoek (NWO)"

Copyright © 2012 by J.C. Romers
This work is licensed under the Creative Commons Attribution 3.0 NL licence.
Cover design by Wendely Wesselink © 2012
Typeset by L^AT_EX. Printed and bound by

Contents

1	Preface	7
1.1	Circles and winding numbers	8
1.2	Topological excitations	10
1.3	Topological insulators	13
1.4	Topological quantum field theory	15
1.5	Anyons and TQC	16
2	TQFTs in 2D	19
2.1	The Aharonov-Bohm effect	19
2.2	Anyons in 2D TQFTs	22
2.2.1	Fusion, braiding, spin and all that	22
2.2.2	The S -matrix and the Verlinde formula	23
2.3	Topological symmetry breaking	26
2.3.1	Generalities	26
2.3.2	Example: breaking $SU(2)_4$ to $SU(3)_1$	29
2.4	Observables and diagrammatics	30
2.4.1	Condensate and the embedding index q	32
2.4.2	The broken modular S - and T -matrices	32

3	Discrete Gauge Theories	35
3.1	Kitaev's Toric Code and the \mathbb{Z}_2 gauge theory	36
3.1.1	Euclidean formalism	38
3.1.2	Phase structure	39
3.2	Quantum Double and Discrete Gauge Theories	41
3.2.1	Electric and magnetic symmetries	41
3.2.2	Realizing a discrete gauge theory	42
3.2.3	Unified framework: quantum double	46
3.3	Euclidean approach to DGTs	53
3.3.1	Lattice actions and observables	53
3.3.2	Order parameters and phase indicators	56
3.4	$D(\overline{D}_2)$ theory: algebraic analysis	65
3.4.1	Breaking: $(\vec{e}, 1)$ condensate	66
3.4.2	Breaking: (X_1, Γ^0) condensate	69
3.5	$D(\overline{D}_2)$ theory: lattice analysis	70
3.5.1	Monte Carlo considerations	70
3.5.2	Results	73
3.6	Summary	87
3.7	Fusion rules for $D(\overline{D}_2)$ DGT	88
4	The quantum Hall effect and spin textures	89
4.1	Quantum Hall physics	89
4.1.1	Integer quantum Hall effect	89
4.1.2	Fractional quantum Hall effect and the CFT connection	91
4.1.3	Paired quantum Hall states and the colorful construction	93
4.2	Charged Spin Textures in quantum Hall systems	98
4.2.1	Skyrmions in the integer quantum Hall effect	98
4.2.2	Construction of CST wave functions over the MR state .	101
4.2.3	Properties of CSTs over the MR state	108
4.3	Spin texture read out of a qubit	112
4.4	Summary	119
5	Conclusions and outlook	121

Mystische Erklärungen. — Die mystischen Erklärungen gelten für tief; die Wahrheit ist, dass sie noch nicht einmal oberflächlich sind.

Friedrich W. Nietzsche

Die fröhliche Wissenschaft [1]

CHAPTER 1

Preface

I call our world Flatland, not because we call it so, but to make its nature clearer to you, my happy readers, who are privileged to live in Space.

Edwin A. Abbott

Flatland [2]

The thesis in front of you is the result of four years of research in theoretical physics. The original research on which it is based is centred around two topics in condensed matter theory — a lattice model for discrete gauge theories and spin textures in quantum Hall states — that are superficially rather different. This introductory chapter serves as a guide on how to localize these topics in the field of modern condensed matter theory and hopefully it will convince you, the reader, that their common denominator justifies both their presence in this work.

The key concept here is *topological order*. These words characterize a family of novel states of matter, starting with the quantum Hall state. A quick

analysis at the time of writing [3] reveals that the use of the word “topological” in all the articles placed in the cond-mat subject class at arXiv.org has increased fourfold over the last ten years (from roughly 50 times per million words at the start of 2002 to about 200 times per million words in 2012). This branch of mathematics has worked its way through nearly all disciplines of physics, touching upon subjects such as the Aharonov-Bohm effect [4], magnetic monopoles [5, 6], topological quantum field theory [7], the quantum Hall effect [8] and more recently the discovery of a periodic table, the “Table of Ten” [9, 10] — based on abstract mathematical work on the classification of symmetric spaces by Cartan [11, 12] in the 1920’s — of topological insulators and superconductors.

1.1 Circles and winding numbers

To make more explicit what we are talking about when we discuss topology in physics, let us first define the notion of topological equivalence in a very pedestrian fashion:

Two objects are topologically equivalent if one can continuously deform one into the other without cutting and pasting.

This immediately captures the essence of the best-known example of topological equivalence, namely the one between a doughnut and a coffee cup. One can imagine continuously deforming one into the other without punching an extra hole or glueing parts together and creating a new hole.

The kind of topological equivalence suitable for our purposes is often one between maps. These maps could be between physical space or spacetime and some internal space (leading to solitons and instantons respectively), the Brillouin zone and the space of gapped free fermion Hamiltonians (resulting in the celebrated “Table of Ten” for topological insulators and superconductors) *et cetera*, but for the moment we restrict ourselves to the simplest of examples: the set of maps between circles and circles.

Consider a circle S_1 parametrized by an angle $\theta \in [0, 2\pi)$. We can define a smooth map ϕ

$$\begin{aligned} \phi : S_1 &\rightarrow S_1, \\ \theta \in [0, 2\pi) &\mapsto \phi(\theta) \in [0, 2\pi), \end{aligned} \tag{1.1}$$

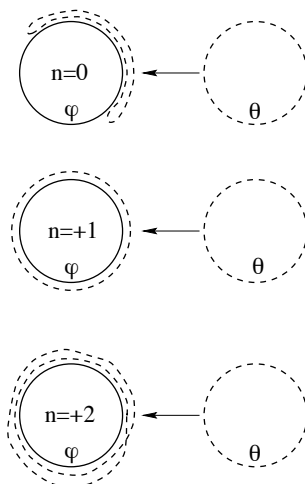


Figure 1.1: Different maps from the circle parametrized by θ to the circle parametrized by ϕ . The winding number n counts how many times the map winds around the range as the domain is traversed once. Figure from Ref. [13].

from this circle to another circle. These maps are characterized by an integer called the winding number, see Figure 1.1. This counts how many times ϕ wraps around the circle as θ runs from 0 to 2π . This is clearly a topological property, since no smooth deformation can change this number. The fact that maps between manifolds fall into topologically distinct classes lies at the root of all that follows below. Maps such as (1.1) can naturally be concatenated to form new map

$$\begin{aligned} \phi_3 = \phi_1 \star \phi_2 : S_1 &\rightarrow S_1, \\ \theta &\mapsto \begin{cases} \phi_1(2\theta) & \text{if } \theta \in [0, \pi) \\ \phi_2(2\theta - 2\pi) & \text{if } \theta \in [\pi, 2\pi) \end{cases} \end{aligned} \quad (1.2)$$

such that the winding number of map ϕ_3 is the sum of winding numbers of ϕ_1 and ϕ_2 . This endows the equivalence classes of maps from circles to circles with a group structure. An obvious generalization of this structure is the study of equivalence classes of maps from d -dimensional spheres to some manifold M . The term for this set of equivalence classes is the d -th homotopy

group of M , $\pi_d(M)$.

It is straightforward to see that the winding numbers of the maps in Eq. (1.2) add up, therefore $\pi_1(S_1) = \mathbb{Z}$. For higher dimensional manifolds and more complex target spaces the problem becomes highly nontrivial, but luckily many cases of interest have been worked out in the mathematical literature.

1.2 Topological excitations

Spin models A classical model for a ferromagnet in two dimensions is the $O(3)$ sigma model, basically the continuum limit of the Heisenberg ferromagnet. Its action in the absence of external fields is given by

$$S = \frac{1}{g} \int d^3x \partial^\mu \mathbf{n} \cdot \partial_\mu \mathbf{n}, \quad (1.3)$$

where $\mathbf{n}(x)$ is a real three-dimensional vector field subject to the constraint

$$\mathbf{n}(x) \cdot \mathbf{n}(x) = 1, \text{ for all } x,$$

which means this vector takes values on the surface of a two-sphere S_2 ; the action (1.3) also respects the symmetries of the sphere — in other words it is invariant under global $O(3)$ rotations, hence the name of the theory.

The ground state of this model is a ferromagnetic state, with all the vectors pointing in the same direction

$$\mathbf{n}(x) = \mathbf{n}_0 \text{ for all } x, \quad (1.4)$$

since in this field configuration all the derivatives evaluate to zero. Such a state breaks the global $O(3)$ symmetry so one expects to find Goldstone bosons; in this case they are spin wave excitations.

In addition to these gapless excitations, the system described by Eq. (1.3) also carries gapped particle-like excitations in its spectrum. These are associated with classical field configurations that cannot be continuously deformed to the polarized ground state (1.4) and are thus topologically distinct from them.

We established that the field takes values on the surface of a two-sphere. If we compactify two-dimensional real space M to a two-sphere — by identi-

fying all points at infinity — the map defined by \mathbf{n}

$$\begin{aligned}\mathbf{n} : S_2 &\rightarrow S_2, \\ x &\mapsto \mathbf{n}(x),\end{aligned}$$

can be classified by an integer, since $\pi_2(S_2) = \mathbb{Z}$. This number is referred to as the Pontryagin index or topological charge and a field configuration carrying one unit of this charge is a *skyrmion* [14]. A remarkable aspect of topological charge is that although it is a very non-local quantity, invariant under local deformations, it can be expressed as an integral of a local quantity, the Pontryagin density ρ_{top}

$$\rho_{\text{top}} = \frac{1}{4\pi} \mathbf{n} \cdot \partial_x \mathbf{n} \times \partial_y \mathbf{n}.$$

In Chapter 4 we find generalizations of skyrmions which we call Charged Spin Textures (since they also carry electric charge) that are in a sense half-skyrmions.

Gauge theories Let us consider a Yang-Mills theory with compact gauge group G and a Higgs field ϕ which breaks the symmetry spontaneously due to its potential $V(\phi)$

$$S = \int d^d x \left\{ -\frac{1}{4} F_{\mu\nu}^a F^{a\mu\nu} - \frac{1}{2} D_\mu \phi D^\mu \phi - V(\phi) \right\}. \quad (1.5)$$

We will study the possibility of topologically nontrivial solutions in a Euclidean spacetime $M = \mathbb{R}^d$. To obtain a solution with finite action, we demand the terms of equation (1.5) to vanish separately at infinity. For the Higgs field this means that

$$\frac{\partial V}{\partial \phi} \Big|_{x \in \partial M} = 0.$$

Say we have a particular solution ϕ_0 that minimizes the potential. Then, because of the symmetry in (1.5), any $\phi = g\phi_0$ is a minimum of V for all elements $g \in G$. Now suppose the symmetry is not completely broken, because the field ϕ does not transform under a faithful representation of G . Then there

exists a residual symmetry group H , given by the stabilizer of ϕ_0 ,

$$H = \{h | h \in G, h\phi_0 = \phi_0\}$$

which allows us to split each element in G into a group product of an element in the coset G/H and an element in H

$$g = kh, \quad h \in H, \quad k \in G/H.$$

The manifold of vacua is therefore not the full group V , but the coset space G/H

$$g\phi_0 = k\phi_0 \simeq G/H,$$

and since ϕ need not be a constant function at the boundary of spacetime ∂M

$$\phi(\partial M) = k(\partial M)\phi_0.$$

We can construct a map from the boundary of space to the vacuum manifold

$$k(\partial M) : \partial M \rightarrow G/H.$$

The boundary of the spacetime manifold in d dimensions can be thought of as a hypersphere S_X^{d-1} , where the X has been added to emphasize this concerns spacetime, as opposed to group space. The maps k in equation (1.6) fall into different topological classes that cannot be continuously deformed in one another. They are therefore labeled by the elements of the homotopy group of the vacuum manifold of order $(d-1)$, $\pi_{d-1}(G/H)$.

This observation tells us what possible pointlike topological defects are possible in the theory. For example, in \mathbb{R}^4 the boundary of spacetime is topologically equivalent to the three-sphere S^3 . From homotopy theory it is known that $\pi_3(S^3) = \mathbb{Z}$. This means that the instantons [15], as the pointlike topologically nontrivial solutions are called, are here labeled by an integer.

To classify higher dimensional objects, we need to consider different homotopy groups than the previously given π_{d-1} . If d is the dimension of spacetime, and D is the dimension of the topological defect in spacetime, the relevant homotopy group becomes $\pi_{d-D-1}(G/H)$. In this discussion we consistently use a spacetime point of view, so for example in \mathbb{R}^4 an instanton is a point, a monopole is linelike since it moves through space and time and a fluxtube sweeps out an area in spacetime - thus being a two-dimensional

object. Some of the more common topological excitations in gauge theories are collected in Table 1.1.

d	D	Homotopy group	Name
3	0	$\pi_2(G/H)$	Instanton
3	1	$\pi_1(G/H)$	Fluxtube
4	0	$\pi_3(G/H)$	Instanton
4	1	$\pi_2(G/H)$	Monopole
4	2	$\pi_1(G/H)$	Fluxtube

Table 1.1: Names and relevant homotopy groups for some topological excitations in gauge theories. The dimensionality of spacetime is d , the dimensionality of the defect in spacetime is D and the vacuum manifold is G/H .

One has to be very careful as how to physically interpret these objects. The zero-dimensional defects in any spacetime dimensionality are instantons; they are localized in both space *and* time. Therefore they are often interpreted as tunneling events between degenerate vacua and turn out to have drastic effects [16] when fermions are included in the theory — the appearance of fermionic zero modes.

In Chapter 3 we study discrete gauge theories in 2+1 dimensions. These theories contain a particular type of soliton, namely a magnetic fluxes. What makes them special is the fact that their topological charge can be an element of a non-Abelian group, which leads to the phenomenon of flux metamorphosis [17] and non-Abelian anyons.

1.3 Topological insulators

So far we have seen examples of topology arise in mappings between coordinate space(time) and field configurations, leading to solitons and instantons. A more recent discovery was the appearance of topologically non-trivial maps in perhaps the most elementary of all states of matter, the band insulator [9, 10].

In a band insulator, the energy spectrum has a gap separating the occupied and empty bands. Assuming that the topological properties of the system are invariant under smooth deformations of the band structure that keep the gap

open, the Hamiltonian of any band insulator can be cast in a simplified form, often denoted by Q , in which all occupied (unoccupied) states have energy -1 ($+1$):

$$Q(k) = \mathbb{1} - 2 \sum_{a \in \text{occ}} |u_a(k)\rangle \langle u_a(k)|, \quad (1.6)$$

where we denote the Bloch states by $|u_a(k)\rangle$. Say there are n unoccupied bands and m occupied ones; since a reshuffling of either the occupied bands or the unoccupied bands leaves the operator (1.6) invariant,

$$Q(k) \in \frac{U(n+m)}{U(n) \times U(m)} \simeq G_{m,m+n}(\mathbb{C}), \quad (1.7)$$

the latter symbol meaning a complex Grassmannian manifold, having the property $G_{m,m+n} \simeq G_{n,m+n}(\mathbb{C})$.

The operator Q is thus a map from the d -dimensional Brillouin zone (which is a d -dimensional torus \mathbb{T}^d) to a Grassmannian

$$\begin{aligned} Q : \mathbb{T}^d &\rightarrow G_{m,m+n}, \\ k &\mapsto Q(k), \end{aligned}$$

which can have non-trivial winding numbers depending on the dimensionality of space. Now we make a further simplification: we will compactify the toroidal topology of the Brillouin zone to a sphere. The topological invariants arising from maps from this sphere to the Grassmannian are called *strong topological invariants* in the literature, whereas the extra topological invariants arising from the fact the torus has an extra number of non-contractible loops compared to the sphere are called *weak topological invariants*. Most attention in the literature has been given to the former, and this reduces the problem to studying the homotopy groups of Grassmannian manifolds.

It turns out that [10]

$$\begin{aligned} \pi_d(G_{m,m+n}) &= 0 \text{ for } d \text{ odd,} \\ \pi_d(G_{m,m+n}) &= \mathbb{Z} \text{ for } d \text{ even.} \end{aligned}$$

In the absence of further symmetries in the Hamiltonian, the story ends here. The above equation physically means that in even dimensional spaces there exist states of non-interacting fermionic band insulators that are topolog-

ically distinct from the atomic insulator — in $d = 2$, this is the integer quantum Hall effect. However, if the system has time-reversal symmetry (TRS), particle-hole symmetry (PHS) or chiral symmetry (CS), further conditions can be imposed on the target Grassmannian in Eq. (1.7). These conditions make that the homotopy properties of the map (1.8) change and different types of topologically non-trivial states of matter might appear: all in all there turn out to be ten different classes of them, their periodic table is often referred to as the “Table of Ten”.

Although the work in this thesis only touches upon one of these systems, the integer quantum Hall effect, in the introduction of Chapter 4, this classification has proven to be so fundamental to our understanding of topological states of matter that it deserves to be in any overview of the field.

1.4 Topological quantum field theory

Although we dedicate the entire next chapter to the subject of topological quantum field theory (TQFT), here might be the right place to introduce them on a somewhat more conceptual level. A possible definition is that a TQFT is a quantum field theory that does not feature the metric on the spacetime on which it is defined in its formulation; therefore all physical observables are independent of continuous deformations of that spacetime. Practically¹ this means that the only interactions in such a theory are topological in nature: basically generalizations of the interactions that take place between the electrically charged particle and the magnetic flux in the Aharonov-Bohm effect.

Let us restrict ourselves to 2+1 dimensions since it is an interesting case and also the situation exclusively encountered in the research presented in this thesis. Operators that create particle-antiparticle pairs, propagate them through time and annihilate them are loops embedded in the three-dimensional spacetime². Topologically speaking therefore these operators are embeddings of circles into \mathbb{R}^3 , which is exactly the subject of the mathematical discipline of knot theory. Indeed it was shown by Witten in Ref. [7] that a mathematical invariant of knots — the Jones polynomial — can be expressed as the expectation value of a Wilson loop in a Chern-Simons theory, an example of a

¹The word “practically” is used here in one of its loosest definitions.

²Strictly speaking, they are loops with a framing, since particles can have nontrivial spin. It is therefore maybe more illuminating to think of these loops as ribbons.

TQFT.

An important point of TQFTs that will not be touched upon in the remainder of this thesis is the appearance of edge modes in these systems. When a TQFT is formulated on a manifold with a boundary, the bulk will remain gapped but often the edge will be described by a Conformal Field Theory (CFT). For Chern-Simons theories this leads to a beautiful duality between the edge and the bulk: the CFT describing the gapless edge modes is the same as the CFT whose conformal blocks span the Hilbert space of the bulk wave function in the presence of external charges. Each particle sector in the bulk has a corresponding particle sector on the edge, which is the rationale behind quantum Hall interference experiments, where quasiparticles run along the edges of a Hall bar and tunnel through the bulk Hall medium.

In Chapter 3 we study a different TQFT, a gauge theory with a finite discrete gauge group: a Discrete Gauge Theory (DGT). We show that the measurement of a topological object, namely a Hopf link of two loops, allows one to find the modular S -matrix of the theory. This matrix, together with the topological spins of the different particle sectors allows one to recover the fusion rules of the theory and is therefore of central importance to the study of TQFTs. In a sense, it is an order parameter for TQFTs, since we also show that this object can be measured in vacua of broken symmetry, where it can be used to reconstruct the (S -matrix of the) effective low-energy TQFT.

1.5 Anyons and TQC

Three-dimensional spacetime — the Flatland mentioned in the quote at the beginning of this chapter — is unique in the sense that particle statistics there is not restricted to being either bosonic or fermionic. The worldline of a point particle going around another point particle in spacetimes of dimension larger than three can always be contracted to a point. Since taking one particle “full circle” around another one is equivalent to interchanging them twice, this operation cannot have any action on the multiparticle wave function in these higher-dimensional spacetimes. The effect of doing half of this operation (a single interchange or *braiding*) can therefore only be a multiplication by ± 1 , where the plus sign is for bosons and the minus sign for fermions.

In 2+1 dimensions, such worldlines are not contractible, and can therefore leave the wave function with an arbitrary phase factor. A single interchange

will result in half this phase, and since this phase can in principle have any value, particles having this property have been dubbed *anyons* [18, 19]. This argument only tells us that anyons *could* exist in 2+1 dimensions, of course not that they should: there are many theories in 2+1d that contain only bosons and/or fermions. However, the TQFTs mentioned thusfar — DGTs and Chern-Simons theories — support stable anyons in their spectrum.

The situation can become even more exotic. The Moore-Read fractional quantum Hall (fqH) state, a system studied in Chapter 4, is a physical system in which the interactions between the quasihole excitations are strictly topological as long as they are well separated. If one carries out the computation, one finds that the state of the system with four quasipoles pinned at fixed locations is doubly degenerate. An interchange of two quasipoles in this four-particle state turns out not to give only a phase on the wave function, but acts as a unitary matrix on the two dimensional space of states. Since matrices need not commute, these anyons were called “non-Abelian”.

This discovery led to the idea of topological quantum computation (TQC) [20]: the two degenerate states could be used as a qubit. The information in this qubit is protected from the environment since the only way by which one can go from one state vector to the other is by the very non-local operation of braiding. Perturbations from the environment are always local in nature and tunneling between the basis states of the qubit is therefore exponentially suppressed in the system size. The computational operations on qubits in this scheme are realized by different braidings and the readout of the register would be performed by fusing the excitations together. In Section 4.3 we propose a scheme for the readout of a Moore-Read fqH quantum register that could work if the elementary quasipoles carry spin textures as has been conjectured in Ref. [21].

So far, the only system in Nature that is conjectured to carry non-Abelian anyons as its excitations is the fqH state at filling $\nu = \frac{5}{2}$. If its physics is indeed shown to be adequately captured by the Moore-Read state this is a leap forward for condensed matter physics. However, the experiments to demonstrate the non-Abelian statistics have proven to be notoriously difficult. Recent experiments [22] look promising, but the smoking gun is still lacking.

CHAPTER 2

Topological quantum field theories in 2D

In this chapter we discuss the properties of topological quantum field theories (TQFTs) in two spatial dimensions. We do not yet care about any particular microscopic model having a TQFT as an effective field theory describing one of its phases. Moreover, for the moment we also ignore the precise form of the Hamiltonian or Lagrangian describing the effective field theory. Our starting point is the fact that these theories have (possibly non-Abelian) anyons as their quasiparticle excitations which are gapped and that interact with one another solely through generalized Aharonov-Bohm (A-B) effects.

This chapter contains no original research by the author, but serves as an introduction to the subject matter and to establish the formalism that will be used later in this thesis.

2.1 The Aharonov-Bohm effect

To obtain some physical intuition on TQFTs, let us connect them with a theory that is perhaps more familiar, namely quantum electrodynamics (QED). In the following we discuss the Aharonov-Bohm effect [4], the archetypical

topological interaction. QED possesses these A-B interactions in addition to its interactions that are mediated by local degrees of freedom (e.g. photons). A TQFT is a theory in which all local degrees of freedom are absent and only such generalized A-B effects persist.

Quantum electrodynamics is the simplest case of a Yang-Mills theory, where the gauge group is Abelian, namely $U(1)$. Imposing a local symmetry on the Dirac action requires the introduction of a new field, the A_μ gauge field. This field acts as a potential for the electric and magnetic fields. However, the E and B fields are not affected by a gauge transformation, whereas the A_μ field, by its very nature, transforms. It is therefore common usage to refer to the latter as an *unphysical* field, whereas the former describe the local physical degrees of freedom. After fixing the gauge to only allow time-independent transformations,

$$\begin{aligned} A_\mu &= (\phi, \mathbf{A}), \\ \mathbf{E} &= -\nabla\phi, \\ \mathbf{B} &= \nabla \times \mathbf{A}. \end{aligned}$$

That this is not a complete picture can be understood by the following gedanken-experiment. Put a very long solenoid somewhere in space, for example along the z -axis. This will create some magnetic field inside the solenoid, but outside of it, there are no physical fields. Inside the solenoid therefore

$$\begin{aligned} \mathbf{E} &= \mathbf{0}, \\ \mathbf{B} &= B\mathbf{z}, \\ \mathbf{A} &= \left(-\frac{By}{2}, \frac{Bx}{2}, 0 \right), \end{aligned}$$

where we use \mathbf{z} for a unit vector in the z -direction, B for the magnitude of the magnetic field and x , y and z for ordinary Cartesian coordinates. Outside the solenoid, the following situation is realized:

$$\begin{aligned} \mathbf{E} &= \mathbf{0}, \\ \mathbf{B} &= \mathbf{0}, \\ \mathbf{A} &= \left(-\frac{BR^2y}{2r^2}, \frac{BR^2x}{2r^2}, 0 \right), \end{aligned}$$

in which R is the radius of the solenoid and r is the distance from the center of the solenoid.

Now consider an interference experiment with two electrons and the solenoid. One part of the electron wavefunction will travel underneath the solenoid and the other part will go over it. The two parts will interfere with a phase difference that is observable.

The phase acquired by an electron moving in the background of a gauge field can be determined by minimal substitution, or — more geometrically — by interpreting the gauge field as a connection. We will do the latter, and find for the phase θ acquired after parallel transport along a path C

$$\theta(C) = \frac{-e}{\hbar} \int_C \mathbf{A} \cdot d\mathbf{r}.$$

The phase difference between the two paths is then, using Stokes' theorem:

$$\begin{aligned} \Delta\theta &= \theta(C_1) - \theta(C_2) = \int_{C_1 \cup -C_2} \mathbf{A} \cdot d\mathbf{r} \\ &= \frac{e}{\hbar} \oint_{C_1 \cup -C_2} \mathbf{A} \cdot d\mathbf{r} \\ &= \frac{e}{\hbar} \int_S \nabla \times \mathbf{A} \cdot d\mathbf{s} \\ &= \frac{e}{\hbar} \int_S \mathbf{B} \cdot d\mathbf{s} = \frac{e}{\hbar} \Phi, \end{aligned}$$

where $C_1 \cup -C_2$ denotes the path obtained by first traversing C_1 , and then C_2 in opposite direction. S is the surface spanned by this curve and Φ the total magnetic flux piercing S , which in this situation is of course equal to the magnetic flux created by the solenoid.

Thus: the electrons pass only through parts of space where the electric and magnetic fields are zero, but there is a physically observable effect. This effect only depends on the number of turns taken around the flux, i.e. it is a function of the topology of the path. It is therefore the prototype of a nonlocal topological interaction.

2.2 Anyons in 2D TQFTs

In this section we set the stage and fix the notation for much of the rest of this thesis. We study phases of systems that are described by a TQFT in $2 + 1$ dimensions, that is systems that only interact through generalized Aharonov-Bohm interactions. We label the different sectors or (anyonic) particle species by a, b, c, \dots . The two interactions between two particles in a TQFT are fusion and braiding.

2.2.1 Fusion, braiding, spin and all that

Fusion We describe fusion by the rule

$$a \times b = \sum_c N_c^{ab} c, \quad (2.1)$$

where the integer multiplicities N_c^{ab} give the number of times c appears in the fusion product of a and b . The fusion algebra is associative and commutative, and has a unique identity element denoted as “1” that represents the vacuum. Each sector a has a unique conjugate \bar{a} (representing the corresponding anti anyon) with the property that their fusion product contains the identity:

$$a \times \bar{a} = 1 + \sum_{c \neq 1} N_c^{a\bar{a}} c.$$

Braiding The particles in a $2 + 1$ dimensional TQFT can have fractional spin and statistics. Rotating a particle a by 2π (also called *twisting*) multiplies the state vector by a phase equal to the *spin factor* θ_a

$$|a\rangle \xrightarrow{\text{twist}} \theta_a |a\rangle,$$

generalizing the usual $+1$ (-1) known from bosons (fermions) in $3 + 1$ dimensions. Adiabatically moving a particle a around another particle b in a channel c is called a *braiding* and can have a nontrivial effect on the state vector of the system, given by $\theta_c / \theta_a \theta_b$.

Quantum dimensions The quantum dimensions d_a of particle species a are another set of important quantities in a TQFT. These numbers satisfy the fu-

sion rules (2.1), i.e. $d_a d_b = \sum_c N_c^{ab} d_c$. The quantum dimension of an anyonic species is a measure for the effective number of degrees of freedom, corresponding to the internal Hilbert space of the corresponding particle type. The Hilbert space dimension of a system with N identical particles of type a grows as $(d_a)^N$ for N large. In general, the quantum dimensions d_a will be real numbers; however for DGTs they are integers. The total quantum dimension \mathcal{D} of the theory is given by

$$\mathcal{D} = \sqrt{\sum_i d_a^2},$$

and the topological entanglement entropy of the ground state [23, 24] is proportional to $\log \mathcal{D}$.

2.2.2 The S -matrix and the Verlinde formula

The modular group Instead of the fusion coefficients N_c^{ab} an alternative specification of a (modular) topological field theory is by its representation of the modular group $SL(2, \mathbb{Z})$ generated by the S and T -matrices

$$S^2 = (ST)^3 = \mathcal{C}, \quad S^* = \mathcal{C}S = S^{-1}, \quad T^* = T^{-1}, \quad \mathcal{C}^2 = 1, \quad (2.2)$$

with \mathcal{C} the charge conjugation matrix. The corresponding matrix elements can be expressed in the fusion coefficients and spin factors:

$$S_{ab} = \frac{1}{\mathcal{D}} \sum_c N_c^{a\bar{b}} \frac{\theta_c}{\theta_a \theta_b} d_c, \quad (2.3)$$

$$T_{ab} = e^{-2\pi i(\bar{c}/24)} \theta_a \delta_{a,b} \quad (2.4)$$

where \mathcal{D} is the total quantum dimension and the constant \bar{c} is the conformal central charge of the corresponding conformal field theory. The central charge of a discrete gauge theory is zero, so in that case the T -matrix is just the diagonal matrix containing the spin factors.

The torus and the Verlinde formula Since the number of ground states of a TQFT on the torus is equal to the number of particle sectors, we label the different ground states by the set $\{|a\rangle\}$ for each sector a . We define operators T_a and \tilde{T}_a that create, propagate and annihilate particle-antiparticle pairs of

species a around either of the two noncontractible loops of the torus. All of these operators define vacuum to vacuum amplitudes since no localized particle excitations are left after traversing the loop and annihilating the pair.

However, these sets of operators do act nontrivially in the space of ground states¹. To be precise, we pick a basis in which the operators T_a take us from one ground state to another

$$T_a|0\rangle = |a\rangle,$$

whereas the operators \tilde{T}_a act diagonally

$$\tilde{T}_a|b\rangle = \lambda_a^{(b)}|b\rangle.$$

Since the sets of operators T_a and \tilde{T}_a correspond to the creation of particles, among themselves they satisfy the fusion algebra (2.1)

$$T_a T_b = \sum_c N_{ab}^c T_c, \quad \tilde{T}_a \tilde{T}_b = \sum_c N_{ab}^c \tilde{T}_c. \quad (2.5)$$

Now there turns out to be a highly non-trivial relation, the Verlinde formula, between the fusion coefficients N_{ab}^c and the modular S -matrix [26]. Recall that the S -matrix basically interchanges the two non-contractible loops of the torus and therefore the roles of the T and \tilde{T} operators. Equivalently it transforms from a basis in which the \tilde{T}_a are diagonal to one in which the T_a are diagonal, since the choice made in the beginning which of the two acts diagonally was arbitrary.

The S -matrix together with the relations (2.5) can be used to find two equivalent expressions for the superposition of ground states that is the result of creating, propagating and annihilating two particles around a non-contractible loop of the torus. In Figure 2.1 we have given a graphical representation of the different steps of this procedure.

At the end of the day, the result is the equality

$$\sum_c N_{ab}^c |c\rangle = \sum_{c,d} S_{cd}^+ \lambda_b^{(d)} S_{ad} |c\rangle. \quad (2.6)$$

Since the basis $\{|a\rangle\}$ spans the space, the equality holds for each term in the

¹For Abelian TQFTs the proof is rather simple and explained in for example [20]. In fact this phenomenon was first studied in the context of gauge theories by 't Hooft [25]. For non-Abelian theories the most straightforward arguments come from studying CFT partition functions [26].

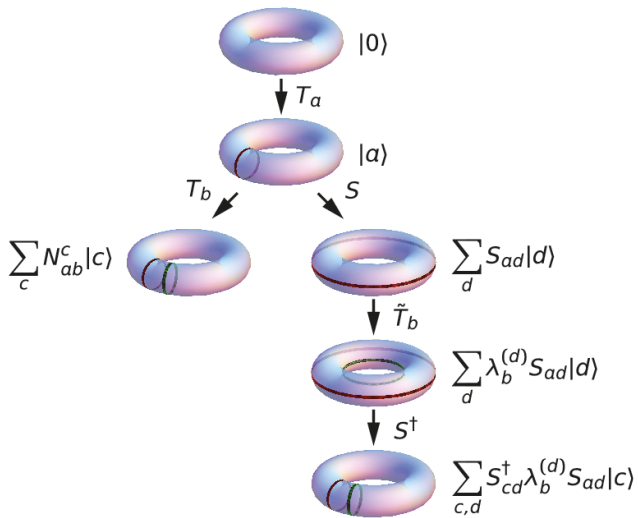


Figure 2.1: Derivation of the Verlinde formula (2.7). Next to each figure is the Hilbert space vector, next to each arrow is the operation used to get from one vector to the other.

sum separately.

We can go further and determine the \tilde{T} eigenvalues λ . Fusion with the vacuum sector does nothing and is unique, $N_{a1}^b = \delta_a^b$ for all a and b . We use this property in equation (2.6),

$$\begin{aligned} N_{1b}^c = \delta_b^c &= \sum_d S_{cd}^+ \lambda_b^{(d)} S_{1d}, \\ 1 &= \sum_d S_{bd}^+ \lambda_b^{(d)} S_{1d}. \end{aligned}$$

If we want this to hold for all choices of b , the only possible choice for the eigenvalues is

$$\lambda_b^{(d)} = \frac{S_{bd}}{S_{1d}},$$

resulting in the celebrated Verlinde formula

$$N_{ab}^c = \sum_d \frac{S_{ad} S_{bd} S_{cd}^+}{S_{1d}}. \quad (2.7)$$

2.3 Topological symmetry breaking

2.3.1 Generalities

In this section we briefly recall topological symmetry breaking, the phenomenon that a phase transition to another topological phase occurs due to a Bose condensate [27, 28]. The analogy with ordinary symmetry breaking is clear if one thinks of the particle as representations of some quantum group, and assumes that a bosonic degree of freedom i.e. with $\theta_c = 1$ – fundamental or composite – condenses. The breaking can then be analyzed, either from the quantum group (Hopf algebra) point of view, or from the dual or representation theory point of view [29].

Let us illustrate this by an example of ordinary group breaking. Suppose we have a gauge group $SU(3)$ and a Higgs triplet that acquires a vacuum expectation value $\Phi = (1, 0, 0)$, then the $SU(2)$ subgroup working on the last two entries will leave Φ invariant. Equivalently this $SU(2)$ subgroup may be characterized by the way the $SU(3)$ triplet decomposes under the $SU(2)$ action as $3 \rightarrow 2 + 1$ where the singlet on the right corresponds exactly to the new

$SU(2)$ invariant groundstate. In that sense one may select a specific residual gauge symmetry by choosing an appropriate Higgs representation which has a singlet under that residual group in its branching. For example if we want to break an $SU(3)$ group to the $SO(3)$ subgroup which is characterized by the branching rule 3 (as well as $\bar{3}$) $\rightarrow 3$ then we may choose the Higgs field to be in the 6-dimensional irrep of $SU(3)$, because then $3 \times 3 = \bar{3} + 6 \rightarrow 3 \times 3 = 1 + 3 + 5$, from which follows that $6 \rightarrow 5 + 1$ and again the singlet on the right corresponds to the $SO(3)$ invariant vacuum state Φ .

In the case of general quantum groups it is this branching rule approach which is the most natural and powerful in the context of TQFT because the fusion algebra corresponds to the representation ring of the quantum group. A general treatment with ample examples can be found in reference [29]. Let us point out some essential features of this procedure that one has to keep in mind. As the quantum group centralizes the chiral algebra in the operator algebra of a CFT, one expects that reducing the quantum group will correspond to enlarging the chiral algebra, and this turns out to be the case. In contrast to ordinary group breaking, the topological symmetry breaking procedure involves two steps, firstly the condensate reduces the unbroken fusion algebra (also called a braided modular tensor category) \mathcal{A} to an intermediate algebra denoted by \mathcal{T} . This algebra however may contain representations that braid nontrivially with the condensed state, i.e. with the new vacuum and if that is the case, these representation will be confined and will be expelled from the bulk to the boundary of the sample. Confinement implies that in the bulk only the unconfined sectors survive as particles and these are characterized by some subalgebra $\mathcal{U} \subset \mathcal{T}$. Let us briefly describe the two steps separately.

From \mathcal{A} to \mathcal{T} Assuming that a certain bosonic irrep c will condense due to some underlying interaction in the system, implies that c will be identified with the vacuum of \mathcal{T} . For our purposes, a boson is a sector with trivial (integer) spin, though in fact in the context of $2 + 1$ dimensions one has to also require that fusion of this field with itself has a channel with trivial braiding.

The definition of the new vacuum requires to a redefinition of fields. Firstly, fields in \mathcal{A} that appear in the orbit under fusion with the condensed field c are identified in \mathcal{T} , so, if $c \times a = b$ then $a, b \rightarrow a'$. Secondly, if a field b forms a fixed point under fusion with the condensate c , then the field will split at least in two parts: $b \rightarrow \sum_i b_i$. The identifications and splittings of representations can be summarized by a rectangular matrix n_a^t that specifies the

“branching” or “restriction” of fields a from in \mathcal{A} to \mathcal{T} with fields t, r, s, \dots :

$$a \rightarrow \sum_t n_a^t t$$

This *branching matrix* is a rectangular matrix (the number of particle types in the \mathcal{A} and \mathcal{T} theories is not equal in general) of positive integers. We will also consider the transpose of this matrix denoted as n_t^a which specifies the “lift” of the fields $t \in \mathcal{T}$ to fields $a \in \mathcal{A}$:

$$t \rightarrow \sum_a n_t^a a = \sum_{a \in t} a$$

One may now derive the fusion rules \mathcal{T} from the fusion algebra (2.1). Because of the identifications, it is often the case that the intermediate algebra \mathcal{T} though being a consistent fusion algebra, is not necessarily braided, in more technical terms, it satisfies the “pentagon” equation but not the “hexagon” equation. The physical interpretation of this fact is that the sectors in \mathcal{T} do not yet constitute the low-energy effective theory. This is so because sectors t that have an ambiguous spin factor, meaning that not all θ_a of the lift $a \in t$ are equal, will be connected to a domain wall and hence are confined in the new vacuum. The confined excitations will be expelled to the edges of the system or have to form hadronic composites that are not confined. Yet the \mathcal{T} algebra plays an important role: in Ref. [30] for example, it was shown that the \mathcal{T} algebra governs the edge/interface degrees of freedom in the broken phase.

From \mathcal{T} to \mathcal{U} Some of the sectors in \mathcal{T} will survive in the bulk, some will be confined. The physical mechanism behind confinement in $2 + 1$ dimensional topological field theories is nontrivial braiding with the condensate. The vacuum state or order parameter should be single valued if carried adiabatically around a localized particle-like excitation. If it is not single valued that would lead to a physical string or “domain wall” extending from the particle that carries a constant energy per unit length. The unconfined algebra \mathcal{U} consists of the representations in \mathcal{T} minus the confined ones, it is this algebra that governs the low energy effective bulk theory. The confined representations can be determined in the following way. First we define the “lift” of a representation in \mathcal{T} as the set of representations $b \in \mathcal{A}$ that restrict to t . Now, if all of the representations in the lift of t braid trivially with the lift of the vacuum, the

sector t is part of \mathcal{U} . Otherwise, it is confined. One may prove that the \mathcal{U} algebra closes on itself with consistent fusion rules, while consistent braiding is achieved by assigning the (identical) spin factors of the parent sectors of the unbroken theory to the \mathcal{U} fields.

Let us finally mention a useful quantity, the so-called *quantum embedding index* q [31], which is a real number characterizing the topological symmetry breaking. This quantity is defined as

$$q = \frac{\sum_a n_u^a d_a}{d_u}, \quad (2.8)$$

where the index a runs over the sectors of the unbroken phase \mathcal{A} , that correspond to lift of any sector u or t of the algebra \mathcal{U} or \mathcal{T} ; the n_u^a is the lift of sectors u to their parents a and d_a is the quantum dimension of the representation a . Observe that this expression is independent of the particular sector u , which is a non-trivial result explained in Ref. [31].

Choosing for u the new vacuum, we have $d_u = 1$ and obtain that q just equals the total quantum dimension of the lift of the \mathcal{U} (or \mathcal{T}) vacuum in the unbroken \mathcal{A} theory. The quantum embedding index is the analogue for the embedding index defined by Dynkin for the embedding of ordinary groups [32]. As an aside we mention that the change in topological entanglement entropy of the disk changes also by $\log(D_{\mathcal{A}}/D_{\mathcal{U}}) = \log q$ in a transition from an \mathcal{A} to a \mathcal{U} phase [31].

2.3.2 Example: breaking $SU(2)_4$ to $SU(3)_1$

Let us to conclude this discussion on topological symmetry breaking and illustrate the procedure with a very straightforward example, namely the breaking of the quantum group $\mathcal{A} = SU(2)_4$. It has 5 irreps labeled by $\Lambda = 0, \dots, 4$ with spinfactors $\theta_a = 1, \frac{1}{8}, \frac{3}{8}, \frac{5}{8}, 1$. The $\Lambda = 4$ is the only boson and we assume it to condense. The lift of the new vacuum corresponds to the $\Phi = 0 + 4$ of \mathcal{A} , and hence the embedding index $q = d_0 + d_4 = 1 + 1 = 2$. The 1 and 3 reps of \mathcal{A} are identified, but because they have different spin factors, the corresponding \mathcal{T} representation will be confined. In \mathcal{U} we are therefore left with the $\Lambda = 2$ rep. which splits because it is a fixed point under fusion with the condensate as $4 \times 2 = 2$. We write $2 \rightarrow 2_1 + 2_2$. The values for the spin and the quantum dimensions and the fusion rules for these representations fully

determine the unconfined quantum group to be $\mathcal{U} = SU(3)_1$. We recall that the nomenclature of the groups is linked to the chiral algebra, it is therefore not surprising that the $SU(2)_4$ quantum group breaks to the *smaller* quantum-group $SU(3)_1$ which is related to a *larger* chiral algebra. For the chiral algebras one has the conjugate embedding $SU(2)_4 \subset SU(3)_1$ which is a conformal embedding. This conformal embedding in turn is induced by the $SO(3) \subset SU(3)$ embedding mentioned at the beginning of this subsection.

2.4 Observables and diagrammatics

There is a powerful diagrammatic language to express the equations describing the TQFT, which we will use to relate the values of observables as they can be measured in the different phases. In this thesis we will use the notation and definitions given by Bonderson [33]. Particle species are represented by lines, fusion and splitting by vertices. A twist is represented by a left or right twist on a particle line:

$$\begin{array}{c} \uparrow \\ | \\ \text{loop} \\ | \\ a \end{array} = \theta_a \begin{array}{c} | \\ | \\ a \end{array}, \quad \begin{array}{c} \text{loop} \\ | \\ \uparrow \\ | \\ a \end{array} = \theta_a^* \begin{array}{c} | \\ | \\ a \end{array}. \quad (2.9)$$

The evaluation of simple diagrams is rather straightforward, and complicated diagrams can be simplified using braid relations and the so-called F symbols which follow from associativity of the fusion algebra. The simplest examples are the closed loop of type a that evaluates to the quantum dimension d_a :

$$\begin{array}{c} \text{circle} \\ | \\ a \end{array} = d_a, \quad (2.10)$$

whereas the twisted loop equals $d_a\theta_a$:

$$\begin{array}{c} \text{twisted loop} \\ | \\ a \end{array} = \theta_a d_a \quad (2.11)$$

Of particular interest are the generators of the modular group, S_{ab}

$$\left(\begin{array}{c} \text{circle with two arrows} \\ a \quad b \end{array} \right) = S_{ab} = \frac{1}{D} \sum_c N_c^{a\bar{b}} \frac{\theta_c}{\theta_a \theta_b} d_c, \quad (2.12)$$

and $T_{ab} = e^{-2\pi i(\bar{c}/24)} \theta_a \delta_{a,b}$, where the \bar{c} is the central charge of the theory, not to be confused with a particle type.

The importance of the rather abstract diagrammatic notation is that the diagrams directly correspond to observables in the Euclidean lattice gauge theory formulation in Chapter 3. In the Euclidean three dimensional formulation of topological theories the values these diagrams have, correspond to the vacuum expectation values of the corresponding anyon loop operators, for example in the unbroken phase one may measure

$$\left\langle \begin{array}{c} \text{circle with arrow} \\ a \end{array} \right\rangle_0 = d_a, \quad (2.13)$$

where the LHS is now defined as the value of the path integral with the nonlocal loop operator for particle species a inserted and the RHS is obtained if we are probing the system in the unbroken phase governed with the groundstate denoted as 0 and governed by the algebra \mathcal{A} . We use the subscript 0 because the value of the same diagram may be different if it is evaluated in a different phase with a groundstate that we will denote by Φ .

Our objective in Chapter 3 is to verify the theoretical predictions of the topological symmetry breaking scheme in a class of Euclidean gauge theories that are expected to exhibit transitions between different topological phases. We will numerically evaluate the expectation values of various topological diagrams using Monte Carlo simulations, and in this section we calculate the predicted outcomes of a variety of possible measurements from theory. The strategy has two steps, (i) the determination of the condensate — including the measurement of the embedding index q — by evaluating the basic nonlocal open string order parameters, given by Eq. (3.29), (ii) measuring the so-called broken modular S -matrix and from that construct the S -matrix of the \mathcal{U} phase. We also will see that the condensate fixes the branching and lift matrices and having determined those we can also predict the outcome of measurements of other topological diagrams corresponding to the lifts of \mathcal{U} fields to \mathcal{A} fields .

2.4.1 Condensate and the embedding index q

We measure the open string operators in the model. Note that in our pictorial representation time flows upward, so a vertical line physically represents the creation, propagation and annihilation of a *single* particle. For the particular case of a DGT, which we study in this work, these lines have a realization as operators on a spacetime lattice, see Eq. (3.29).

If the symmetry is unbroken we will have for any nontrivial field a that

$$\langle L_{a\bar{a}} \rangle_0 = \left\langle \left| \begin{array}{c} | \\ \uparrow a \\ | \end{array} \right\rangle_{\Phi=0} \right\rangle = 0. \quad (2.14)$$

because the diagram represents the creation and subsequent annihilation of a single a -particle. However in the broken situation the expectation value will be nonzero for all fields $\phi_i \in \mathcal{A}$ in the condensate which we denote by Φ . So writing,

$$\Phi = 0 + \sum_i \phi_i \quad (2.15)$$

we obtain that in general,

$$\left\langle \left| \begin{array}{c} | \\ \uparrow a \\ | \end{array} \right\rangle_{\Phi} \right\rangle = \delta_{a\phi_i} d_a. \quad (2.16)$$

This in turn implies that it is simple to measure q as

$$\sum_{a \in \mathcal{A}} \left\langle \left| \begin{array}{c} | \\ \uparrow a \\ | \end{array} \right\rangle_{\Phi} \right\rangle = \left\langle \left| \begin{array}{c} | \\ \uparrow 0 \\ | \end{array} \right\rangle_{\Phi} \right\rangle + \sum_i \left\langle \left| \begin{array}{c} | \\ \uparrow \phi_i \\ | \end{array} \right\rangle_{\Phi} \right\rangle = d_0 + \sum_i d_{\phi_i} = q \quad (2.17)$$

2.4.2 The broken modular S - and T -matrices

The great advantage of switching to the modular data, that is studying the S - and T -matrices, is that unlike the fusion coefficients these generators can be directly measured using the anyon loop operators that arise naturally in a three dimensional Euclidean formulation of the theory. We will evaluate the expectation value of these S -matrices numerically in the lattice formulation of multiparameter discrete gauge theories in Chapter 3. The measured S - and

T -matrix elements do not satisfy the relations (2.2) directly; however, using the measurements the full S - and T -matrices of the \mathcal{U} theory, which do satisfy the modular group relations, can be constructed. In the unbroken theory the measured S -matrix elements $\langle S_{ab} \rangle$ correspond to the expectation values of the Hopf link with one loop colored with representation a and the other with representation b :

$$\langle S_{ab} \rangle_0 = \frac{1}{\mathcal{D}} \left\langle a \left(\bigcirc \bigcirc \right)_b \right\rangle_0 = S_{ab},$$

where S_{ab} is the S -matrix of the unbroken \mathcal{A} theory. We can however also determine the modular S -matrix of the residual \mathcal{U} theory S_{uv} directly from measurements if we take the splittings of certain fields $a \Rightarrow \{a_i\}$ into account appropriately. We will show how to do this for the DGTs in detail in Chapter 3 and will arrive at an explicit formula and algorithm to determine S_{uv} :

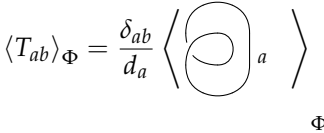
$$S_{uv} = \frac{1}{q} \sum_{a_i, b_j} n_u^{a_i} n_v^{b_j} \langle S_{a_i b_j} \rangle_{\Phi}. \quad (2.18)$$

This expression involves not only the branching (lift) matrix $n_u^{a_i}$, but also the what we will call the *broken S -matrix* defined as $\tilde{S}_{a_i b_j} = \langle S_{a_i b_j} \rangle_{\Phi}$, which, because of the splitting, clearly involves a larger size matrix than the modular S -matrix of the original \mathcal{A} phase. From the broken S -matrix we may directly read off S_{uv} , the S -matrix of the effective low energy TQFT governed by \mathcal{U} . An important observation is that the values of the S -matrix elements in a broken phase will be different from the ones in the unbroken phase, for example because of the contribution of the *vacuum exchange diagram* \tilde{S} depicted below, in which the condensed particle is exchanged giving a nonzero contribution in the broken phase while it would give a vanishing contribution in the unbroken phase:

$$\tilde{S}_{a_i b_j} = \frac{1}{q^2} \left(\text{diagram} \right)$$

In the explicit calculations later on we show that this *vacuum exchange diagram* leads to a change in the S -matrix which depends on the subindices introduced above. It turns out that it is also possible to calculate the broken S -matrix from first principles, this will be discussed in a forthcoming paper [34].

As to be expected one finds identical rows and columns in the broken S -matrix, for components that are identified, whereas the entries for confined fields will be zero. With this prescription the formalism outlined above is applicable in any phase of the theory including the unbroken one where there is no splitting and the vacuum exchange diagram gives a vanishing contribution. The measured T -matrix on the other hand is given by

$$\langle T_{ab} \rangle_{\Phi} = \frac{\delta_{ab}}{d_a} \left\langle \left(\text{Diagram} \right)_a \right\rangle_{\Phi}$$


again with $\langle T_{ab} \rangle_0 = T_{ab}$. After measuring or calculating the S - and T -matrices in a given phase, we can reconstruct the fusion coefficients with the help of the Verlinde formula [26],

$$N_{ab}^c = \sum_x \frac{S_{ax} S_{bx} S_{\bar{c}x}}{S_{1x}}. \quad (2.19)$$

To conclude, we have in this section summarized the basic features of a TQFT and considered some aspects of topological phase transitions induced by a Bose condensate, furthermore we explained how the measurement of the L -, S -, and T -operators in the broken phase fully determine the quantum group of a (broken) topological phase. The general scheme to analyse the breaking pattern of a some multiparameter TQFT is to first use the open string operators to probe which fields are condensed in the various regions of parameter space. In a given broken phase we can subsequently compute/measure what we will call the broken S -matrix \bar{S}_{a_i, b_j} , where as mentioned the subindex labels the splitting of the corresponding \mathcal{A} field. From the broken S -matrix we can read off the S -matrix of the \mathcal{U} theory. In Chapter 3 we will explicitly execute this program for discrete gauge theories.

CHAPTER 3

Discrete Gauge Theories

This chapter is based on the following publications:

- F. A. BAIS AND J. C. ROMERS. Anyonic order parameters for discrete gauge theories on the lattice. *Ann. Phys. (N.Y.)*, 324:1168–1175, 2009, arXiv:0812.2256 [cond-mat.mes-hall]
- F. A. BAIS AND J. C. ROMERS. The modular S-matrix as order parameter for topological phase transitions. *New J.Phys.*, 14:035024, 2012, arXiv:1108.0683 [cond-mat.mes-hall]

In this chapter we study a lattice realization of a particular example of a TQFT, a discrete gauge theory (DGT) based on a finite group H [17, 37]. We define these models on a three-dimensional Euclidean spacetime lattice and find that the action in general allows for many coupling constants, which results in a rich phase diagram. We define gauge-invariant observables (loop operators) in one-to-one correspondence with the various particle sectors in the theory.

We then turn to a concrete example based on the group \overline{D}_2 , the double

dihedral group, which is the group of order eight that is spanned by the unit quaternions. We use these operators to determine the effective low-energy TQFT in various phases of broken topological symmetry. This is done by interpreting the modular S -matrix S_{ab} (see Section 2.2.2) as the expectation value of the Hopf link of two loop operators corresponding to particle types a and b , and measuring this quantity in the various vacua of the theory. In the unbroken vacuum the familiar modular S -matrix is recovered, whereas in broken vacua the values of this matrix change. We provide a method to recover the S -matrix of the effective low-energy theory, thus providing a method to determine the symmetry breaking purely in terms of observable quantities.

The measurement of these observables and thus the mapping of the phase diagram is achieved with the aid of Monte Carlo simulations. Also the order of several phase transitions is established.

3.1 Kitaev's Toric Code and the \mathbb{Z}_2 gauge theory

To connect with other work on topologically ordered systems, let us first go to a Hamiltonian formalism. This is formally done by taking a timeslice of the spacetime lattice which we will define later on in Section 3.3.1 and taking the limit in which the temporal spacing goes to zero [38]. The Hamiltonian of (2+1)-dimensional \mathbb{Z}_2 gauge theory on a square *spatial* lattice is

$$H = -\frac{1}{2}\lambda \sum_l (P_l - 1) - \sum_p \frac{1}{2} (Q_{p1} Q_{p2} Q_{p3} Q_{p4} - 1), \quad (3.1)$$

where the operators P_l and Q_l act on links, the second term is a sum over the elementary plaquettes of the lattice where $p1 \dots p4$ are the links of a single plaquette and λ is the coupling constant. The operators satisfy

$$\{Q_l, P_l\} = 0, \quad P_l^2 = Q_l^2 = 1,$$

which means a possible representation can be given in terms of Pauli matrices $P_l = \sigma_3$, $Q_l = \sigma_1$ acting on spin- $\frac{1}{2}$ bosons living on the links. Loosely speaking the P_i operators are the complex exponent of the electric fields and the Q_i operators the complex exponents of the magnetic fields. Note that a closed string of P_i operators generates a Wilson loop, whereas a closed string of Q_i operators creates a closed Dirac-string. Gauge transformations act on the star

of four links $i1 \dots i4$ adjacent to a site i

$$G_i = P_{i1}P_{i2}P_{i3}P_{i4},$$

and to build the *gauge invariant* Hilbert space, one has to implement a Gauss law for physical states $|\psi\rangle$

$$(1 - G_i)|\psi\rangle = 0 \quad \text{for all sites } i. \quad (3.2)$$

Now we can make the connection with work by Kitaev [20] and Wen [39]. Their models (Toric code, \mathbb{Z}_2 string nets) correspond to Hamiltonian \mathbb{Z}_2 DGT where the coupling $\lambda = 0$ and the gauge constraint (3.2) is not strictly enforced. Setting $\lambda = 0$ makes the theory purely topological, the ground state is an equal weight superposition of all states

$$\prod_{l \in C} Q_l |0\rangle, \quad (3.3)$$

where C is a closed loop of links and $|0\rangle$ is the state with the property $P_l|0\rangle = |0\rangle$ for all links l . Viewing the link variables as spin- $\frac{1}{2}$ bosons, this vacuum state corresponds to all the spins being in the up state. Since the expectation value of any loop operator (3.3) in the ground state is equal to one. These loops are Wilson loops in the gauge theory language and Wilson loops are the natural observables in a gauge theory. Since they are independent of size and their value only depends on linking with other loops or strings, the theory is topological.

Toric code models with perturbations (corresponding to $\lambda \neq 0$ but small) have been studied in the literature [40, 41] and it was found that the topological properties like the ground state degeneracy are robust against such small perturbations. In our Euclidean formulation one gets the perturbations for free but there exists also a strictly topological limit. For the DGT based on \mathbb{Z}_2 this is discussed in the next Section 3.1.1 and it is mentioned later on for the richer \overline{D}_2 model.

By not enforcing the gauge constraint (3.2) strictly but adding it as a term to the Hamiltonian, these models allow for massive open strings. Such open strings are not gauge-invariant at their endpoints and therefore correspond to external charges.

3.1.1 Euclidean formalism

The \mathbb{Z}_2 gauge theory in the Euclidean approach, where we discretize both space and time, is described by the action

$$S = -\beta \sum_p U_{p1} U_{p2} U_{p3} U_{p4}, \quad (3.4)$$

where the sum is again over all plaquettes (now both spatial and temporal) and the U variables are numbers ± 1 . Gauge transformations act on a site and multiply all links ending on the site by -1 . The partition sum

$$\mathcal{Z} = \sum_{\{U\}} e^{-S}$$

and the expectation value of *gauge invariant* operators \mathcal{O}

$$\langle \mathcal{O} \rangle = \frac{1}{\mathcal{Z}} \sum_{\{U\}} \mathcal{O}(\{U\}) e^{-S},$$

are the quantities of interest here. The gauge invariance, which in the Hamiltonian formulation was enforced by projecting out states from the Hilbert space, is now manifest in the action and the operators. The partition sum is over all gauge field configurations, but since all sums are finite, gauge fixing is not required¹.

If the coupling β is large, the dominant contribution from the partition sum will be from field configurations where all plaquettes $UUUU = +1$. In the limit $\beta \rightarrow \infty$ this is strictly true, and one is left with a topological quantum field theory, as was the case for the Hamiltonian (3.1) with $\lambda = 0$. For β small there is a confining phase, the phase transition is at $\beta = 0.7613$ [42].

In most of this work, we study the topological properties of a DGT, for a general group H . To show that for finite coupling constant β this *topological limit* is good approximation, let us perturbatively calculate the expectation value of a Wilson loop in this \mathbb{Z}_2 theory. The Wilson loop $W(C)$ is the product

¹This even holds for continuous groups, since we integrate over the group instead of the algebra.

of U variables around a closed loop C

$$\langle W(C) \rangle = \frac{1}{Z} \sum_{\{U\}} UU \dots U e^{-S}.$$

For large β , the action is minimized by configurations for which all plaquettes are $+1$. The first order perturbation comes from those configurations in which one link is -1 . In three dimensions, this excites 4 plaquettes, so the Boltzmann weight for such configurations is $e^{-4\beta}$ smaller than for those with no excited plaquettes.

If the lattice has size $N \times N \times N$, there are $3N^3$ links. For a contour C of length L ,

$$\langle W(C) \rangle \approx \frac{1 - Le^{-4\beta} + (3N^3 - L)e^{-4\beta}}{1 + 3N^3e^{-4\beta}} \approx 1 - 2Le^{-4\beta} + O(e^{-8\beta}).$$

This shows the corrections to the purely topological result $W(C) = 1$ are, for β several times larger than the critical point, negligible for simulations of reasonable lattice sizes: for a Wilson loop size 10×10 , $\beta = 3.0$ yields corrections only in the third digit.

Another gauge-invariant quantity is the 't Hooft loop, which lives on a loop C' of the dual lattice. Such a loop pierces a number of plaquettes p , and the 't Hooft operator

$$H(C') = \prod_{p \in C'} e^{-2\beta} U_{p1} U_{p2} U_{p3} U_{p4},$$

flips the sign of the coupling $\beta \rightarrow -\beta$ for these plaquettes. This forces a \mathbb{Z}_2 magnetic flux through these plaquettes. We will define operators generalizing the 't Hooft and Wilson loops for general non-Abelian DGTs shortly.

3.1.2 Phase structure

The action (3.4) can realize three phases when one also allows for negative coupling. For large positive β , the phase mentioned before is realized, where almost all plaquettes² are $+1$. For large negative β , almost all plaquettes

²This works for a square 3D lattice with periodic boundary conditions. We have not investigated other lattices, but one can imagine that types of frustration might occur here.

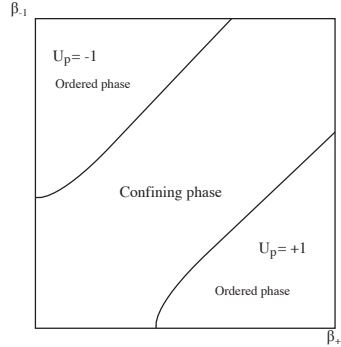


Figure 3.1: Phase diagram for a pure \mathbb{Z}_2 gauge theory.

are -1 . For small $|\beta|$, a confining phase where the magnetic \mathbb{Z}_2 flux has condensed is realized.

To study the phase diagram of a (non-Abelian) DGT in full, we find it convenient to formulate the action in the *class basis*, instead of the *irrep basis*. This means we do not take the character of the group element of the plaquette product $UUUU$ in the action, but we define delta functions on each class. We will explain in detail how this works in Section 3.3.1. For \mathbb{Z}_2 the phase diagram is one-dimensional, but the introduction of a second coupling constant will get rid of the need for negative couplings:

$$S = - \sum_p (\beta_{+1} \delta_{+1}(U_{p1} U_{p2} U_{p3} U_{p4}) + \beta_{-1} \delta_{-1}(U_{p1} U_{p2} U_{p3} U_{p4})), \quad (3.5)$$

where $\delta_A(U)$ for a group element U and a conjugacy class A gives $+1$ if $U \in A$ and zero otherwise. For non-Abelian groups this formulation makes the phase diagram much more intuitive, for \mathbb{Z}_2 it is rather artificial. In Figure 3.1 the phase diagram of the pure \mathbb{Z}_2 gauge theory is shown as a function of the conjugacy class couplings β_{+1} and β_{-1} . Later in this thesis we present similar phase diagrams for the \overline{D}_2 gauge theory.

It is well-known that the inclusion of matter coupled to the gauge fields complicates the phase diagram strongly. The question of whether there exist good order parameters to distinguish the phases in coupled gauge-matter systems is interesting in its own right and highly non-trivial [43], but it is not

something we will go into here.

3.2 Quantum Double and Discrete Gauge Theories

The excitations in gauge theories fall into two classes, which we call electric and magnetic. The electric excitations are the fields that transform nontrivially under the gauge group, either put into the theory as external charges or by explicitly introducing extra dynamical terms in the action. An example is the particle-antiparticle pair put into the \mathbb{Z}_2 gauge theory by insertion of a Wilson loop in the action.

The magnetic class of excitations are the topologically nontrivial solutions to the gauge field equations. As has been discussed in section 1.2, there exists a great many of such solutions, but we will apply the notion “magnetic” solely to the solitonic excitations. In planar physics, see table 1.1, these are the fluxes.

3.2.1 Electric and magnetic symmetries

In what follows, we will discuss the way in which both the electric and magnetic excitations of a discrete gauge theory transform under gauge transformations, followed by a part on more exotic excitations, the dyons, which carry both magnetic and electric charge. After this, the mathematical framework of the *quantum double* [44], in which these notions stick together, will be built up [45].

In this discussion, spacetime is continuous. This restricts the gauge freedom: if we want the map defining a gauge transformation to be smooth and continuous, it has to be a constant in the case of a discrete group. Therefore only global gauge transformations are allowed in what follows³.

The discrete group under consideration is denoted H , group elements are $g, h \in H$, and a Hilbert space formalism with Dirac notation is used for the fields. Matrix indices are suppressed.

Electric charges The electric excitations of a theory are described by some field $|v^\alpha(x)\rangle$. Here α is an index labeling the representation under which the field transforms when acted upon by a gauge transformation. The field takes

³This might sound counterintuitive. However, the defining property of a gauge transformation is not that it is local but that it does nothing to physical Hilbert space vectors.

values in the vector space V_α associated with the representation α and may take different values at different spatial locations x . However, for convenience, we will drop this coordinate.

Let us perform a gauge transformation by an element $g \in H$:

$$|v^\alpha\rangle \mapsto D_\alpha(g)|v^\alpha\rangle,$$

where $D_\alpha(g)$ is the matrix representing g in representation α . This works well for single particle states. If we want to describe the action of the gauge group on multiparticle states, we have to make use of the direct product representation. An n -particle state is given by the direct product of single particle Hilbert space vectors

$$|v^\alpha\rangle \otimes |v^\beta\rangle \otimes |v^\gamma\rangle \dots \quad (3.6)$$

This product is in general not irreducible anymore, even if the original representations α, β, \dots were. To simplify the gauge action on the combination, we can use the Clebsch-Gordan decomposition:

$$|v^\alpha\rangle \otimes |v^\beta\rangle = \bigotimes_{\xi} N_{\xi}^{\alpha\beta} |v^{\xi}\rangle,$$

where $N_{\xi}^{\alpha\beta}$ is called the multiplicity of the ξ irrep in the product of α and β . It is given here for a product between two representations, but it can be generalized to n -particle states by repeated application.

Magnetic charges We have seen that electric charges are labeled by the representations of the group. Since any representation can be decomposed into irreps, the fundamental electric particles are labeled by the irreps of the group H .

We now wish to construct a similar labeling for the magnetic sectors of the theory. To achieve this we need to study the emergence of a DGT in detail in a more physical setting than before.

3.2.2 Realizing a discrete gauge theory

To gain insight as to how the magnetic sectors of a discrete gauge theory are labeled, consider how we can realize a discrete gauge theory to begin with. Let us start with a G gauge theory, where G is a simply connected continuous

group, for example $SU(2)$. By using the Higgs mechanism, this theory can be transformed into a H gauge theory, with H a discrete group. To this end, we require a scalar field in some representation of G invariant under the subgroup H .

By letting the mass of the Higgs field go to infinity, the only excitations present in the gauge-Higgs system above are the magnetic fluxes. Parallel transport can be realized by the untraced Wilson line operator along some open or closed curve C

$$P \exp\left(ig \int_C A \cdot dx\right). \quad (3.7)$$

This object will in principle take values in the full gauge group G . Let us use this object to take the Higgs field at a certain point x , transport it along C , and close C such that we end up at the same point x again. We desire the Higgs field to be single valued, so operator (3.7) should act trivially upon it. Since the Higgs field has invariance under the discrete subgroup H , we see that for all closed curves C , the untraced Wilson loop takes values in H . Therefore, magnetic fluxes are labeled by group elements of H , as a Wilson loop operator measures the magnetic flux within the loop.

However, in the non-Abelian case, this is not the complete story. Let us consider charges introduced in the theory that are not H -invariant and their transport around a flux. First we work in a gauge where the flux is labeled by $g \in H$. If we parallel transport a charge in representation α around it, the topological interaction between them works as

$$|v^\alpha\rangle \mapsto D_\alpha(g)|v^\alpha\rangle. \quad (3.8)$$

Let us compare this event to another situation, where we first perform a global gauge transformation by the group element h . This transformation has two effects: it acts on the internal space of the α charge with the element h and it will change the flux to some unknown value g' . The parallel transport equivalent to equation (3.8) is now given by

$$D_\alpha(h)|v^\alpha\rangle \mapsto D_\alpha(g')D_\alpha(h)|v^\alpha\rangle = D_\alpha(g'h)|v^\alpha\rangle.$$

After this parallel transport, let us transform back to the original gauge by performing a transformation with element h^{-1} . The effect of parallel transport

is now as follows:

$$|v^\alpha\rangle \mapsto D_\alpha(h^{-1}g'h)|v^\alpha\rangle.$$

Since we work in the same gauge as in equation (3.8), the result should be the same. Therefore we arrive at the equality

$$g' = hgh^{-1}.$$

This is the transformation law for a flux labeled by a group element g under a gauge transformation h . The gauge invariant notion for the magnetic sectors of the theory is thus not given by individual group elements, but by the conjugacy classes of H .

However, although the above effect is inherently quantum mechanical, it still is not a complete treatment of the full quantum theory. We have neglected the fact that these fluxes might be in a superposition of classical states. To make this more clear in our notation and also pave the way for the quantum double treatment, from now on we will also denote fluxes as kets in a vector space. The vector space of interest here is the group algebra $\mathbb{C}H$, the space of formal linear combinations of group elements

$$\mathbb{C}H = \left\{ \sum_i c_i |g_i\rangle \mid c_i \in \mathbb{C}, |g_i\rangle \in H \right\}. \quad (3.9)$$

Concluding what we have learned so far: the electric sectors of the theory are labeled by the irreducible representations α and the magnetic sectors are labeled by the conjugacy classes A . Now let us study how the fluxes interact.

Interactions between fluxes and flux metamorphosis Consider the situation where two fluxes in states g_1 and g_2 are next to each other, the former to the left of the latter. An electric charge transported around the two will be acted upon by the product of the two,

$$|v^\alpha\rangle \mapsto D_\alpha(g_1g_2)|v^\alpha\rangle. \quad (3.10)$$

Let us now define a counterclockwise interchange, or *braid*, operator for this pair. What is the effect of such an interchange on the internal space of the fluxes, that moves g_2 to the left of g_1 , in a counterclockwise manner?

Let us gauge the system such that the flux starting as g_1 remains unchanged and g_2 transforms into g'_2 . We know that an electric charge at a large distance having topological interactions with the pair should not feel any effect of the interchange, leading to

$$g_1 g_2 = g'_2 g_1 \quad (3.11)$$

$$g'_2 = g_1 g_2 g_1^{-1}. \quad (3.12)$$

This class of topological interactions between magnetic fluxes, called *flux metamorphosis* [17] appear only when there are nonAbelian magnetic sectors present, otherwise the conjugation in equation (3.12) is trivial.

In terms of the braid operator \mathcal{R} acting on the two-particle Hilbert space of the two pure fluxes we can formulate this as follows:

$$\begin{aligned} \mathcal{R} : CH \otimes CH &\rightarrow CH \otimes CH \\ \mathcal{R}|g_1\rangle \otimes |g_2\rangle &= |g_1 g_2 g_1^{-1}\rangle \otimes |g_1\rangle. \end{aligned}$$

As a corollary we can also derive the action of moving a flux around another flux, back to its original location, called a *monodromy*

$$\mathcal{R}^2 |g_1\rangle \otimes |g_2\rangle = |(g_1 g_2) g_1 (g_1 g_2)^{-1}\rangle \otimes |g_1 g_2 g_1^{-1}\rangle. \quad (3.13)$$

The product of the two fluxes after the monodromy is still $g_1 g_2$, as should be the case.

Determining unknown flux The interactions between fluxes can be used to determine the magnetic charge of an unknown flux. The group elements form an orthonormal basis for the group algebra CH in the sense $\langle g_i | g_j \rangle = \delta_{ij}$, which allows us to determine the flux of an unknown magnetic excitation $|h\rangle$ by performing a series of interference experiments. We do this by calculating the matrix element

$$\langle h | \otimes \langle g_i | \mathcal{R} | g_i \rangle \otimes | h \rangle = \langle g_i | h g_i h^{-1} \rangle \langle h | (g_i h) h (g_i h)^{-1} \rangle \quad (3.14)$$

$$= \delta_{g_i, h g_i h^{-1}} \delta_{h, (g_i h) h (g_i h)^{-1}}. \quad (3.15)$$

By repeating this experiment for all fluxes g_i , we obtain a set of matrix elements unique for the flux h , allowing this flux to be uniquely established.

Dyonic sectors Discrete gauge theories also carry dyons in their spectrum, sectors with both magnetic and electric quantum numbers [45]. Let us start out with a magnetic flux, and try to attach some electric charge to it. Say we first try to attach a representation α of the full discrete group H to a given flux in a conjugacy class A . The ket describing this dyonic state is given by

$$|g, v^\alpha\rangle = |g\rangle \otimes |v^\alpha\rangle \in \mathbf{CH} \otimes V_\alpha, \quad (3.16)$$

where v^α is a vector in the carrier space V_α of the representation α and g lives in the group algebra \mathbf{CH} . Let us try to probe this sector using test excitations to find out which electric representation is present, in an experiment akin to equation (3.14). We arrive at the matrix element

$$\begin{aligned} \langle g, v^\alpha | \otimes \langle g_i | \mathcal{R} | g_i \rangle \otimes |g, v^\alpha\rangle &= \langle g, v^\alpha | g_i g g_i^{-1}, D_\alpha(g_i) v^\alpha \rangle \langle g_i | (g_i g) g_i (g_i g)^{-1} \rangle \\ &= \langle v^\alpha | D_\alpha(g_i) v^\alpha \rangle \delta_{g, g_i g g_i^{-1}}. \end{aligned}$$

The delta function in this expression restricts the set of group elements we can use to calculate nonzero matrix elements to the group elements that commute with g . The physical origin of this is clear: if we probe the long-distance electric charge of a dyonic sector with a flux not commuting with the magnetic charge on the dyon, the internal flux state of the dyon ends up orthogonal to its original orientation.

The above means that not all charges can unambiguously be attached to a given flux. Only charges forming a representation of the centralizer ${}^g N$, the set of elements in H commuting with g , can be implemented in a consistent manner.

3.2.3 Unified framework: quantum double

Let us recall what we have seen so far. Electric sectors are labeled by irreducible representations α of the gauge group and the internal space of an electric excitation is the carrier space of its representation V_α . Magnetic sectors are labeled by the conjugacy classes A of the gauge group. Since a magnetic excitation can be in a linear superposition of classical fluxes, its internal space is the group algebra \mathbf{CH} . The dyonic sectors are labeled by both electric and magnetic quantum numbers, but its electric representations are restricted to those of the centralizer ${}^g N$ of the flux g .

We will now construct all of the above in a more unified framework. We denote a general state in a discrete gauge theory as

$$|h, v^\alpha\rangle \in V_\alpha^A,$$

where we have defined the combined Hilbert space V_α^A for general discrete gauge theory sectors labeled by a class A and a centralizer charge α . Let us define two operators that can work on the internal states of particles. The first operator, P_g , projects out the flux g

$$P_g|h, v^\alpha\rangle = \delta_{g,h}|h, v^\alpha\rangle,$$

whereas the second operator, which we denote by g , performs a global gauge transformation

$$g|h, v^\alpha\rangle = |ghg^{-1}, D_\alpha(g)v^\alpha\rangle.$$

These operators do not commute, and realize the algebra

$$\begin{aligned} P_g P_{g'} &= \delta_{g,g'} P_g \\ h P_g &= P_{hgh^{-1}} h \end{aligned}$$

The set of combined flux projections and gauge transformations $\{P_g h\}_{g,h \in H}$ generates the quantum double $D(H)$, a Hopf algebra. We will give all the definitions of Hopf algebra operations in what follows, but first we will construct irreducible representations and see they correspond directly to the electric, magnetic and dyonic sectors of a discrete gauge theory.

Constructing irreps We now turn to finding the irreducible representations for this Hopf algebra: this allows us to label all of the sectors in the spectrum. The representation theory of the quantum double $D(H)$ of a finite group H was first worked out in [46] but here we follow the discussion presented in [37].

Let A be a conjugacy class in H . We will label the elements within A as follows:

$$\{^A h_1, ^A h_2, \dots, ^A h_k\} \in A,$$

for a class A of order k . In general, the centralizers for the different group elements within a conjugacy class are different, but they are isomorphic to

one another. Let ${}^A N \subset H$ be the centralizer for the first group element in the conjugacy class $A, {}^A h_1$.

The set ${}^A X$ relates the different group elements within a conjugacy class to the first defining element h_1

$${}^A X = \left\{ {}^A x_1, {}^A x_2, \dots, {}^A x_k \mid {}^A h_i = {}^A x_i {}^A h_1 {}^A x_i^{-1} \right\}. \quad (3.17)$$

This still leaves a lot of freedom, but we fix our convention such that ${}^A x_1 = e$. The centralizer ${}^A N$, being a group, will have different irreps, which we label by α . The vector space for a representation α is spanned by a basis ${}^\alpha v_j$. The total Hilbert space that combines magnetic and electric degrees of freedom, V_α^A , is then spanned by the set of vectors

$$\left\{ |{}^A h_i, {}^\alpha v_j\rangle \right\},$$

where i runs over the elements of the conjugacy class, $i = 1, 2, \dots, \dim A$ and j runs over the basis vectors of the carrier space of α , $j = 1, 2, \dots, \dim \alpha$.

To see that this basis is a natural one to act on with our flux measurements and gauge transformations, consider an irreducible representation Π_α^A of some combined projection and gauge transformation $P_h g$

$$\Pi_\alpha^A(P_h g) |{}^A h_i, {}^\alpha v_j\rangle = \delta_{h, g {}^A h_i g^{-1}} |g {}^A h_i g^{-1}, \sum_m D_\alpha(\tilde{g})_{mj}^\alpha v_m\rangle,$$

where the element \tilde{g} is the part of the gauge transformation g that commutes with the flux ${}^A h_1$, defined as

$$\tilde{g} = {}^A x_k^{-1} g {}^A x_k, \quad (3.18)$$

with ${}^A x_k$ implicitly defined by ${}^A h_k = g {}^A h_i g^{-1}$. This indeed commutes with the element ${}^A h_1$:

$${}^A h_k = g {}^A x_i {}^A h_1 {}^A x_i^{-1} g^{-1} \rightarrow {}^A h_1 {}^A x_k^{-1} = {}^A x_k^{-1} g {}^A x_i {}^A h_1 {}^A x_i^{-1} g^{-1}$$

So

$$\begin{aligned}
 {}^A h_1 \tilde{g} &= {}^A h_1^A x_k^{-1} g^A x_i \\
 &= {}^A x_k^{-1} g^A x_i^A h_1^A x_i^{-1} g^{-1} g x_i \\
 &= {}^A x_k^{-1} g x_i h_1 = \tilde{g}^A h_1.
 \end{aligned}$$

Ribbon element By viewing a dyon as a combination of a magnetic flux and an electric charge with some spatial separation between the two, we can define an operator that signals the spin of the excitation. Since spin is the eigenvalue of a state belonging to the operator that rotates the state by 2π , the following operator, called the ribbon element c , will do the job

$$c = \sum_{g \in H} P_g g.$$

It is a central element in $D(H)$ and hence can be used to label its irreps. Letting c work on a given state leads to the relation

$$\Pi_\alpha^A \left(\sum_g P_g g \right) |{}^A h_i, \alpha v_j\rangle = |{}^A h_i, \sum_m D_\alpha({}^A h_1)_{mj}^\alpha v_m\rangle,$$

And since the element ${}^A h_1$ commutes with all elements in the centralizer ${}^A N$ the operator c , by Schur's lemma, needs to be proportional to the unit matrix

$$D_\alpha({}^A h_1) = e^{2\pi i s_{(A,\alpha)}} 1_{\alpha},$$

where we have defined the topological spin s of each sector of $D(H)$. This is related to the "twist" defined earlier in Section 2.2.1 by

$$\theta_{(A,\alpha)} = e^{2\pi i s_{(A,\alpha)}}.$$

Coproduct We can also use the Hopf algebra language to act on multiparticle states. The coproduct Δ , the coalgebraic dual to multiplication

$$\Delta : D(H) \rightarrow D(H) \otimes D(H),$$

is the natural object for this purpose which satisfies a property called *coassociativity*:

$$(\Delta \otimes \text{id}) \circ \Delta = (\text{id} \otimes \Delta) \circ \Delta,$$

where id is the identity map. Given the flux projectors P_h and gauge transformations g , the concrete construction is as follows:

$$\Delta(P_h g) = \sum_{h'h''=h} P_{h'} g \otimes P_{h''} g.$$

The constraint in this sum means we project out all combinations of fluxes that carry total flux h and implement a gauge transformation by the group element g on both excitations.

In the case of $D(H)$ with H an Abelian group, the coproduct also satisfies cocommutativity. We first define τ , the flip operator:

$$\begin{aligned} \tau : D(H) \otimes D(H) &\rightarrow D(H) \otimes D(H) \\ P_h g \otimes P_{h'} g' &\mapsto P_{h'} g' \otimes P_h g, \end{aligned}$$

then cocommutativity amounts to $\Delta = \tau \circ \Delta$.

On the representation level the comultiplication leads to the definition of the tensor product or fusion rules of states.

Counit In an algebra, there exists the unit element that makes multiplication act as the identity map. In our Hopf algebra, the element doing the same for comultiplication is the *counit*

$$\epsilon : D(H) \rightarrow \mathbb{C},$$

which acts in such a way that

$$(\epsilon \otimes \text{id}) \circ \Delta = \text{id} = (\text{id} \otimes \epsilon) \circ \Delta.$$

On the representation level, this is precisely what is expected from the vacuum irrep. Fusing a given irrep with the vacuum sector, be it from the right or the left, should keep a state invariant

$$\Pi_1^\epsilon \otimes \Pi_\alpha^A \simeq \Pi_\alpha^A \simeq \Pi_\alpha^A \otimes \Pi_1^\epsilon.$$

Fusion The direct product of two irreducible representations of a group is in general not irreducible anymore. It decomposes into a direct sum of irreps, with multiplicities given by the Clebsch-Gordan coefficients. For direct products of irreps of a Hopf algebra, there is an analogous decomposition

$$\Pi_\alpha^A \otimes \Pi_\beta^B = \bigotimes_{C,\gamma} N_{\alpha\beta C}^{AB\gamma} \Pi_\gamma^C,$$

where the coefficients can be calculated from the Verlinde formula, see [?]. This relation describes the possible channels Π_γ^C two particles Π_α^A and Π_β^B can fuse into. Alternatively, one can use it to work out the different decay channels for a single particle state that can be regarded as a composite of Π_α^A and Π_β^B .

Braiding and the universal R -matrix In the scattering experiments described by equation (3.14), we already alluded to the braid operator \mathcal{R} . We will now explicitly present a construction. Acting on a two-particle state, we want the right particle to be acted upon by the flux of the left particle and then have their positions interchanged. It is useful to decompose the braid operator into into the latter part, which is the flip operator τ and the former part, called the *universal R -matrix*

$$R = \sum_h (P_h, e) \otimes (1, h) \in D(H) \otimes D(H).$$

The first term projects out the flux of the first particle, which is then implemented on the second. Combining this with the representation functions and the flip operator gives us the braid operator

$$\mathcal{R}_{\alpha\beta}^{AB} = \tau \circ (\Pi_\alpha^A \otimes \Pi_\beta^B)(R).$$

Quasi-cocommutativity It can be checked that the braiding operator and the coproduct commute, which is expected from physical considerations, since the local interchange of two particles cannot affect the long-range properties of the pair

$$\Delta(P_h g) \mathcal{R} = \mathcal{R} \Delta(P_h g). \quad (3.19)$$

This is a consequence of the relation:

$$(\tau \circ \Delta(P_h g))R = R\Delta(P_h g)$$

Quasi-triangularity Given two particles, the effect of braiding the second around the first and then letting the first decay should equal letting the decay process take place first and then braiding the second particle around the decay products.

By using explicit matrix notation, we can specify the action of the R -matrix on three-particle states. Let us first write the universal R -matrix as follows: $R = \sum_k R_l^k \otimes R_r^k$. Now, for actions on three-particle states, we define R_{ij} , the triple product with R_l^k on position i , R_r^k on position j and 1 on the other position. For example:

$$R_{23} = \sum_k 1 \otimes R_l^k \otimes R_r^k$$

$$R_{31} = \sum_k R_r^k \otimes 1 \otimes R_l^k$$

The physical condition described above is then formulated as the quasi-triangularity conditions, illustrated in Figure 3.2:

$$(\Delta \otimes \text{id})R = R_{13}R_{23} \quad (3.20)$$

$$(\text{id} \otimes \Delta)R = R_{13}R_{12} \quad (3.21)$$

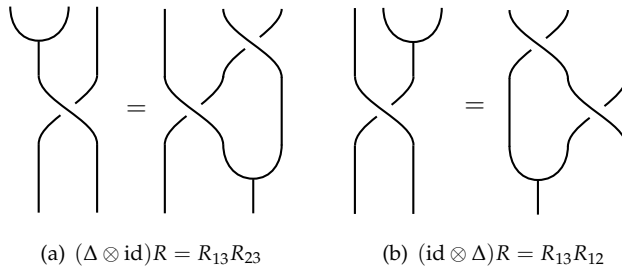


Figure 3.2: Quasi-triangularity conditions.

Modular data from the quantum double To conclude we give a simple expression for the modular S -matrix that can be obtained by calculating the trace of the monodromy matrix

$$S_{(A,\alpha)(B,\beta)} = \frac{1}{|H|} \sum_{g \in A, h \in B, [g,h]=e} \text{Tr}_\alpha(x_g^{-1} h x_g)^* \text{Tr}_\beta(x_h^{-1} g x_h)^*, \quad (3.22)$$

where $[g, h]$ is the group theoretical commutator: $[g, h] = ghg^{-1}h^{-1}$.

3.3 Euclidean approach to DGTs

Until now, what we have done is to set the stage for DGTs. We have shown that they can arise by breaking a Yang-Mills theory by some exotic Higgs condensate invariant under a *discrete subgroup* H of the continuous gauge group. Now we take a different viewpoint on these matters by directly formulating a DGT on a spacetime lattice. We show that the centralizer charge appearing in the dyonic sectors of the theory makes a reappearance in the order parameters, which are generalizations of the Wilson and 't Hooft loops.

3.3.1 Lattice actions and observables

We discretize three-dimensional spacetime into a set of sites i, j, \dots using a rectangular lattice. The gauge field U_{ij} [47], which takes values in the gauge group H , lives on the links ij, jk, \dots connecting sets of neighboring sites. The links are oriented in the sense that $U_{ij} = U_{ji}^{-1}$.

We note that the gauge field U_{ij} takes care of the parallel transport of matter fields that are charged under the gauge group from site i to site j . An ordered product of links along a closed loop is gauge invariant up to conjugation by a group element and measures the holonomy of the gauge connection. Gauge transformations are labeled by a group element $g_i \in H$ and are performed at the sites of the lattice. The gauge field transforms as

$$U_{ij} \mapsto g_i U_{ij} g_j^{-1}, \quad (3.23)$$

where the orientation of the links (incoming or outgoing) has to be taken into account as shown in Figure 3.3.

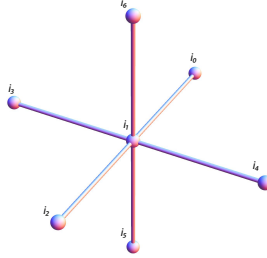


Figure 3.3: In our convention a gauge transformation g at location i_1 transforms $U_{i_1 i_2} \rightarrow g U_{i_1 i_2}$, $U_{i_1 i_4} \rightarrow g U_{i_1 i_4}$, $U_{i_1 i_6} \rightarrow g U_{i_1 i_6}$, $U_{i_0 i_1} \rightarrow U_{i_0 i_1} g^{-1}$, $U_{i_3 i_1} \rightarrow U_{i_3 i_1} g^{-1}$, $U_{i_5 i_1} \rightarrow U_{i_5 i_1} g^{-1}$.

The standard form for the lattice gauge field action makes use of the ordered product of links around a plaquette $ijkl$:

$$U_p = U_{ijkl} = U_{ij} U_{jk} U_{kl} U_{li},$$

which transforms under conjugation by the gauge group,

$$U_p \mapsto g_i U_p g_i^{-1}.$$

The gauge action per plaquette which corresponds to the Yang-Mills form $F_{\mu\nu}^2$ in the continuum limit for $H = SU(N)$, is given by

$$S_p = - \sum_{\alpha} \beta_{\alpha} \chi_{\alpha} (U_p), \quad (3.24)$$

where χ_{α} is the group character in irrep α and β_{α} is inversely proportional to the square of the coupling constant for irrep α . This is known, for $H = SU(2)$ and the sum over representations limited to the fundamental one, as the Wilson action [47].

For $SU(N)$ gauge theories one usually only includes the fundamental representation and is thus left with only one coupling constant. This is not necessary however: gauge invariance of the action is ensured by the fact the characters are conjugacy class functions, and therefore we will consider actions where the number of independent couplings equals the number of conjugacy

classes i.e. the number of irreps (for a finite group these numbers are finite and equal).

For our purposes, namely the study of magnetic condensates in DGTS, equation (3.24) is not the most convenient to work with. We perform a change of basis in the space of coupling constants to write it as a sum over delta functions on conjugacy classes A : $\delta_A(h) = 1$ if $h \in A$, and 0 otherwise. In this basis the action becomes

$$S_p = - \sum_A \beta_A \delta_A(U_p) , \quad (3.25)$$

similar to the action of the \mathbb{Z}_2 gauge theory (3.5), where the conjugacy classes are just $+1$ and -1 .

This formulation allows us in particular to directly control the mass of the different fluxes in the theory, which will ease the search for different vacua in the phase diagram. Increasing the coupling constant for a certain conjugacy class (magnetic flux) A will increase the contribution of configurations carrying many A fluxes to the path integral. Likewise, setting all β_A to zero except β_e , the coupling constant for the trivial conjugacy class, will result in an "empty" vacuum and therefore an unbroken phase.

To perform the transformation to the conjugacy class basis, we need to make use of the following orthogonality relations valid for all finite groups H

$$\int_H dg \chi_\alpha(g) \chi_\beta^*(g) = \delta_{\alpha,\beta} , \quad (3.26)$$

$$\begin{aligned} \sum_{\alpha \in \mathcal{R}} \chi_\alpha(g) \chi_\alpha^*(h) &= \frac{|H|}{|A|} \text{ if } g, h \in A \\ &= 0 \text{ otherwise,} \end{aligned} \quad (3.27)$$

where $|H|$ is the order of the group H , $|A|$ is the order of the conjugacy class A , $\chi_\alpha(\cdot)$ is the character in irrep α , \mathcal{R} is the set of irreps and group integration is defined as

$$\int_H dg f(g) = \frac{1}{|H|} \sum_{g \in H} f(g).$$

Equations (3.26) and (3.27) show that the irreducible representations of a group H form an orthonormal set for functions on conjugacy classes of H . We thus expect the conjugacy class delta function to be expressible in terms

of characters

$$\delta_A(g) = \sum_{\alpha \in \mathcal{R}} c_\alpha \chi_\alpha(g),$$

for some set of constants $\{c_\alpha\}$. We multiply both sides of this expression by a character of the same group element in another irrep β and perform the integrations by use of the orthogonality relations (3.26) and (3.27)

$$\begin{aligned} \int_H dg \chi_\beta^*(g) \delta_A(g) &= \sum_{\alpha \in \mathcal{R}} c_\alpha \int_H dg \chi_\beta^*(g) \chi_\alpha(g), \\ \frac{|A|}{|H|} \chi_\beta^*(A) &= \sum_{\alpha \in \mathcal{R}} c_\alpha \delta_{\alpha\beta} = c_\beta, \end{aligned}$$

where the slightly abusive notation $\chi_\alpha(A)$ means the character of any group element of A in the representation α . This shows that

$$\delta_A(g) = \sum_{\alpha \in \mathcal{R}} \frac{|A|}{|H|} \chi_\alpha^*(A) \chi_\alpha(g), \quad (3.28)$$

which in turn implies that the the difference between (3.24) and (3.25) is just a change of basis:

$$\sum_{A \in \mathcal{C}} \beta_A(\beta_\alpha) \delta_A(g) = \sum_{\alpha \in \mathcal{R}} \beta_\alpha \chi_\alpha(g),$$

where \mathcal{C} is the set of conjugacy classes and $\beta_A(\beta_\alpha)$ is given by

$$\beta_A = \sum_\alpha \beta_\alpha \chi_\alpha(A).$$

To probe the physics of the system for a fixed set of values of the coupling constants in the action, we will use a set of order parameters and phase indicators. These order parameters are in one-to-one correspondence with the set of fundamental anyonic excitations of the theory.

3.3.2 Order parameters and phase indicators

We distinguish two different sets of order parameters that are closely related to one another. The first is the set of closed *loop operators*, that physically correspond to the creation, propagation and annihilation of an anyon-anti-anyon

pair in spacetime. The second is the set of open *string operators* that create, propagate and annihilate a single anyon. In the background of a trivial vacuum, only the loops can have nonzero expectation values, since the creation of a single particle would violate the conservation of the quantum numbers of the vacuum in such a background. This means that the open strings tell us something about possible Bose condensates, whereas the closed loops tell us about the behaviour of external particles put into this background. We define the open string operators only for the purely magnetic sectors, since in this work we only study magnetic condensates⁴.

First we will define the loop operators, which are a generalization of the Wilson and 't Hooft loops. They create a particle-antiparticle pair from the vacuum and annihilate them at a later time. These loops allow us to calculate Aharonov-Bohm type phases and determine which anyonic excitations will be confined. In $SU(N)$ gauge theories, the Wilson loop for a free excitation, e.g. in the Higgs phase of $SU(2)$ theory, in general falls off as e^{-cP} , with P the perimeter of the loop, whereas a confined excitation, such as the $\mathbf{3}$ charge of an external quark source in pure $SU(3)$ gauge theory describing QCD, falls off as $e^{-c'A}$, with A the area of the loop.

Because the excitations in a DGT are gapped, numerically we find that the expectation values of loop operators are constant as a function of size. The argument for this behaviour for the \mathbb{Z}_2 theory is in Section 3.1.1. Although only strictly true in the limit of infinite coupling constant, the gap suppresses the dependence on size so strongly, we will assume that the theory is a purely topological one in the region of coupling constant space in which we are interested.

Let us draw a closed loop on the dual lattice, this loop pierces a set of plaquettes C through which we will force magnetic flux. Now draw another loop, this time on the real lattice, such that (i) each point of this loop lies on the corner of a plaquette in C and (ii) the two loops do not link⁵. The combination of the two loops establishes a framing: we have selected a location for the electric charge of a flux-charge composite. This framing also provides us with

⁴Electric condensates break the gauge group H to some subgroup K by the conventional Higgs breaking, this implies in the present context that $D(H)$ will be broken to $D(K)$, which in turn means that the fluxes in the coset G/H are confined [28].

⁵One can also write down a magnetic and electric loop that link for example once. This gives the worldribbon a twist and the expectation value of such an operator allows one to calculate the topological spin for a given excitation.

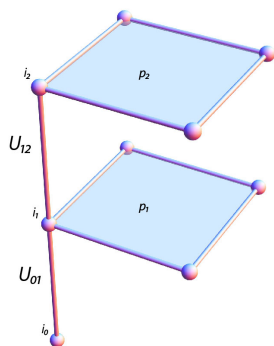


Figure 3.4: The first two plaquettes appearing in expression (3.29). The ordered product U_p of links around a plaquette p needs to be taken with an orientation that has to be constant throughout the loop.

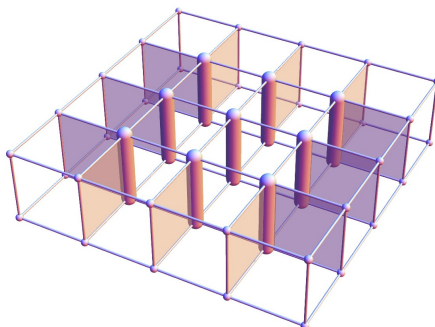


Figure 3.5: A set of plaquettes forming a closed loop on the lattice. The fat links constitute the h -forest.

a point and orientation on each plaquette from which to take the plaquette product U_p : for non-Abelian groups the product of the four links depends on which corner you start.

To insert a flux h in a plaquette $p \in C$, we have to “twist” the Boltzmann factor of this particular plaquette by locally changing the action from $S(U_p)$ to $S(h^{-1}U_p)$: if the minimum of the action was previously obtained for $U_p = e$, it is now shifted to $U_p = h$. We want to perform this twisting procedure for all plaquettes in C .

The notion of a group element as a magnetic flux is not gauge-invariant: under a gauge transformation by g , a flux h transforms as $g h g^{-1}$. Therefore it is necessary to sum over the group elements h in a conjugacy class A in some way.

One can go about this in two different, and inequivalent, ways.

- The authors in Ref. [48] only studied pure magnetic flux loops (without electric charge) and performed a sum over the conjugacy class for each plaquette in C individually. This leaves a gauge-invariant expression, but the loop loses its framing, since a conjugation by the element U_{01} maps

$$h^{-1}U_{01}U_{12}U_{23}U_{30} \rightarrow U_{01}h^{-1}U_{12}U_{23}U_{30},$$

for a plaquette spanned by group elements $U_{01} \dots U_{30}$.

- When dealing with nontrivial braiding properties of loop operators it is necessary to choose a basepoint i_0 in space with respect to which all operators are defined, it provides a calibration that serves as a “flux bureau of standards”, borrowing a term from [49]. This point can be anywhere in spacetime and does not need to be on the loop. We then define a function $k_{i_p}(h, \{U_{ij}\})$ of h and the gauge field variables $\{U_{ij}\}$ for the twist element that has to be inserted into the plaquette product for plaquette p , where i_p is the corner of the plaquette chosen in the framing

$$k_{i_p} = k_{i_p}(h, \{U_{ij}\}) = U_{i_0 i_p}^{-1} h^{-1} U_{i_0 i_p}.$$

With this notation and the above considerations, the anyonic operator

$\Delta^{(A,\alpha)}$ is given by ⁶:

$$\Delta^{(A,\alpha)}(C) = \sum_{h \in A} \prod_{p_j \in C} D_\alpha \left(x_{U_{j-1,j}^{-1} k_j U_{j-1,j}}^{-1} U_{j-1,j} x_{k_j} \right) e^{S(U_{p_j}) - S(k_j U_{p_j})}. \quad (3.29)$$

Here p_j iterates over the plaquettes in C and D_α is the representation function of the centralizer irrep α of ${}^A N$. The link $U_{j-1,j}$ neighbours the plaquette p_j , and the combination in brackets always takes values in the centralizer subgroup of the conjugacy class A . The exponential of the difference of two actions changes the minimal action configuration to one containing flux h for the plaquette under consideration.

The operator in expression (3.29) is a generalization of the Wilson and 't Hooft loops, and by constructing it we have established the desired one to one correspondence between irreducible representations of the quantum-group and loop operators for the pure discrete gauge theory. If we fill in for A the trivial conjugacy class, the exponent vanishes and the x group elements are equal to the group unit, so after we multiply out the D_α -matrices we are left with

$$\Delta^{(e,\alpha)}(C) = \chi_\alpha (U_{1,2} U_{2,3} \cdots U_{n-1,n} U_{n,1}),$$

where the product of U s is an ordered product along the loop on the lattice.

On the other hand, if we replace α by the trivial representation, we are left with

$$\Delta^{(A,1)}(C) = \sum_{h \in A} \prod_{p_j \in C} e^{S(U_{p_j}) - S(h^{p_j} U_{p_j})},$$

which is comparable to the order parameter proposed in Ref. [48], but the gauge invariance with respect to the transformations (3.23) is ensured in a different way. We sum over the conjugacy class only once and insert the flux in a gauge invariant way by parallel transporting it along the loop from a fixed basepoint. The operator in Ref. [48] sums over the conjugacy class for each individual plaquette. This way also gauge invariance is achieved, but the loop loses its framing, and therefore is not suitable to describe true anyonic charges.

The open magnetic string operators are a variant of expression (3.29) where

⁶This definition is different from our original definition [35] by a factor of $\frac{1}{|A|}$. This definition gives the correct S -matrix elements directly.

the set of plaquettes C corresponds to an open string on the dual lattice. Looking at the h -forest configurations, it can immediately be seen that such a string, corresponding to the creation and subsequent annihilation of a single particle, has zero expectation value in the trivial vacuum. For these strings to acquire a non zero expectation value a *vacuum exchange contribution* is required, which we will focus on now.

The vacuum exchange contribution. We use the set of operators $\{\Delta^{(A,\alpha)}\}$ to measure the elements of the S -matrix by picking two loops C_1 and C_2 that link each other once

$$\langle S_{(A,\alpha)(B,\beta)} \rangle = \langle \Delta^{(A,\alpha)}(C_1) \Delta^{(B,\beta)}(C_2) \rangle. \quad (3.30)$$

In the trivial vacuum the $S_{(A,\alpha)(B,\beta)}$ -matrix elements of fluxes $g \in A$ and $h \in B$ for which $ghg^{-1}h^{-1} = [g,h] \neq e$ evaluate to zero (this is what we measure using the operators (3.29) and calculate algebraically (3.22)). If we however measure the S -matrix elements of such noncommuting fluxes in a broken vacuum nonzero matrix elements can appear.

This is most easily explained by considering an example. The main contribution to a single loop of pure magnetic flux is of the form pictured in Figure 3.5. This configuration is called the h -forest state in earlier literature [48]. Modulo gauge transformations this is the dominant configuration in the trivial vacuum that contributes to a loop of flux labeled by conjugacy class A , where $g \in A$. Expression (3.29) contains a sum over these group elements within a conjugacy class, but let us for now focus on one of the group elements. Each link in this configuration has value e , except for the fat links in Figure 3.5, they have value h . That this configuration leads to a loop or tube of flux is easily seen: within the forest each plaquette has a value $eh eh^{-1} = e$, whereas at the edges the value is $eh ee = h$ (depending on the orientation of the plaquette product). This is also the easiest way to see the origin of the Aharonov-Bohm effect on the lattice: an electric charge loop having linking number 1 with the flux loop will have exactly one link with value h in it, therefore its value will be $\chi_\alpha(h)$.

Consider now the dominant configuration that contributes to the S -matrix element $S_{(A,1)(B,1)}$. We again pick two group elements $g \in A$, $h \in B$ and draw a similar diagram. This is shown in Figure 3.6. By similar logic this causes the plaquettes at the boundary of either forest to have value g respectively

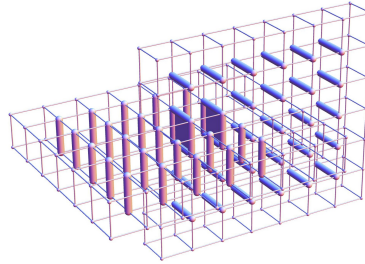


Figure 3.6: The vacuum exchange contribution. Double h -forest, configuration contributing to the S -matrix measurement of two non commuting fluxes. The fat links are the g -forest and h -forest and the shaded plaquettes are a string of $[g, h]$ flux connecting the the two loops.

h . Inside the forests most plaquettes still have value e , however there are some plaquettes that are different. There is a tube of plaquettes that have value $[g, h]$, where the two forests intersect. In general this group theoretical commutator is not equal to identity element for nonAbelian groups. This is the physical reason behind the appearance of zeroes in the S -matrix for nonAbelian theories. This tube of plaquettes represents a flux $[g, h]$ going from the one loop to the other. In the trivial vacuum this flux will be gapped, so the contribution of this diagram to the path integral expectation value will be negligible.

However, a different situation appears when we are in a vacuum where the flux $[g, h]$ has Bose condensed. We cannot give a single configurations that contributes dominantly to the path integral (there are many), but we can say that configurations like the one in Figure 3.6 are now contributing since the mass for the flux $[g, h]$ has disappeared.

Thus we expect that in the measurements there will be cases where zeroes in the original S -matrix will obtain a nonzero value in the broken phase.

An auxiliary A_N gauge symmetry The operators (3.29) are invariant with respect to the local H gauge transformations (3.23). However, in our formula-

tion of the operators we have tacitly introduced another, auxiliary ${}^A N$ gauge symmetry that is less obvious. A crucial property that allows one to determine the topological symmetry breaking pattern in detail is that the loop operators do transform nontrivially under this symmetry. In a non trivial ground state, these symmetries may be broken and will therefore lead to the lifting of certain degeneracies related with the splitting of fields in the topological symmetry breaking process. So this hidden symmetry turns out to be a blessing in disguise.

Let us first note that there is no preferred choice for the coordinate system (3.17) we define for the conjugacy classes. Once a certain choice $\{x_{h_i}\}$ has been made such that $h_i = x_{h_i} h_1 x_{h_i}^{-1}$, a set $\{x'_{h_i}\}$ with

$$x'_{h_i} = x_{h_i} n_{h_i}, \quad [n_{h_i}, h_i] = e, \quad (n_{h_i} \in {}^A N) \quad (3.31)$$

will do just as well. In the trivial vacuum, the S -matrix is invariant with respect to this transformation. This is most easily seen by looking at the algebraic expression (3.22), but it is also confirmed by our measurements of (3.30).

This invariance can be understood on the operator level by multiplying out the representation matrices of the centralizer in equation (3.29). Generally this will lead to terms of the form

$$\mathrm{Tr}_\alpha \tilde{g} = \mathrm{Tr}_\alpha (x_{h_k}^{-1} g x_{h_i}),$$

where g is the product of links on the loop and $h_k = g h_i g^{-1}$, implying that indeed $\tilde{g} \in {}^A N$. When the loop is linked with another loop, the element g will in general be in the conjugacy class of the flux of this other loop. Under the transformation (3.31) of the conjugacy class coordinate system, the above expression will transform as

$$\mathrm{Tr}_\alpha (n_{h_k}^{-1} x_{h_k}^{-1} g x_{h_i} n_{h_i}) = \mathrm{Tr}_\alpha (n_{h_i} n_{h_k}^{-1} x_{h_k}^{-1} g x_{h_i}),$$

due to the cyclicity of the trace. This elucidates the invariance of the S -matrix in the trivial vacuum under the translation of the x_{h_i} : non-commuting fluxes never have a non-zero matrix element, and if $[g, h] = e$, we have that $h_i = h_k$ and therefore $n_{h_i} n_{h_k}^{-1} = e$. In a non-trivial ground state where non-commuting fluxes may have non-zero S -matrix elements due to a vacuum interchange

contribution, the transformation (3.31) may manifest itself in different measured matrix elements. This means that in such cases the entry (A, α) may split into multiple entries $\{(A_i, \alpha_i)\}$. As we are interested in these multiple entries, we will in our calculations always include the nontrivial behavior of our observables under this auxiliary ${}^A N$ action. This turns out to be one of two mechanism responsible for the splitting of irreps of \mathcal{A} into multiple irreps of \mathcal{U} , the other of which we turn to now.

An auxiliary $H/{}^A N$ symmetry There is another symmetry, but now on the level of the fusion algebra that turns out to be useful. Suppose in the theory there exists a rule of the form

$$(A, \alpha) \times (e, \beta) = (A, \alpha), \quad (3.32)$$

where (e, β) is some one-dimensional purely electric representation. This turns out to be the case whenever the representation $\Pi^{(e, \beta)}(\cdot)$ evaluates to unity for all elements in ${}^A N$, the normalizer of conjugacy class A . We can prove this using the explicit expression for the fusion coefficients in terms of the quantum double characters [37]:

$$N_{(C, \gamma)}^{(A, \alpha)(B, \beta)} = \frac{1}{|H|} \sum_{g, h} \text{Tr} \left[\Pi^{(A, \alpha)} \otimes \Pi^{(B, \beta)} (\Delta(P_h g)) \right] \text{Tr} \left[\Pi^{(C, \gamma)} (P_h g) \right]^*. \quad (3.33)$$

Picking $(B, \beta) = (e, \beta)$ and $(C, \gamma) = (A, \alpha)$,

$$\begin{aligned} N_{(A, \alpha)}^{(A, \alpha)(e, \beta)} &= \frac{1}{|H|} \sum_{g, h} \text{Tr} \left[\Pi^{(A, \alpha)} \otimes \Pi^{(e, \beta)} \left(\sum_{h_1 h_2 = h} P_{h_1} g \otimes P_{h_2} g \right) \right] \cdots \\ &\quad \cdots \text{Tr} \left[\Pi^{(A, \alpha)} (P_h g) \right]^* \\ &= \frac{1}{|H|} \sum_{g, h} \text{Tr} \left[\Pi^{(A, \alpha)} (P_h g) \otimes \Pi^{(e, \beta)} (P_e g) \right] \text{Tr} \left[\Pi^{(A, \alpha)} (P_h g) \right]^* \\ &= \frac{1}{|H|} \sum_{g \in {}^A N, h \in A} \text{Tr} \left[\Pi^{(A, \alpha)} (P_h g) \right] \text{Tr} \left[\Pi^{(A, \alpha)} (P_h g) \right]^* = 1, \end{aligned}$$

where in the latter line we have made use of the orthogonality of the characters. We assumed $\Pi^{(e, \beta)}(P_e g) = 1$ for all $g \in {}^A N$. The sum over h is restricted

since if $h \notin A$ the matrix element will be zero and the sum over g is restricted since if $g \notin A$ the matrix element will be off-diagonal and thus not contribute to the trace.

So we see that the fusion rule (3.32) leads to a degeneracy in the calculation of S -matrix elements since by definition

$$\left\langle \begin{array}{c} \text{Diagram 1} \\ (A,\alpha) \quad (C,\gamma) \\ 0 \end{array} \right\rangle = \left\langle \begin{array}{c} \text{Diagram 2} \\ (A,\alpha) \\ (e,\beta) \\ (C,\gamma) \\ 0 \end{array} \right\rangle .$$

The diagrammatic equation shows two representations, (A, α) and (C, γ) , on the left-hand side (LHS) of an equals sign. These are represented as two circles with arrows, one above the other. On the right-hand side (RHS), there are three representations stacked vertically: (A, α) at the top, (e, β) in the middle, and (C, γ) at the bottom. Each representation is shown as a vertical line with a loop or arrow. The entire equation is enclosed in large angle brackets with a subscript 0 at the bottom.

However, on the operator level this equality does not hold. Indeed, when we probe the LHS of this equation in a non-trivial vacuum the result will in general differ from the RHS. In particular, it turns out that the different \mathcal{U} representations that lift to the same \mathcal{A} representations (A, α) differ precisely by such a fusion. So this degeneracy may be lifted in the broken phase and give rise to a additional splittings of certain entries (A, α) . Consequently in our numerical calculations we have to explicitly keep track of the presence of such electric representations (e, β) , that satisfy (3.32) and see whether they give rise to additional splittings.

To conclude this section, we remark that we have very explicitly indicated how one gets from the modular S -matrix S_{ab} to the extended or broken S -matrix $\tilde{S}_{a,b}$, from which the topological data of the broken \mathcal{U} phase can be immediately read off.

3.4 $D(\overline{D}_2)$ theory: algebraic analysis

The group \overline{D}_2 contains eight elements that can be represented by the set of 2×2 -matrices

$$\{\mathbb{1}, -\mathbb{1}, \pm i\sigma_1, \pm i\sigma_2, \pm i\sigma_3\}, \tag{3.34}$$

where the σ_i , $i = 1, 2, 3$ are the Pauli spin matrices. We denote the conjugacy classes as $e = \{\mathbb{1}\}$, $\bar{e} = \{-\mathbb{1}\}$, $X_1 = \{i\sigma_1, -i\sigma_1\}$, $X_2 = \{i\sigma_2, -i\sigma_2\}$, $X_3 = \{i\sigma_3, -i\sigma_3\}$ and the irreducible group representations as 1 , the trivial irrep, J_1, J_2, J_3 three one-dimensional irreps and χ the two-dimensional irrep given

by (3.34). The character table is given on the left hand side of Table 3.1. The

\overline{D}_2	e	\bar{e}	X_1	X_2	X_3	\mathbb{Z}_4	$\mathbb{1}$	$i\sigma_i$	$-\mathbb{1}$	$-i\sigma_i$
1	1	1	1	1	1	Γ^0	1	1	1	1
J_1	1	1	1	-1	-1	Γ^1	1	i	-1	$-i$
J_2	1	1	-1	1	-1	Γ^2	1	-1	1	-1
J_3	1	1	-1	-1	1	Γ^3	1	$-i$	-1	i
χ	2	-2	0	0	0					

Table 3.1: Character table of the group \overline{D}_2 and of \mathbb{Z}_4 as a centralizer of the conjugacy class X_i .

centralizer groups for the conjugacy classes e and \bar{e} are both \overline{D}_2 since the elements in these conjugacy classes constitute the center of the group. The conjugacy classes X_i , $i = 1, 2, 3$ have non-trivial \mathbb{Z}_4 centralizer subgroups, of which the character table is given on the right hand side of Table 3.1. The irreducible representations of the quantum double are labeled by a combination (A, α) of a conjugacy class A and a centralizer irrep α . The full set of fusion rules for the $D(\overline{D}_2)$ theory is given in 3.7. All in all, there are 22 sectors: the trivial flux paired with the five irreps of \overline{D}_2 , the \bar{e} flux paired with the five irreps of \overline{D}_2 and the three X_i fluxes paired with the four \mathbb{Z}_4 irreps. The sectors that involve an X_i flux or a χ irrep have quantum dimension 2, the others have unit quantum dimension. One obtains that the total quantum dimension for the theory $D_A = 8$.

3.4.1 Breaking: $(\bar{e}, 1)$ condensate

In this case the lift of the new vacuum is $\phi = (e, 1) + (\bar{e}, 1)$, which implies that $q = d_{(e,1)} + d_{(\bar{e},1)} = 2$. To determine the effective low energy theory we fuse ϕ with all particle sectors of the theory and look for the irreducible combinations that appear. As before the notation (A, α) stands for a particle with magnetic

flux A and electric charge α .

$$\begin{aligned}
\phi \times (e, 1) &= (e, 1) + (\bar{e}, 1) \\
\phi \times (e, J_i) &= (e, J_i) + (\bar{e}, J_i) \\
\phi \times (e, \chi) &= (e, \chi) + (\bar{e}, \chi) \quad (*) \\
\phi \times (\bar{e}, 1) &= (e, 1) + (\bar{e}, 1) \\
\phi \times (\bar{e}, J_i) &= (e, J_i) + (\bar{e}, J_i) \\
\phi \times (\bar{e}, \chi) &= (e, \chi) + (\bar{e}, \chi) \quad (*) \\
\phi \times (X_i, \Gamma^0) &= (X_i, \Gamma^0) + (X_i, \Gamma^0) \\
\phi \times (X_i, \Gamma^1) &= (X_i, \Gamma^1) + (X_i, \Gamma^3) \quad (*) \\
\phi \times (X_i, \Gamma^2) &= (X_i, \Gamma^2) + (X_i, \Gamma^2) \\
\phi \times (X_i, \Gamma^3) &= (X_i, \Gamma^1) + (X_i, \Gamma^3) \quad (*)
\end{aligned}$$

The lines marked with (*) have components on the right hand side that carry different spin factors, implying that they are confinement in the broken phase. Studying the fusion rules of the surviving combinations of irreps leads to the conclusion that the effective \mathcal{U} theory is $D(\mathbb{Z}_2 \otimes \mathbb{Z}_2)$. We denote the four different irreps and conjugacy classes of the group $\mathbb{Z}_2 \otimes \mathbb{Z}_2$ by the labels $++, +-, -+, --$, the first (second) symbol standing for the first (second) \mathbb{Z}_2 . This means $\mathcal{D}_{\mathcal{T}}^2 = 32$ and $\mathcal{D}_{\mathcal{U}}^2 = 16$. The branchings of \mathcal{A} irreps into the

unconfined \mathcal{U} theory are

$$\begin{aligned}
(e, 1) + (\bar{e}, 1) &\rightarrow (++, ++), & d_{(++ , ++)} &= 1 \\
(e, J_1) + (\bar{e}, J_1) &\rightarrow (++, +-), & d_{(++ , +-)} &= 1 \\
(e, J_2) + (\bar{e}, J_2) &\rightarrow (++, -+), & d_{(++ , -+)} &= 1 \\
(e, J_3) + (\bar{e}, J_3) &\rightarrow (++, --), & d_{(++ , --)} &= 1 \\
(X_1, \Gamma^0)_1 &\rightarrow (-+, ++), & d_{(-+ , ++)} &= 1 \\
(X_1, \Gamma^0)_2 &\rightarrow (-+, +-), & d_{(-+ , +-)} &= 1 \\
(X_1, \Gamma^2)_1 &\rightarrow (-+, -+), & d_{(-+ , -+)} &= 1 \\
(X_1, \Gamma^2)_2 &\rightarrow (-+, --), & d_{(-+ , --)} &= 1 \\
(X_2, \Gamma^0)_1 &\rightarrow (+-, ++), & d_{(+-, ++)} &= 1 \\
(X_2, \Gamma^0)_2 &\rightarrow (+-, -+), & d_{(+-, -+)} &= 1 \\
(X_2, \Gamma^2)_1 &\rightarrow (+-, +-), & d_{(+-, +-)} &= 1 \\
(X_2, \Gamma^2)_2 &\rightarrow (+-, --), & d_{(+-, --)} &= 1 \\
(X_3, \Gamma^0)_1 &\rightarrow (--, ++), & d_{(-- , ++)} &= 1 \\
(X_3, \Gamma^0)_2 &\rightarrow (--, --), & d_{(-- , --)} &= 1 \\
(X_3, \Gamma^2)_1 &\rightarrow (--, +-), & d_{(-- , +-)} &= 1 \\
(X_3, \Gamma^2)_2 &\rightarrow (--, -+), & d_{(-- , -+)} &= 1
\end{aligned}$$

which all have quantum dimension $d_u = 1$, while the confined fields are

$$\begin{aligned}
(e, \chi) + (\bar{e}, \chi) &\rightarrow t_1, & d_{t_1} &= 2 \\
(X_1, \Gamma^1) + (X_1, \Gamma^3) &\rightarrow t_2, & d_{t_2} &= 2 \\
(X_2, \Gamma^1) + (X_2, \Gamma^3) &\rightarrow t_3, & d_{t_3} &= 2 \\
(X_3, \Gamma^1) + (X_3, \Gamma^3) &\rightarrow t_4, & d_{t_4} &= 2
\end{aligned}$$

and have $d_t = 2$.

3.4.2 Breaking: (X_1, Γ^0) condensate

There is an obvious symmetry in the fusion rules between the three (X_i, Γ^0) particle sectors. We choose to study the case where the (X_1, Γ^0) condensates. This gives for the new vacuum $\phi = (e, 1) + (\bar{e}, 1) + (X_1, \Gamma^0)$, from which follows that $q = 4$ in this case. We now read off the lifts of the \mathcal{T} fields on the right:

$$\begin{aligned}
\phi \times (e, 1) &= (e, 1) + (\bar{e}, 1) + (X_1, \Gamma^0) \\
\phi \times (e, J_i) &= (e, J_i) + (\bar{e}, J_i) + \delta_{1i}(X_1, \Gamma^0) + \eta_{1i}(X_1, \Gamma^2) \\
\phi \times (e, \chi) &= (e, \chi) + (\bar{e}, \chi) + (X_1, \Gamma^1) + (X_1, \Gamma^3) \\
\phi \times (\bar{e}, 1) &= (e, 1) + (\bar{e}, 1) + (X_1, \Gamma^0) \\
\phi \times (\bar{e}, J_i) &= (e, J_i) + (\bar{e}, J_i) + \delta_{1i}(X_1, \Gamma^0) + \eta_{1i}(X_1, \Gamma^2) \\
\phi \times (\bar{e}, \chi) &= (e, \chi) + (\bar{e}, \chi) + (X_1, \Gamma^1) + (X_1, \Gamma^3) \\
\phi \times (X_1, \Gamma^0) &= (X_1, \Gamma^0) + (X_1, \Gamma^0) + (e, 1) + (\bar{e}, 1) + (e, J_1) + (\bar{e}, J_1) \\
\phi \times (X_1, \Gamma^1) &= (X_1, \Gamma^1) + (X_1, \Gamma^3) + (e, \chi) + (\bar{e}, \chi) \\
\phi \times (X_1, \Gamma^2) &= (X_1, \Gamma^2) + (X_1, \Gamma^2) + (e, J_2) + (\bar{e}, J_2) + (e, J_3) + (\bar{e}, J_3) \\
\phi \times (X_1, \Gamma^3) &= (X_1, \Gamma^1) + (X_1, \Gamma^3) + (e, \chi) + (\bar{e}, \chi) \\
\phi \times (X_i, \Gamma^0) &= (X_i, \Gamma^0) + (X_i, \Gamma^0) + (X_k, \Gamma^0) + (X_k, \Gamma^2) \quad (i \neq k \neq 1) \\
\phi \times (X_i, \Gamma^1) &= (X_i, \Gamma^1) + (X_i, \Gamma^3) + (X_k, \Gamma^1) + (X_k, \Gamma^3) \\
\phi \times (X_i, \Gamma^2) &= (X_i, \Gamma^2) + (X_i, \Gamma^2) + (X_k, \Gamma^0) + (X_k, \Gamma^2) \\
\phi \times (X_i, \Gamma^3) &= (X_i, \Gamma^1) + (X_i, \Gamma^3) + (X_k, \Gamma^1) + (X_k, \Gamma^3)
\end{aligned}$$

We have used the symbol δ_{ij} which is 1 when i and j are equal and is zero otherwise, and η_{ij} which is 1 when i and j are not equal and is zero when i and j are. The \mathcal{U} theory is $D(\mathbb{Z}_2) \simeq \mathbb{Z}_2 \otimes \mathbb{Z}_2$. This means $\mathcal{D}_{\mathcal{T}}^2 = 16$ and $\mathcal{D}_{\mathcal{U}}^2 = 4$. The lifts of the unconfined fields are:

$$\begin{aligned}
(e, 1) + (\bar{e}, 1) + (X_1, \Gamma^0)_1 &\rightarrow (+, +), \quad d_{(+,+)} = 1 \\
(e, J_1) + (\bar{e}, J_1) + (X_1, \Gamma^0)_2 &\rightarrow (+, -), \quad d_{(+,-)} = 1 \\
(X_2, \Gamma^0)_1 + (X_3, \Gamma^0)_1 &\rightarrow (-, +), \quad d_{(-,+)} = 1 \\
(X_2, \Gamma^2)_1 + (X_3, \Gamma^2)_1 &\rightarrow (-, -), \quad d_{(-,-)} = 1
\end{aligned}$$

and of the confined fields:

$$\begin{aligned}
(e, J_2) + (\bar{e}, J_2) + (X_1, \Gamma^2)_1 &\rightarrow t_1, \quad d_{t_1} = 1 \\
(e, J_3) + (\bar{e}, J_3) + (X_1, \Gamma^2)_2 &\rightarrow t_2, \quad d_{t_2} = 1 \\
(e, \chi) + (\bar{e}, \chi) + (X_1, \Gamma^1) + (X_1, \Gamma^3) &\rightarrow t_3, \quad d_{t_3} = 2 \\
(X_2, \Gamma^0)_2 + (X_3, \Gamma^2)_2 &\rightarrow t_4, \quad d_{t_4} = 1 \\
(X_3, \Gamma^0)_2 + (X_2, \Gamma^2)_2 &\rightarrow t_5, \quad d_{t_5} = 1 \\
(X_2, \Gamma^1) + (X_2, \Gamma^3) + (X_3, \Gamma^1) + (X_3, \Gamma^3) &\rightarrow t_6, \quad d_{t_6} = 2
\end{aligned}$$

3.5 $D(\overline{D}_2)$ theory: lattice analysis

The five couplings $\{\beta_A\}$ for conjugacy class A that appear in the action of the $D(\overline{D}_2)$ theory

$$S_p = \sum_p - \{ \beta_e \delta_e(U_p) + \beta_{\bar{e}} \delta_{\bar{e}}(U_p) + \beta_{X_1} \delta_{X_1}(U_p) + \beta_{X_2} \delta_{X_2}(U_p) + \beta_{X_3} \delta_{X_3}(U_p) \}, \quad (3.35)$$

are inversely proportional to the masses of the fluxes A . For example if we put all couplings to zero except for β_e , which we make large (at least as large as 2.0 as we will see shortly), the trivial vacuum is realized: this is the configuration where for all plaquettes $U_p = e$. Deviations from this configuration occur because of quantum fluctuations, but since all excitations are gapped they will be exponentially suppressed. The gap in this vacuum is easily calculated to be of the order of $4\beta_e$, since the smallest excitation above the configuration in which all plaquettes are e is one in which one link has a value $h \neq e$. This excites four plaquettes and changes the action (3.35) by a value of $4\beta_e$.

3.5.1 Monte Carlo considerations

For the other, nontrivial phases in this theory, the dominant configurations contributing to the path integral are not so readily identified. To gain insight into what configurations contribute we use a Monte Carlo simulation, in particular a modified *heat bath* algorithm. Bluntly applying this algorithm to our problem leads to various complications, therefore we briefly point out the method, the complications and how we have resolved them.

The procedure starts with some initial configuration of link variables $\{U\}_1$. We then update all links in lexicographic order, a process called a sweep, and arrive at a new configuration $\{U\}_2$. The updating process for each link proceeds as follows. Consider the link U_{ij} . We identify which plaquettes contain this link: in three dimensions, there are four such plaquettes. Now we calculate, for each element $g \in H$, what the sum of the plaquette actions for each of these four plaquettes would be if U_{ij} were to have the value g . This gives a set of numbers

$$\{S_{g_1}, S_{g_2}, \dots, S_{g_{|H|}}\},$$

where S_{g_k} is the sum of the four plaquette actions with U_{ij} equal to g_k . We now calculate a localized partition sum $Z_{U_{ij}}$:

$$Z_{U_{ij}} = \sum_{g \in H} e^{-S_g},$$

which can be used to calculate a set of probabilities $\{p(g)\}_{g \in H}$ for each group element g

$$p(g) = \frac{e^{-S_g}}{Z_{U_{ij}}}.$$

After a given number of sweeps n_0 , the Monte Carlo algorithm arrives at the minimum of the action and the path integral expectation value of the operator O

$$\langle O \rangle = \frac{\int DU O[U] e^{-S[U]}}{\int DU e^{-S[U]}} \quad (3.36)$$

is given by taking the average of $O[\{U\}_n]$, the value of O at gauge field configuration $\{U\}_n$:

$$\langle O \rangle_{\text{MC estimate}} = \frac{1}{m} \sum_{n=n_0+1}^{n_0+m} O[\{U\}_n]. \quad (3.37)$$

However, for our purposes this scheme is troublesome for two reasons: it is tacitly assumed that the presence of the operator O in (3.36) does not change the value of the minimum of the action S and furthermore the loops of magnetic flux are very non-local objects and therefore highly unlikely to appear when using a local updating algorithm. This is illustrated in Figure 3.7.

The shift upward of the functional $S[U]$ is due to the presence of a magnetic flux string and the shift to the left is due to the non-locality of the magnetic excitations. The latter shift also occurs when a single loop of flux is inserted.

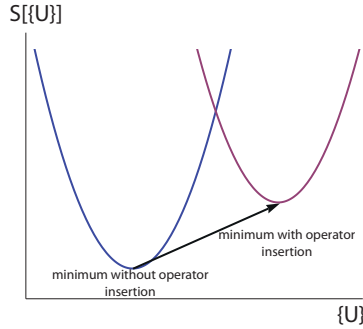


Figure 3.7: Schematic drawing of the action as a functional of the gauge field configuration $\{U\}$. The insertion of non-commuting fluxes shifts the minimum of the action to a different location in the configuration space (due to the non-local nature of the excitations) and to a different value (due to the presence of a string).

The minimum of the action in the calculation of an S -matrix element (3.30) is altered by the insertions of the loop operators: the configuration for two non-commuting fluxes carries a string (see the discussion around Figure 3.6) that is massive and thus costs a finite amount of action. There is no way to get rid of this string and therefore the minimum value of the action in the presence of the two loops is shifted. We therefore have to amend the standard MC algorithm. Defining

$$\begin{aligned} S &= S_{\min} + \delta S \quad \text{without operator insertion,} \\ \tilde{S} &= \tilde{S}_{\min} + \delta \tilde{S} \quad \text{with operator insertion,} \end{aligned}$$

and noticing that around the minimum the actions behave identically, implying that δS and $\delta \tilde{S}$ are the same functions, expression (3.36) becomes

$$\langle O \rangle = \frac{\int DU e^{-(\tilde{S}_{\min} - S_{\min})} O[U] e^{-\delta S[U]}}{\int DU e^{-\delta S[U]}}. \quad (3.38)$$

This leads to a modified Monte Carlo average

$$\langle O \rangle_{\text{MC estimate}} = \frac{1}{m} e^{-(S_{\min} - S_{\min})} \sum_{n=n_0+1}^{n_0+m} O[\{U\}_n]. \quad (3.39)$$

We now describe two approaches to the second problem in our MC measurements: the low probability that the local updating algorithm will converge to a gauge field configuration containing a (set of) magnetic flux loop(s). We will assume a single loop of pure magnetic flux is inserted, as nothing substantial will change in the case of multiple loops or the addition of dyonic charge.

The first approach is based on the observation, illustrated in Figure 3.5, that we know the gauge field configuration (up to gauge transformations) that extremizes the action in the trivial vacuum with the insertion of a loop of magnetic flux: the h -forest. We can therefore use this configuration as an *ansatz* in the MC algorithm. We start with a “cold lattice”, all links $U_{ij} = e$, except for the h -forest, for these links we set $U_{ij} = h$. This is an extremum of the action if we set all $\beta_{A \neq e} = 0$ and $\beta_e \gg 1$. To perform a measurement at some other value of the coupling constants, we can slowly change the coupling constants towards the desired values, performing a few MC updates after each step. The second approach is a more physical one. We initialize the lattice directly at the desired point in coupling constant space. The trick is then not to insert the loop all at once, but to slowly grow it, as illustrated in Figure 3.8. We start by twisting the action for four plaquettes around one link, as shown by the shaded plaquettes in the top left of Figure 3.8. After this, a number of MC updates are performed. Then the set of plaquettes that have a twisted action is changed as in the top right corner of the Figure. Again a number of MC updates is performed and so on. We have checked that in the trivial vacuum one obtains the h -forest configuration using this procedure. Both of methods to insert flux loops have been used by us and we have verified that they lead to completely equivalent results.

3.5.2 Results

In this subsection we present the results of our Monte Carlo simulations. The first quantity we measured was the free energy as a means to map out a suitable subspace of the parameter space. It gives us an indication of the validity

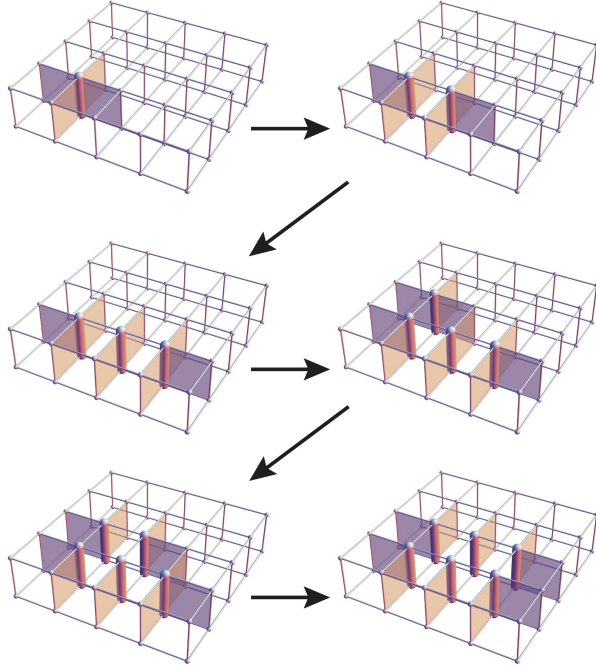


Figure 3.8: Growing a flux loop in multiple steps. The shaded plaquettes have a twisted action, and the fat links show the convergence towards a h -forest state.

of our naive intuition about where nontrivial condensates should occur.

Once we have found some region where symmetry breaking occurs we measure the open string expectation values to determine the respective condensates. After that we measure the unbroken and broken S -matrix elements. Using the straightforward algorithm involving the auxiliary symmetries of our loop operators discussed in section 3.3.2, allows us to find the branching matrix $n_u^{a_1}$ as well as the S -matrix of the effective \mathcal{U} theory in the broken phase.

Mapping out the phase diagram The space of coupling constants in our theory is five-dimensional but it is not our goal to analyse it completely. We have

restricted our search to some representative regions where nontrivial condensates do indeed occur. To study the location of the corresponding phase transitions we measured the free energy F , which we define as the expectation value of the plaquette action, averaged over the spacetime lattice. The left

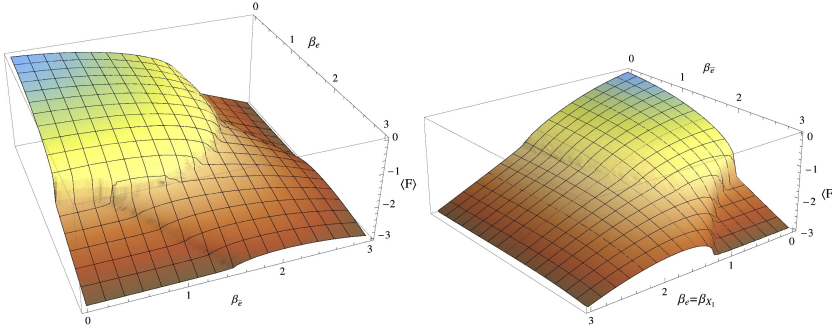


Figure 3.9: Plots of the free energy F for two-dimensional planes through the origin of the parameter space of the lattice model. In the left figure we have the $(\beta_e, \beta_{\bar{e}})$ plane and in the right figure we have the $(\beta_e = \beta_{X_1}, \beta_{\bar{e}})$ plane. See text for further comments.

plot of Figure 3.9 shows F as a function of $(\beta_e$ and $\beta_{\bar{e}})$ and all other couplings equal zero. For small values of all the couplings appearing in the action (3.35), we are in the completely confining phase of the gauge theory, where all the open string operators of magnetic flux have a non-zero expectation value, and all loop operators carrying electric charge are confined. This corresponds to the plateau in the graph where F is maximal and tends to zero.

The regions where the magnetic flux $(\bar{e}, 1)$ and (X_1, Γ^0) have condensed can be anticipated on theoretical grounds by realizing that the coupling β_A is inversely proportional to the mass of flux A . In fact, when we look at the subgroup K_A generated by the elements in conjugacy class A , in particular

$$\begin{aligned} K_{\bar{e}} &= \{\mathbb{1}, -\mathbb{1}\} \\ K_{X_1} &= \{\mathbb{1}, -\mathbb{1}, i\sigma_1, -i\sigma_1\}, \end{aligned}$$

and set the couplings for the conjugacy classes containing the elements in K_A equal to one another, there is an extra gauge invariance $U_p \rightarrow k U_p$ for an

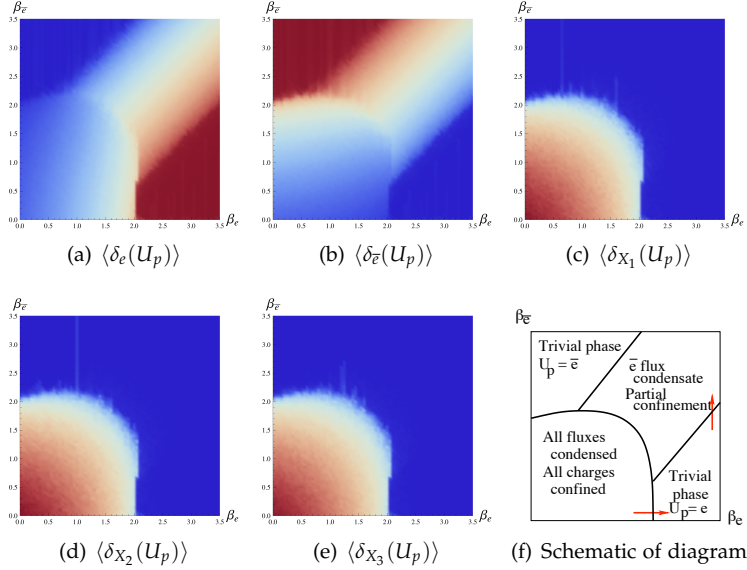


Figure 3.10: Space-time averaged expectation value of $\delta_A(U_p)$ for each conjugacy class A . Shown is a $(\beta_e, \beta_{\bar{e}})$ -plane in coupling constant space where the other three couplings are zero. The color coding is such that red is the highest and blue the lowest value in each figure. In (f) we have identified the meaning of the various regions and the transition lines, where the red arrows indicate the trajectories used to determine whether the transitions are first or second order (see Figures 3.13f and 3.14f).

element $k \in A$ in the plaquette action (3.35). In particular

$$S = \beta (\delta_e(U_p) + \delta_{\bar{e}}(U_p))$$

is invariant with respect to $U_p \rightarrow -1U_p$ and

$$S = \beta (\delta_e(U_p) + \delta_{\bar{e}}(U_p) + \delta_{X_1}(U_p))$$

is invariant with respect to $U_p \rightarrow k U_p$, where $k \in \{-1, i\sigma_1, -i\sigma_1\}$.

These left multiplications are exactly the kind appearing in the definition of the (loop) order parameters (3.29). Therefore one can establish, even without

reverting to MC measurements, that the above actions, for large values of β , produce the desired flux condensates.

One may verify this reasoning in the Figures 3.10 and 3.11 where we have probed the phase diagram more in detail by measuring the spacetime averaged expectation value of $\delta_A(U_p)$ for all conjugacy classes A as a function of the relevant coupling parameters β . The red color indicates high values for the expectation value and we see that for all coupling parameters near zero all fluxes are condensed and thus all charges will be confined. This is what traditionally is called the “strong coupling phase ($g \sim 1/\beta \gg 1$). Looking at the colorings for the various operators one readily identifies the various phases as indicated in the schematics of the subfigures (f). For example the symmetry with respect to the diagonal of the Figures 3.10a and 3.10b, shows that there are “Ising” like ordered phases, one with all plaquette values $U_p = e$ and the other with all $U_p = \bar{e}$. The in-between region is the region with the \bar{e} flux condensate. Note that if the \bar{e} flux would be the only one that phase would continue all the way to the origin, end we would exactly end up with the Z_2 pure gauge theory phase diagram.

In the region with β_e larger than approximately 2.0 and all other couplings near zero, the trivial vacuum is realized. All string operators with nontrivial magnetic flux have zero expectation value there.

There is a very direct way to determine the condensate as well as the quantum embedding index q (see (2.8)). This is by measuring the expectation value of the open string for each pure flux A and then summing over all fluxes. In the $(\bar{e}, 1)$ vacuum we obtain

$$\left\langle \left| \begin{array}{c} \uparrow \\ (e,1) \end{array} \right\rangle_{\Phi} = \left\langle \left| \begin{array}{c} \uparrow \\ (\bar{e},1) \end{array} \right\rangle_{\Phi} = 1.0,$$

so $q = 2$, whereas in the (X_1, Γ^0) vacuum

$$\left\langle \left| \begin{array}{c} \uparrow \\ (e,1) \end{array} \right\rangle_{\Phi} = \left\langle \left| \begin{array}{c} \uparrow \\ (\bar{e},1) \end{array} \right\rangle_{\Phi} = 1.0, \quad \left\langle \left| \begin{array}{c} \uparrow \\ (X_1, \Gamma^0) \end{array} \right\rangle_{\Phi} = 2.0,$$

so in this case $q = 4$. In Figure 3.12 we show the measurement of the vacuum expectation value for the $(\bar{e}, 1)$ open string as a function of the coupling constant $\beta_{\bar{e}}$, which demonstrates that such measurements clearly indicate where

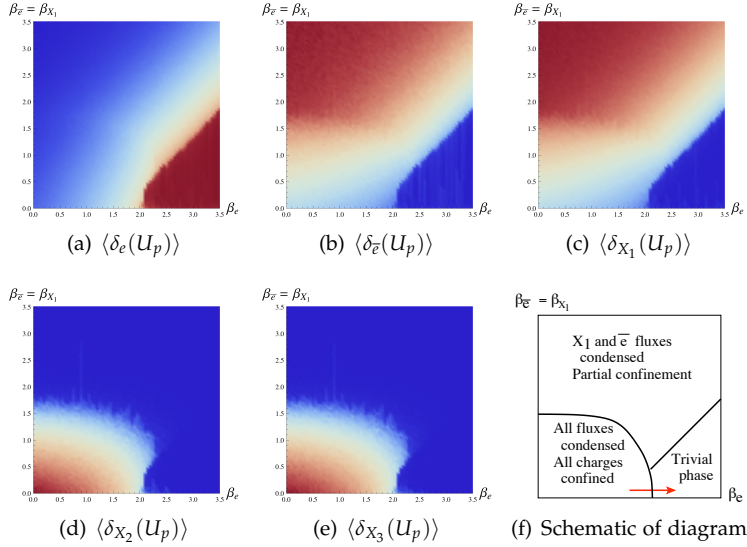


Figure 3.11: Space-time averaged expectation value of $\delta_A(U_p)$ for each conjugacy class A . Shown is a $(\beta_e, \beta_{\bar{e}} = \beta_{X_1})$ -plane in coupling constant space where the other two couplings are zero. The color coding is such that red is the highest and blue the lowest value in each figure. In (f) we have identified the meaning of the various regions and the transition lines, where the red arrow indicates the trajectory used to determine whether the transition is first or second order (see Figure 3.13f).

the transition takes place.

Order of phase transitions There is one more issue we like to address in our simulations, that is to determine the order of the transitions we have identified. A conventional approach is to search for a hysteresis effect across a first order transition (see for example [50] where this approach is used to study \mathbb{Z}_N gauge theory in 2+1d), but because of the relative modest size of the lattices used this is not an optimal approach. A method that is working much better is to directly probe the system at a given sequence of coupling constants around the transition and to see whether there is a coexistence region

where both phases occur in the sampling⁷. To perform these measurements we use the parallel tempering method [51] to overcome local minima in the action landscape. The idea behind this method is to initialize a range of lattices simultaneously, all at different couplings along a trajectory in coupling constant space starting in phase one and ending in phase two. The updates of this ensemble then consist of the updates of each of the individual lattices and, occasionally, a swap of two adjacent lattices. The swap between lattices **1** and **2** is accepted with a probability

$$p(\mathbf{1} \leftrightarrow \mathbf{2}) = \min \left\{ 1, \frac{\exp(S_1(\mathbf{1}) + S_2(\mathbf{2}))}{\exp(S_2(\mathbf{1}) + S_1(\mathbf{2}))} \right\},$$

where $S_1(\mathbf{2})$ means using the action (in particular, the set of couplings) of lattice **1** to evaluate the field configuration of lattice **2** et cetera. One can prove that this satisfies detailed balance. In effect, each lattice will perform a random walk through coupling constant space along the chosen trajectory, allowing a "cold" lattice to thermalize in the "high temperature" region, thus overcoming the local minima of the action.

We have made measurements for the trajectories indicated by the arrows in the Figures 3.10f and 3.11f. The results of these measurements for the horizontal arrow is given in Figure 3.13 and for the vertical arrow in Figure 3.14. We find that in that the horizontal trajectory the transition from the strongly coupled phase corresponding to the left peak in Figure 3.13 to the trivial phase corresponding to the right peak indeed goes through a coexistence region corresponding to the values of the coupling parameter where both peaks are present as in subfigures 3.13b and 3.13c.

The result for the vertical trajectory corresponding to the transition from the trivial phase to the broken (X_1, Γ_0) phase is given in figure 3.14, where we see that the peak shifts continuously implying that the transition is second order. We can understand this transition as follows. In this region of coupling constant space, all fluxes except the \bar{e} flux are very heavy. This means the ground state is essentially that of a \mathbb{Z}_2 gauge theory. Since \mathbb{Z}_2 gauge theory in 3 dimensions is Kramers-Wannier dual [52, 53] to the three-dimensional Ising model, it has the same phase structure [42]. We therefore expect this phase transition to lie in the same universality class.

⁷We would like to thank Simon Trebst for pointing this out to us.

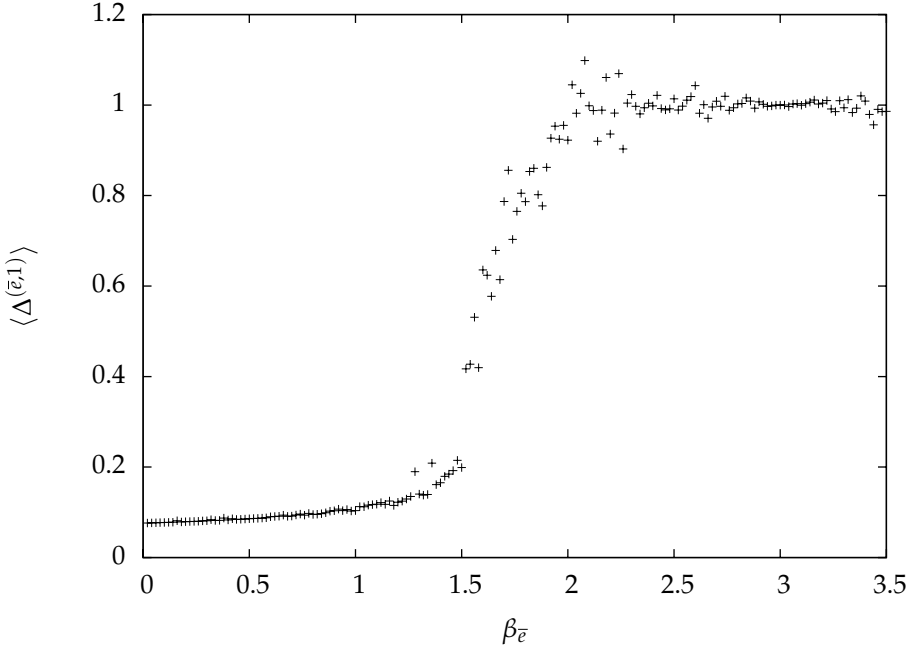


Figure 3.12: Vacuum expectation value of the $(\bar{e}, 1)$ open string as a function of the coupling constant $\beta_{\bar{e}}$, showing that the nonlocal open string operators are good order parameters to characterize topological phase transitions. Length of the string: 4 plaquettes, measurements on a 16^3 lattice, $\beta_e = 3.0$, other couplings zero.

Measuring the (broken) modular S-matrices We have measured the (broken) S-matrix elements using the simple algorithm involving the auxiliary symmetries of our loop operators. This allows us to obtain the unbroken S-matrix as well as the branching matrix $n_u^{a_1}$ and the S-matrix of the effective \mathcal{U} theory in the various broken phases. Here we exploit the relation (3.22) for the measurement, and relation (2.18) :

$$S_{uv} = \frac{1}{q} \sum_{a_i, b_j} n_u^{a_i} n_v^{b_j} \langle S_{a_i b_j} \rangle_{\Phi},$$

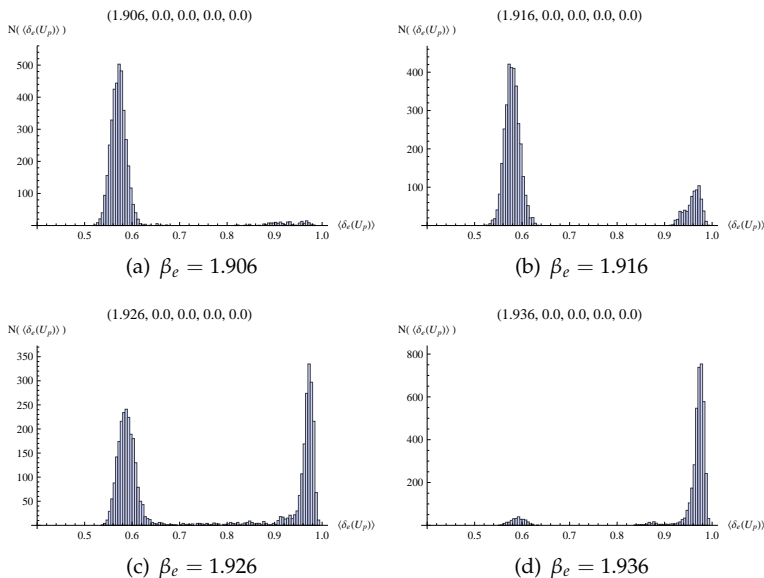


Figure 3.13: The sequence of plots is across the transition from the strongly coupled phase with all fluxes condensed and all charges confined, to the trivial phase. This trajectory corresponds to the horizontal arrow in Figures 3.10f and 3.11f, where $1.906 \leq \beta_e \leq 1.936$ and all other couplings equal zero. Plotted along the x -axis is average expectation value of the percentage of trivial plaquettes with $U_p = e$ and along the y -axis we plot the number of times that that percentage is measured in a simulation of 4000 runs on a 10^3 lattice. The figures clearly show a shift from peak on the left to on the right, with a double peak in between, this is the signature of region where both phases coexist, i.e. of a first order transition.

relating S_{uv} to the measured S -matrix in the broken phase. We first measured the unbroken S -matrix in the $D(\bar{D}_2)$ phase and obtain results identical to the matrix calculated using formula (3.22), the result is given in Table 3.2 and is of course also consistent with the matrix obtained from the relation (2.18) with $\Phi = 0$. The accuracy of the measured matrix elements in represented in the table as integers is smaller than 5%.

The branching matrices n_u^a can be obtained from measuring the broken S -

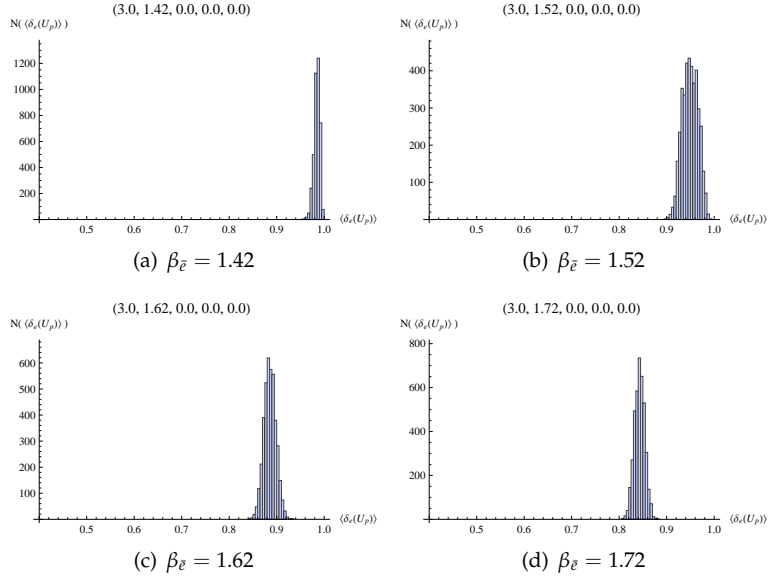


Figure 3.14: The sequence of plots is across the transition from the trivial phase to the phase with the \bar{e} condensate, the trajectory corresponds to the vertical arrow in Figure 3.10f, where $1.42 \leq \beta_{\bar{e}} \leq 1.72$, $\beta_e = 3.0$ and all other couplings equal zero. Plotted along the x-axis is average expectation value of the percentage of trivial plaquettes with $U_p = e$ and along the y-axis we plot the number of times that that percentage is measured in a simulation of 4000 runs on a 10^3 lattice. The figures only feature only a single peak that smoothly moves from one phase to the other, indicating a smooth second order transition, presumably corresponding to the 3D Ising model transition.

matrices. The columns in these matrices correspond to the different \mathcal{U} sectors. If we see two rows or columns with different parents a, b in the \mathcal{A} theory that are proportional to each other, a and b branch to the same \mathcal{U} sector u . Conversely, if different u fields correspond to the same a field that means that the a splits in the broken phase. We have listed the results for the broken S -matrix in the $(\bar{e}, 1)$ vacuum in Table 3.3.

To realize the splittings between the irreducible representations using the auxiliary gauge symmetries alluded to in section 3.3.2, we found the following

	$(e,1)$	$(e,1)$	$(e,1)$	$(e,1)$	(e,χ)	$(\bar{e},1)$	$(\bar{e},1)$	$(\bar{e},1)$	(\bar{e},χ)	(\bar{e},χ)	(X_1,Γ^0)	(X_1,Γ^1)	(X_1,Γ^2)	(X_1,Γ^3)	(X_2,Γ^0)	(X_2,Γ^1)	(X_2,Γ^2)	(X_2,Γ^3)	(X_3,Γ^0)	(X_3,Γ^1)	(X_3,Γ^2)	(X_3,Γ^3)
$(e,1)$	1	1	1	1	2	1	1	1	1	2	2	2	2	2	2	2	2	2	2	2	2	2
$(e,1)$	1	1	1	1	2	1	1	1	1	2	2	2	2	2	2	2	2	2	2	2	2	2
$(e,2)$	1	1	1	1	2	1	1	1	1	2	2	2	2	2	2	2	2	2	2	2	2	2
$(e,3)$	1	1	1	1	2	1	1	1	1	2	2	2	2	2	2	2	2	2	2	2	2	2
(e,χ)	2	2	2	2	4	-2	-2	-2	-2	4	0	0	0	0	0	0	0	0	0	0	0	0
$(\bar{e},1)$	1	1	1	1	-2	1	1	1	1	-2	2	2	2	2	2	2	2	2	2	2	2	2
$(\bar{e},1)$	1	1	1	1	-2	1	1	1	1	-2	2	2	2	2	2	2	2	2	2	2	2	2
$(\bar{e},2)$	1	1	1	1	-2	1	1	1	1	-2	2	2	2	2	2	2	2	2	2	2	2	2
$(\bar{e},3)$	1	1	1	1	-2	1	1	1	1	-2	2	2	2	2	2	2	2	2	2	2	2	2
(\bar{e},χ)	2	2	2	2	4	-2	-2	-2	-2	4	0	0	0	0	0	0	0	0	0	0	0	0
(X_1,Γ^0)	2	2	-2	-2	0	2	2	-2	-2	0	4	0	-4	0	0	0	0	0	0	0	0	0
(X_1,Γ^1)	2	2	-2	-2	0	2	2	-2	-2	0	0	4	0	4	0	0	0	0	0	0	0	0
(X_1,Γ^2)	2	2	-2	-2	0	2	2	-2	-2	0	-4	0	4	0	0	0	0	0	0	0	0	0
(X_1,Γ^3)	2	2	-2	-2	0	2	2	-2	-2	0	0	4	0	-4	0	0	0	0	0	0	0	0
(X_2,Γ^0)	2	-2	2	-2	0	2	-2	2	-2	0	0	0	0	4	0	-4	0	0	0	0	0	0
(X_2,Γ^1)	2	-2	2	-2	0	2	-2	2	-2	0	0	0	0	0	-4	0	4	0	0	0	0	0
(X_2,Γ^2)	2	-2	2	-2	0	2	-2	2	-2	0	0	0	0	-4	0	4	0	0	0	0	0	0
(X_2,Γ^3)	2	-2	2	-2	0	2	-2	2	-2	0	0	0	0	0	4	0	-4	0	0	0	0	0
(X_3,Γ^0)	2	-2	-2	2	0	2	-2	-2	2	0	0	0	0	0	0	0	0	0	4	0	-4	0
(X_3,Γ^1)	2	-2	-2	2	0	2	-2	-2	2	0	0	0	0	0	0	0	0	0	0	-4	0	4
(X_3,Γ^2)	2	-2	-2	2	0	2	-2	-2	2	0	0	0	0	0	0	0	0	0	-4	0	4	0
(X_3,Γ^3)	2	-2	-2	2	0	2	-2	-2	2	0	0	0	0	0	0	0	0	0	0	4	0	-4

Table 3.2: The S-matrix for the (unbroken) $D(\overline{D}_2)$ theory (up to the normalisation factor $1/D_A = 1/8$) as measured in the trivial vacuum. We put integers in the table as the accuracy is below the 5%, i.e. 1 actually stands for read as $1. \pm 0.05$.

construction to suffice. By the symbol \equiv we mean “is realized by inserting the operator(s)”.

$(\bar{e},1)$ vacuum

- $(X_i, \Gamma^0)_1 \equiv \Delta^{(X_i, \Gamma^0)}$.
- $(X_i, \Gamma^0)_2 \equiv \Delta^{(X_i, \Gamma^0)} \Delta^{(e, J_i)}$.
- $(X_1, \Gamma^2)_1 \equiv \Delta^{(X_1, \Gamma^2)}$ with $\{x_{i\sigma_1} = e, x_{-i\sigma_1} = i\sigma_2\}$.
- $(X_1, \Gamma^2)_2 \equiv \Delta^{(X_1, \Gamma^2)} \Delta^{(e, J_1)}$ with $\{x_{i\sigma_1} = e, x_{-i\sigma_1} = i\sigma_2\}$.
- $(X_2, \Gamma^2)_1 \equiv \Delta^{(X_2, \Gamma^2)}$ with $\{x_{i\sigma_2} = e, x_{-i\sigma_2} = i\sigma_1\}$.
- $(X_2, \Gamma^2)_2 \equiv \Delta^{(X_2, \Gamma^2)} \Delta^{(e, J_2)}$ with $\{x_{i\sigma_2} = e, x_{-i\sigma_2} = i\sigma_1\}$.
- $(X_3, \Gamma^2)_1 \equiv \Delta^{(X_3, \Gamma^2)}$ with $\{x_{i\sigma_3} = e, x_{-i\sigma_3} = i\sigma_1\}$.

	$(e,1)$	(e,J_1)	(e,J_2)	(e,J_3)	$(\bar{e},1)$	(\bar{e},J_1)	(\bar{e},J_2)	(\bar{e},J_3)	$(X_1,\Gamma^0)_1$	$(X_1,\Gamma^0)_2$	$(X_1,\Gamma^2)_1$	$(X_1,\Gamma^2)_2$	$(X_2,\Gamma^0)_1$	$(X_2,\Gamma^0)_2$	$(X_2,\Gamma^2)_1$	$(X_2,\Gamma^2)_2$	$(X_3,\Gamma^0)_1$	$(X_3,\Gamma^0)_2$	$(X_3,\Gamma^2)_1$	$(X_3,\Gamma^2)_2$
$(e,1)$	1	1	1	1	1	1	1	1	2	2	2	2	2	2	2	2	2	2	2	2
(e,J_1)	1	1	1	1	1	1	1	1	2	2	2	2	-2	-2	-2	-2	-2	-2	-2	-2
(e,J_2)	1	1	1	1	1	1	1	1	-2	-2	-2	-2	2	2	2	2	2	2	2	2
(e,J_3)	1	1	1	1	1	1	1	1	-2	-2	-2	-2	2	2	2	2	2	2	2	2
$(\bar{e},1)$	1	1	1	1	1	1	1	1	2	2	2	2	2	2	2	2	2	2	2	2
(\bar{e},J_1)	1	1	1	1	1	1	1	1	2	2	2	2	-2	-2	-2	-2	-2	-2	-2	-2
(\bar{e},J_2)	1	1	1	1	1	1	1	1	-2	-2	-2	-2	2	2	2	2	2	2	2	2
(\bar{e},J_3)	1	1	1	1	1	1	1	1	-2	-2	-2	-2	2	2	2	2	2	2	2	2
$(X_1,\Gamma^0)_1$	2	2	-2	-2	2	2	-2	-2	4	4	-4	-4	4	4	-4	-4	4	4	-4	-4
$(X_1,\Gamma^0)_2$	2	2	-2	-2	2	2	-2	-2	4	4	-4	-4	-4	-4	4	4	-4	-4	4	4
$(X_1,\Gamma^2)_1$	2	2	-2	-2	2	2	-2	-2	-4	-4	4	4	4	4	-4	-4	4	4	-4	-4
$(X_1,\Gamma^2)_2$	2	2	-2	-2	2	2	-2	-2	-4	-4	4	4	-4	-4	4	4	-4	-4	4	4
$(X_2,\Gamma^0)_1$	2	-2	2	-2	2	-2	2	-2	4	-4	4	-4	4	4	-4	-4	4	-4	4	-4
$(X_2,\Gamma^0)_2$	2	-2	2	-2	2	-2	2	-2	-4	4	-4	4	4	4	-4	-4	4	-4	4	-4
$(X_2,\Gamma^2)_1$	2	-2	2	-2	2	-2	2	-2	4	-4	4	-4	-4	-4	4	4	-4	-4	4	-4
$(X_2,\Gamma^2)_2$	2	-2	2	-2	2	-2	2	-2	-4	4	-4	4	-4	-4	4	4	-4	-4	4	-4
$(X_3,\Gamma^0)_1$	2	-2	-2	2	2	-2	-2	2	4	-4	-4	4	4	-4	-4	4	4	-4	-4	4
$(X_3,\Gamma^0)_2$	2	-2	-2	2	2	-2	-2	2	-4	4	4	-4	-4	4	4	-4	-4	4	-4	4
$(X_3,\Gamma^2)_1$	2	-2	-2	2	2	-2	-2	2	4	-4	-4	4	-4	-4	4	4	-4	-4	4	4
$(X_3,\Gamma^2)_2$	2	-2	-2	2	2	-2	-2	2	-4	4	4	-4	4	-4	-4	4	-4	-4	4	4

Table 3.3: The broken S-matrix as measured in the $(\bar{e},1)$ vacuum, where the columns and rows of zeroes corresponding to the confined fields are left out. Identifying identical columns and rows we obtain the familiar S-matrix of the $D(\mathbb{Z}_2 \otimes \mathbb{Z}_2)$ theory.

- $(X_3, \Gamma^2)_2 \equiv \Delta^{(X_3, \Gamma^2)} \Delta^{(e, J_3)}$ with $\{x_{i\sigma_3} = e, x_{-i\sigma_3} = i\sigma_1\}$.

(X_1, Γ^0) vacuum

- $(X_i, \Gamma^0)_1 \equiv \Delta^{(X_i, \Gamma^0)}$.
- $(X_1, \Gamma^0)_2 \equiv \Delta^{(X_1, \Gamma^0)} \Delta^{(e, J_1)}$.
- $(X_2, \Gamma^2)_1 \equiv \Delta^{(X_2, \Gamma^2)}$ with $\{x_{i\sigma_2} = e, x_{-i\sigma_2} = i\sigma_1\}$.
- $(X_3, \Gamma^2)_1 \equiv \Delta^{(X_3, \Gamma^2)}$ with $\{x_{i\sigma_3} = e, x_{-i\sigma_3} = i\sigma_1\}$.

We see that in Table 3.3 the columns (rows) for the sectors (e, α) and (\bar{e}, α) for $\alpha = 1, J_1, J_2, J_3$ are identical and thus that the corresponding fields have to be identified. This leaves us with 16 sectors for the broken \mathcal{U} theory. Summing the entries as prescribed by formula (3.5.2) yields exactly the S-matrix of the $D(\mathbb{Z}_2 \otimes \mathbb{Z}_2)$ theory, which is given in Table 3.4.

In Table 3.5 we have listed the result for broken S-matrix in the (X_1, Γ^0) vacuum. here we have to identify the sectors $(e, 1)$, $(\bar{e}, 1)$ and $(X_1, \Gamma^0)_1$, the

\mathcal{U}	$D(\mathbb{Z}_2 \otimes \mathbb{Z}_2)$	$(\bar{e}, 1)$	(e, J_1)	(\bar{e}, J_2)	(e, J_3)	$(X_1, \Gamma^0)_1$	$(X_1, \Gamma^0)_2$	$(X_1, \Gamma^2)_1$	$(X_1, \Gamma^2)_2$	$(X_2, \Gamma^0)_1$	$(X_2, \Gamma^0)_2$	$(X_2, \Gamma^2)_1$	$(X_2, \Gamma^2)_2$	$(X_3, \Gamma^0)_1$	$(X_3, \Gamma^0)_2$	$(X_3, \Gamma^2)_1$	$(X_3, \Gamma^2)_2$
$(e, 1)$	$(+, +, +)$	1	1	1	1	1	1	1	1	1	1	1	1	1	1	1	1
(e, J_1)	$(+, +, -)$	1	1	1	1	1	1	1	1	-1	-1	-1	-1	-1	-1	-1	-1
(e, J_2)	$(+, -, +)$	1	1	1	1	-1	-1	-1	-1	1	1	1	1	-1	-1	-1	-1
(e, J_3)	$(+, -, -)$	1	1	1	1	-1	-1	-1	-1	-1	-1	-1	-1	1	1	1	1
$(X_1, \Gamma^0)_1$	$(-, +, +)$	1	1	-1	-1	1	1	-1	-1	1	-1	1	-1	1	-1	1	-1
$(X_1, \Gamma^0)_2$	$(-, +, -)$	1	1	-1	-1	1	1	-1	-1	-1	-1	-1	-1	1	1	-1	-1
$(X_1, \Gamma^2)_1$	$(-, -, +)$	1	1	-1	-1	-1	-1	1	1	1	-1	1	-1	-1	1	-1	1
$(X_1, \Gamma^2)_2$	$(-, -, -)$	1	1	-1	-1	-1	-1	1	1	-1	1	-1	-1	1	-1	1	-1
$(X_2, \Gamma^0)_1$	$(+, -, +)$	1	-1	1	-1	1	-1	1	-1	1	1	-1	-1	-1	-1	-1	1
$(X_2, \Gamma^0)_2$	$(+, -, -)$	1	-1	1	-1	-1	1	-1	1	1	1	-1	-1	-1	-1	1	-1
$(X_2, \Gamma^2)_1$	$(+, +, +)$	1	-1	1	-1	1	-1	1	-1	-1	-1	1	1	-1	1	-1	-1
$(X_2, \Gamma^2)_2$	$(+, +, -)$	1	-1	1	-1	-1	1	-1	-1	-1	-1	1	1	-1	1	-1	-1
$(X_3, \Gamma^0)_1$	$(-, -, +)$	1	-1	-1	1	1	-1	-1	1	1	-1	1	-1	1	1	-1	-1
$(X_3, \Gamma^0)_2$	$(-, -, -)$	1	-1	-1	1	-1	1	-1	-1	1	1	-1	1	-1	1	-1	-1
$(X_3, \Gamma^2)_1$	$(-, +, +)$	1	-1	-1	1	1	-1	-1	1	-1	1	1	-1	-1	-1	1	1
$(X_3, \Gamma^2)_2$	$(-, +, -)$	1	-1	-1	1	-1	1	-1	-1	-1	-1	1	1	-1	-1	1	1

Table 3.4: The S -matrix of the $\mathcal{U} = D(\mathbb{Z}_2 \otimes \mathbb{Z}_2)$ theory (up to normalisation factor of $1/D_{\mathcal{U}} = 1/4$) as obtained from the broken S -matrix measured in the $(\bar{e}, 1)$ vacuum, after leaving out the rows and columns with only zeroes of the confined fields and after identifying identical rows and columns.

sectors (e, J_1) , (\bar{e}, J_1) and $(X_1, \Gamma^0)_2$, the sectors $(X_2, \Gamma^0)_1$ and $(X_3, \Gamma^0)_1$, and the sectors $(X_2, \Gamma^2)_1$ and $(X_3, \Gamma^2)_1$. These results are all fully consistent with the algebraic analysis presented in Section 3.4.

Let us illustrate the method by calculating a few sample S -matrix elements in the (X_1, Γ^0) condensed vacuum. The \mathcal{U} theory should be $D(\mathbb{Z}_2)$; let us first calculate the $S_{(+,+)(+,+)}$ element, the $(+, +)$ sector being the new vacuum

$$\begin{aligned}
S_{(+,+)(+,+)} &= \frac{1}{q} \left\{ \left\langle S_{(e,1)(e,1)} \right\rangle_{\Phi} + \left\langle S_{(e,1)(\bar{e},1)} \right\rangle_{\Phi} + \left\langle S_{(e,1)(X_1, \Gamma^0)} \right\rangle_{\Phi} + \right. \\
&\quad \left. \left\langle S_{(\bar{e},1)(e,1)} \right\rangle_{\Phi} + \left\langle S_{(\bar{e},1)(\bar{e},1)} \right\rangle_{\Phi} + \left\langle S_{(\bar{e},1)(X_1, \Gamma^0)} \right\rangle_{\Phi} + \right. \\
&\quad \left. \left\langle S_{(X_1, \Gamma^0)(e,1)} \right\rangle_{\Phi} + \left\langle S_{(X_1, \Gamma^0)(\bar{e},1)} \right\rangle_{\Phi} + \left\langle S_{(X_1, \Gamma^0)(X_1, \Gamma^0)} \right\rangle_{\Phi} \right\} = \\
&\quad \frac{1}{4} \frac{1}{8} (1 + 1 + 2 + 1 + 1 + 2 + 2 + 2 + 4) = \frac{1}{2},
\end{aligned}$$

in agreement with Table 3.6. The contributions to the above matrix element would be equal if we had used the S -matrix elements as measured in the trivial vacuum.

To appreciate the importance of the measurements in the broken vacuum,

	$(e,1)$	$(e,1)$	$(\bar{e},1)$	$(\bar{e},1)$	$(X_1,\Gamma^0)_1$	$(X_1,\Gamma^0)_2$	$(X_2,\Gamma^0)_1$	$(X_2,\Gamma^2)_1$	$(X_3,\Gamma^0)_1$	$(X_3,\Gamma^2)_1$
$(e,1)$	1	1	1	1	2	2	2	2	2	2
$(e,1)$	1	1	1	1	2	2	-2	-2	-2	-2
$(\bar{e},1)$	1	1	1	1	2	2	2	2	2	2
$(\bar{e},1)$	1	1	1	1	2	2	-2	-2	-2	-2
$(X_1,\Gamma^0)_1$	2	2	2	2	4	4	4	4	4	4
$(X_1,\Gamma^0)_2$	2	2	2	2	4	4	-4	-4	-4	-4
$(X_2,\Gamma^0)_1$	2	-2	2	-2	4	-4	4	-4	4	-4
$(X_2,\Gamma^2)_1$	2	-2	2	-2	4	-4	-4	4	-4	4
$(X_3,\Gamma^0)_1$	2	-2	2	-2	4	-4	4	-4	4	-4
$(X_3,\Gamma^2)_1$	2	-2	2	-2	4	-4	-4	4	-4	4

Table 3.5: The broken S -matrix for the $D(\overline{D}_2)$ theory as measured in the (X_1,Γ^0) vacuum.

U	$D(\mathbb{Z}_2)$	$(e,1)$	$(e,1)$	$(X_2,\Gamma^0)_1$	$(X_2,\Gamma^2)_1$
$(e,1)$	$(+,+)$	1	1	1	1
$(e,1)$	$(+,-)$	1	1	-1	-1
$(X_2,\Gamma^0)_1$	$(-,+)$	1	-1	1	-1
$(X_2,\Gamma^2)_1$	$(-,-)$	1	-1	-1	1

Table 3.6: The modular S -matrix for the $D(\mathbb{Z}_2)$ theory (up to normalisation factor $1/D_U = 1/2$)

consider the matrix element $S_{(-,+)(-,-)}$. The parents of the $(-,+)$ sector are $(X_2,\Gamma^0)_1$ and $(X_3,\Gamma^0)_1$ and those of the $(-,-)$ are $(X_2,\Gamma^2)_1$ and $(X_3,\Gamma^2)_1$.

$$\begin{aligned}
S_{(-,+)(-,-)} &= \frac{1}{q} \left\{ \left\langle S_{(X_2,\Gamma^0)_1(X_2,\Gamma^2)_1} \right\rangle_{\Phi} + \left\langle S_{(X_2,\Gamma^0)_1(X_3,\Gamma^2)_1} \right\rangle_{\Phi} + \right. \\
&\quad \left. \left\langle S_{(X_3,\Gamma^0)_1(X_2,\Gamma^2)_1} \right\rangle_{\Phi} + \left\langle S_{(X_3,\Gamma^0)_1(X_3,\Gamma^2)_1} \right\rangle_{\Phi} \right\} = \\
&\quad \frac{1}{4} \frac{1}{8} ((-4) + (-4) + (-4) + (-4)) = -\frac{1}{2},
\end{aligned}$$

We see that after completing the calculation along this line we obtain the S -matrix of the $D(\mathbb{Z}_2)$ theory, as given in Table 3.6. Note that if we had used the S -matrix of the unbroken theory, the $S_{(X_2,\Gamma^0)(X_3,\Gamma^2)}$ and $S_{(X_3,\Gamma^0)(X_2,\Gamma^2)}$ would have been zero.

3.6 Summary

- We have defined gauge invariant actions for DGTs on a spacetime lattice featuring coupling constants that lead to a rich phase diagram. By tuning these coupling constants one can realize the different magnetic flux condensates contained in the theory.
- We have established the order of various phase transitions in the theory, demonstrating the strength of the Euclidean approach combined with Monte Carlo techniques.
- We have defined gauge invariant operators that are in one-to-one correspondence with the different particle sectors in a DGT. We have shown that they can be measured by Monte Carlo simulations.
- We have shown that by measuring a Hopf link of two loop operators in the vacuum without Bose condensation one recovers the modular S -matrix of the DGT. Measurement of the same object in symmetry broken vacua returns the “broken S -matrix”, which contains a contribution of the “vacuum exchange diagram”. This broken S -matrix can be used to reconstruct the S -matrix of the effective theory in the symmetry broken vacuum.
- This program is performed in full for the DGT based on the group D_2 .

3.7 Fusion rules for $D(\overline{D}_2)$ DGT

$$\begin{aligned}
(e, J_i) \times (e, J_i) &= (e, 1) \\
(e, J_i) \times (e, J_j) &= (e, J_k) \\
(e, J_i) \times (e, \chi) &= (e, \chi) \\
(e, \chi) \times (e, \chi) &= (e, 1) + \sum (e, J_i) \\
(\bar{e}, 1) \times (e, J_i) &= (\bar{e}, J_i) \\
(\bar{e}, 1) \times (e, \chi) &= (\bar{e}, \chi) \\
(e, J_i) \times (X_i, \Gamma^{0,2}) &= (X_i, \Gamma^{0,2}) \\
(e, J_i) \times (X_j, \Gamma^{0,2}) &= (X_j, \Gamma^{2,0}) \\
(e, \chi) \times (X_i, \Gamma^0) &= (X_i, \Gamma^1) + (X_i, \Gamma^3) \\
(\bar{e}, 1) \times (\bar{e}, 1) &= (e, 1) \\
(\bar{e}, 1) \times (X_i, \Gamma^{0,2}) &= (X_i, \Gamma^{0,2}) \\
(\bar{e}, 1) \times (X_i, \Gamma^{1,3}) &= (X_i, \Gamma^{3,1}) \\
(e, J_i) \times (X_i, \Gamma^{1,3}) &= (X_i, \Gamma^{1,3}) \\
(e, J_i) \times (X_j, \Gamma^{1,3}) &= (X_j, \Gamma^{3,1}) \\
(e, \chi) \times (X_i, \Gamma^{1,3}) &= (X_i, \Gamma^0) + (X_i, \Gamma^2) \\
(X_i, \Gamma^{0,2}) \times (X_i, \Gamma^{0,2}) &= (e, 1) + (\bar{e}, 1) + (e, J_i) + (\bar{e}, J_i) \\
(X_i, \Gamma^0) \times (X_i, \Gamma^2) &= (e, J_j) + (\bar{e}, J_j) + (e, J_k) + (\bar{e}, J_k) \\
(X_i, \Gamma^{0,2}) \times (X_j, \Gamma^{0,2}) &= (X_i, \Gamma^{2,0}) \times (X_j, \Gamma^{0,2}) = (X_k, \Gamma^0) + (X_k, \Gamma^2) \\
(X_i, \Gamma^{0,2}) \times (X_i, \Gamma^{1,3}) &= (X_i, \Gamma^{2,0}) \times (X_i, \Gamma^{1,3}) = (e, \chi) + (\bar{e}, \chi) \\
(X_i, \Gamma^{0,2}) \times (X_j, \Gamma^{1,3}) &= (X_i, \Gamma^{2,0}) \times (X_j, \Gamma^{1,3}) = (X_k, \Gamma^1) + (X_k, \Gamma^3) \\
(X_i, \Gamma^{1,3}) \times (X_i, \Gamma^{1,3}) &= (e, 1) + (e, J_i) + (\bar{e}, J_j) + (\bar{e}, J_k) \\
(X_i, \Gamma^1) \times (X_i, \Gamma^3) &= (\bar{e}, 1) + (\bar{e}, J_i) + (e, J_j) + (e, J_k) \\
(X_i, \Gamma^{1,3}) \times (X_j, \Gamma^{1,3}) &= (X_i, \Gamma^{3,1}) \times (X_j, \Gamma^{1,3}) = (X_k, \Gamma^0) + (X_k, \Gamma^2)
\end{aligned}$$

CHAPTER 4

The quantum Hall effect and spin textures

This chapter is based on the following publications:

- J. C. ROMERS, L. HUIJSE, AND K. SCHOUTENS. Charged spin textures over the Moore-Read quantum Hall state. *New Journal of Physics*, 13(4):045013, 2011, arXiv:1010.0897 [cond-mat]
- J. C. ROMERS AND K. SCHOUTENS. Spin texture readout of a Moore-Read topological quantum register. *Phys. Rev. Lett.*, 2012, arXiv:1111.6032 [cond-mat]

4.1 Quantum Hall physics

4.1.1 Integer quantum Hall effect

We now turn to another example of topological order, the quantum Hall state of matter. In 1980, Von Klitzing experimentally discovered the quantum Hall

effect (qHe) [56]. The classical Hall effect, *i.e.* the fact that a 2DEG in a magnetic field conducts current in a direction perpendicular to the applied voltage, was found to have a quantized relative that appeared in the regime of very strong magnetic fields.

In this regime, the longitudinal and Hall (transverse) conductance as functions of the magnetic field show very special behaviour: the Hall conductance develops plateaus centred around particular values of the magnetic field, whereas the longitudinal conductance vanishes only to reappear at the edge of a plateau. In terms of the *filling fraction* ν of the 2DEG

$$\nu = \frac{N}{N_\phi},$$

where N is the number of electrons in the sample and N_ϕ the number of magnetic flux quanta, the Hall conductivity σ_{xy} was found to be quantized as

$$\sigma_{xy} = \nu \frac{e^2}{h},$$

where e is the electron charge and h is Planck's constant.

It turns out that to describe the systems with ν an integer (the integer qH effect, as opposed to ν a fraction, the fractional qH effect) one can ignore electron-electron interactions and maintain a single particle picture¹. The one-particle eigenstates of the Hamiltonian for a free electron on the plane in a uniform perpendicular magnetic field

$$H = \frac{1}{2m} \left(\mathbf{p} - \frac{e}{c} \mathbf{A} \right)^2, \quad (4.1)$$

in the symmetric gauge

$$\mathbf{A}(\mathbf{r}) = \frac{1}{2} \mathbf{B} \times \mathbf{r},$$

¹The presence of disorder is important though. One can prove (see for example the excellent lecture notes by Girvin [13]) that if translational symmetry is unbroken the Hall conductivity is just a linear function of the magnetic field. In order for plateaus to develop, one needs disorder to break translational symmetry.

are, in the lowest Landau level (LLL), given by

$$\psi_l(z) = z^l e^{-\frac{|z|^2}{4\ell_B}}. \quad (4.2)$$

where $\ell_B = \sqrt{\frac{\hbar c}{eB}}$ is the magnetic length, $z = x + iy$ and $l = 0, \dots, N_\phi$. All these states are degenerate in the single-particle picture and the value of l determines the angular momentum of the state. With these notations in place, the multiparticle wave function for one completely filled Landau level ($\nu = 1$) becomes a Slater determinant

$$\Psi_{\text{iqH}}(z_1, \dots, z_N) = \begin{vmatrix} \psi_0(z_1) & \psi_1(z_1) & \dots & \psi_{N_\phi}(z_1) \\ \psi_0(z_2) & \psi_1(z_2) & \dots & \psi_{N_\phi}(z_2) \\ \vdots & & & \vdots \\ \psi_0(z_N) & \psi_1(z_N) & \dots & \psi_{N_\phi}(z_N) \end{vmatrix},$$

which is a Vandermonde determinant and can be written as

$$\Psi_{\text{iqH}}(z_1, \dots, z_N) = \prod_{i < j} (z_i - z_j) e^{-\frac{\sum_k |z_k|^2}{4\ell_B}}. \quad (4.3)$$

The exponential part of these expressions depends on the geometry of the system under consideration (*i.e.* whether the electrons live on the sphere, the plane *et cetera*), whereas the polynomial part is universal. In what follows we will only be interested in the polynomial part of such wave functions and we will drop the geometry-dependent exponential.

4.1.2 Fractional quantum Hall effect and the CFT connection

In 1982, Tsui et. al. experimentally observed the existence of stable plateaus located at fractional Landau level fillings [57]. Very soon after that, Laughlin [58] proposed a family of wave functions for the plateaus at filling fractions $\nu = \frac{1}{2m+1}$,

$$\Psi_L^{\nu=1/(2m+1)} = \prod_{i < j} (z_i - z_j)^{2m+1}. \quad (4.4)$$

This equation was arrived at by imposing three demands on the wave function:

- The wave function is of a Jastrow form $\prod_{i<j} f(z_i - z_j)$, and odd under interchange of two coordinates since the coordinates describe fermions,
- The multi particle wave function is a sum of products of single particle eigenfunctions (4.2) of the Hamiltonian 4.1,
- It is an eigenstate of total angular momentum, therefore the polynomial is homogeneous.

Moore and Read [59] realized one could obtain the Laughlin wave functions from a Conformal Field Theory (CFT) construction. On a deep level, this is due to the fact that effective field theory of the bulk of a quantum Hall liquid is described by a Chern-Simons (CS) theory and the existence of a bulk-boundary correspondence between CS theory and CFT [7].

For the $\nu = 1/3$ Laughlin state, let us see how this construction works. It turns out the CFT doing the job for the Laughlin states is the compactified boson. We define electron vertex operators²

$$V_{\text{el}}(z) = e^{i\sqrt{3}\varphi}(z),$$

such that the Operator Product Expansion (OPE) of two electron operators satisfies

$$V_{\text{el}}(z_i)V_{\text{el}}(z_j) = (z_i - z_j)^3 e^{i2\sqrt{3}\varphi}(z_j).$$

An N -particle Laughlin wave function is then obtained by calculating the correlator

$$\langle V_{\text{el}}(z_1)V_{\text{el}}(z_2)\dots V_{\text{el}}(z_N)V_{\text{bg}} \rangle, \quad (4.5)$$

where V_{bg} is an operator inserting background electric charge³ such that the correlator is charge neutral. The electric charge can be measured with the operator

$$Q_{\text{el}} = \frac{1}{i\sqrt{3}} \frac{\partial}{\partial \varphi},$$

which is normalized such that the electron operator has charge 1.

²All exponents of operators are implicitly normal ordered, meaning we put all creation operators to the left of the annihilation operators.

³This is a subtle point. Mathematically it is easiest to insert the background compensating charge at infinity, but if one smears the charge evenly over the whole system, the geometrical exponential factor is recovered.

Quasihole operators appear quite naturally in the present setting. Quasiholes should not “feel” the electron liquid in their background, *i.e.* they should have trivial braiding with the electrons. Mathematically, this translates into the absence of branch cuts between electrons and quasiholes. The vertex operator having the lowest *integer* degree OPE with an electron operator is clearly

$$V_{\text{qh}}(w) = e^{i\varphi/\sqrt{3}}(w),$$

which has Q_{el} eigenvalue $\frac{1}{3}$ and OPE

$$V_{\text{qh}}(w_i)V_{\text{qh}}(w_j) = (w_i - w_j)^{\frac{1}{3}}e^{i2\varphi/\sqrt{3}}(w_j),$$

which establishes the fractional statistics: adiabatically transporting one quasihole around another gives a phase factor of $e^{2\pi i/3}$.

4.1.3 Paired quantum Hall states and the colorful construction

In the previous section we have seen that vertex operators of the compact boson CFT generate wave functions of quantum Hall liquids. This is an appealing picture, since it is a unified description in the sense that one can write down operators for both electronic coordinates and quasihole coordinates. However, if we insist on antisymmetry in the electronic coordinates⁴, this construction can only generate wave functions having odd filling fraction $1/(2m + 1)$.

Since plateaus at other filling fractions have been observed experimentally, clearly this is not the whole story. Many proposals for wave functions describing a wider range of filling fractions have been made throughout time, such as a hierarchy picture [63], a composite fermion picture [64] and taking particle-hole conjugates⁵ of certain wave functions [68]. Another route is to

⁴Electrons are fermions, so the multiparticle wave function should be antisymmetric with respect to permutations of the electronic coordinates. Later on, we will often use bosonic variants of such wave functions, for they are easier to study mathematically; the difference is an overall Vandermonde factor. Bosonic quantum Hall wave functions are however also physically relevant: rapidly rotating Bose gases are conjectured to form a quantum Hall liquid at very high rotational frequencies [60, 61, 62].

⁵Since particle-hole conjugacy takes the filling fraction from ν to $1 - \nu$, clearly something of interest is going on at $\nu = \frac{1}{2}$. The consequences of this have been studied [65, 66] and numerical studies [67] have concluded the particle-hole conjugate of the Pfaffian is a more likely candidate

take the CFT picture seriously and construct wave functions by tensoring the compact boson CFT with some other CFT, which is what we will do now.

We want our construction to have the following properties: (i) electron operators should not have branch cuts in their OPEs, and the final wave function should be antisymmetric in the electronic coordinates; (ii) electron operators and quasihole operators should be local with respect to each other: quasiholes should not “feel” the electronic condensate; (iii) the multiparticle wave function should describe a *incompressible* quantum liquid. These requirements constrain the set of CFTs that one might consider. The third requirement, incompressibility, is subject to a lot of debate. It has been suggested that only unitary CFTs can generate incompressible states [69], although non-unitary CFTs have also been studied extensively [70]. Only very recently has a proof been found that the Ising CFT indeed generates an incompressible state [71], by generalizing the plasma analogy that exists for the Laughlin states [72].

Ising CFT The particular CFT of interest here is the Ising CFT, which also describes the Ising model at its phase transition between ordered and disordered phases. The chiral part of this CFT contains three primary fields

$$\mathbb{1}, h_{\mathbb{1}} = 0; \quad \sigma, h_{\sigma} = \frac{1}{16}; \quad \psi, h_{\psi} = \frac{1}{2},$$

where we denote the conformal dimension of the field α by h_{α} . The OPEs of these fields are

$$\begin{aligned} \psi(z_1) \psi(z_2) &= \frac{\mathbb{1}}{z_1 - z_2}, \\ \psi(z_1) \sigma(z_2) &= \frac{\sigma}{(z_1 - z_2)^{1/2}}, \\ \sigma(z_1) \sigma(z_2) &= \frac{\mathbb{1}}{(z_1 - z_2)^{1/8}} + \psi(z_1 - z_2)^{3/8}. \end{aligned} \tag{4.6}$$

The third of these OPEs immediately suggests something new is going on here: the fusion of two σ fields has two possible outcomes. In what follows, we will dress a compact boson operator with an Ising field to write down operators for electrons and quasi holes. In particular, the electron will be augmented with a ψ field, whereas the quasihole carries a σ . The wave function

than the Pfaffian for the state at $\nu = \frac{5}{2}$.

of a state containing multiple quasiholes therefore lives in a multidimensional Hilbert space, and the particular vector in this space depends on the fusion outcome of each pair of quasiholes.

The electron operator carrying a ψ field having the lowest degree OPE with another electron operator while maintaining mutual locality and antisymmetry and the simplest quasihole operator local with respect to the electron operator

$$V_{\text{el}}(z) = \psi e^{i\sqrt{2}\varphi}(z), \quad V_{\text{qh}}(w) = \sigma e^{i\varphi/\sqrt{2}}(w), \quad (4.7)$$

constitute the building blocks of the MR state. If we define the charge of the electron to be one unit, the operator measuring the charge has to be

$$Q_{\text{el}} = \frac{1}{i\sqrt{2}} \frac{\partial}{\partial \varphi},$$

which establishes the charge of the fundamental quasihole as one quarter of an electron.

Moore-Read wave function Inserting the electron operators (4.7) into a correlator (4.5) gives a quantum Hall ground state

$$\Psi_{\text{MR}}^{\nu=1/2} = \prod_{i < j} (z_i - z_j)^2 \text{Pf} \left[\frac{1}{z_i - z_j} \right], \quad (4.8)$$

where the Pfaffian is the antisymmetrized product of pairs of coordinates. Counting powers, it is straightforward to see that this state has filling fraction $\nu = \frac{1}{2}$. Something remarkable has happened here compared to the Laughlin states (4.4). Since the addition of one flux quantum always changes the electric charge in the system by $\Delta Q = \nu e$, and the electric charge of the fundamental quasihole in the MR state is $e/4$, the addition of one flux allows for two *separated* quasiholes each carrying half a flux quantum.

Idealized Hamiltonians Numerical studies of the 2D Coulomb Hamiltonian in a magnetic field (the original article by Laughlin [58] already contained a numerical analysis of the overlap of the wave function now bearing his name with the ground state of a Coulomb Hamiltonian) have provided us with ample evidence that the wave functions above are ground states for certain filling fractions in systems with realistic interactions. However, these Hamiltonians

are complicated and messy and their study is well out of reach of analytical methods. More insight can be obtained by studying idealized model Hamiltonians (or, equivalently, the clustering properties of the wave functions) that capture the essence of the states under consideration while staying analytically tractable.

We start out by considering *bosonic* quantum Hall wave functions. Since all these LLL wave functions are analytic polynomials, one can go from an antisymmetric to a symmetric wave function by dividing out a Vandermonde factor $\prod_{i<j}(z_i - z_j)$. Note that this changes the filling fraction: the bosonic brother of the Laughlin state (4.4) with exponent 3, has exponent 2 and filling $\nu = \frac{1}{2}$ and the bosonic variant of the Moore-Read state (4.8) has filling $\nu = 1$. The bosonic Laughlin state

$$\Psi_L^{\nu=1/2} = \prod_{i<j}(z_i - z_j)^2 \quad (4.9)$$

is the densest zero-energy eigenstate of the Hamiltonian

$$H_L = \sum_{i<j} \delta(z_i - z_j).$$

Similarly, the bosonic Moore-Read state

$$\Psi_{MR}^{\nu=1} = \prod_{i<j}(z_i - z_j) \text{Pf} \left[\frac{1}{z_i - z_j} \right] \quad (4.10)$$

is the densest zero-energy eigenstate of the pairing Hamiltonian

$$H_{\text{pair}} = \sum_{i<j<k} \delta(z_i - z_j) \delta(z_j - z_k), \quad (4.11)$$

which is saying that the wave function should not vanish when two coordinates are put equal whereas it should be identically zero when a third is set to the same value.

Eq. (4.10) can be cast in another form [73] that is especially suited for our purposes and is based on the clustering properties captured in the Hamiltonian (4.11). We start by dividing the coordinates into two groups

$$I = \{z_1, \dots, z_{N/2}\}, \quad II = \{z_{N/2+1}, \dots, z_N\},$$

and write down the following expression

$$\Psi_{\text{MR}}(z_1, \dots, z_N) = \text{Symm}_{I, II} \left[\Psi_{L, I}^{\nu=1/2} \Psi_{L, II}^{\nu=1/2} \right], \quad (4.12)$$

with a bosonic Laughlin wave function at $\nu = 1/2$, Eq. (4.9), for each group separately.

The symmetrization step in (4.12) is performed over all possible partitions of the particles into the groups I and II . The equivalence of (4.10) and (4.12) can be understood by arguing that both are densest zero-energy eigenstates of the Hamiltonian (4.11), that this densest zero-energy eigenstate is unique and that therefore the two wave functions are equal (see [74] for details).

Originally however [73], the equivalence was found using a bosonization of the $Ising \otimes Ising$ CFT; we explain how this works because we require this formulation to calculate the wave function of a state with many fused quasi-holes.

Bosonization The bosonization of the $Ising \otimes Ising$ CFT establishes a mapping between the field content of two independent copies of the $c = 1/2$ $Ising$ CFT and a $c = 1$ compactified boson, as shown below.

$Ising$	\otimes	$Ising$	\leftrightarrow	$c = 1$ boson
1	\otimes	1		1
ψ	\otimes	1		$\frac{1}{\sqrt{2}}(e^{i\varphi} + e^{-i\varphi})$
1	\otimes	ψ		$\frac{1}{i\sqrt{2}}(e^{i\varphi} - e^{-i\varphi})$
σ	\otimes	σ		$\frac{1}{\sqrt{2}}(e^{i\varphi/2} + e^{-i\varphi/2})$

Let us check how this formulation gives the bosonic MR ground state wave function (4.10). Up to an overall Vandermonde factor $\prod_{i < j} (z_j - z_i)$, the bosonized CFT correlator is the one containing an even number of ψ fields, one at each of the electron coordinates. In the bosonized description

$$\langle (e^{i\varphi} + e^{-i\varphi})(z_1) \dots (e^{i\varphi} + e^{-i\varphi})(z_N) \rangle, \quad (4.13)$$

only terms in which the number of factors of $e^{i\varphi}$ and $e^{-i\varphi}$ are equal contribute. We therefore select $N/2$ coordinates $I = \{z_1, \dots, z_{N/2}\}$ for which we take

the positive exponential and take the negative exponential for the other half $II = \{z_{N/2+1}, \dots, z_N\}$. This gives a contribution

$$\prod_{i < j \in I} (z_i - z_j) \prod_{k < l \in II} (z_k - z_l) \prod_{m \in I, n \in II} (z_m - z_n)^{-1}.$$

Combining this with the overall Vandermonde factor and summing over all permutations of the particle coordinates, since the partition into groups I and II was completely arbitrary, we obtain the wave function (4.12).

4.2 Charged Spin Textures in quantum Hall systems

4.2.1 Skyrmions in the integer quantum Hall effect

Experiments have confirmed that the lowest energy excitations in $\nu = 1$ integer quantum Hall (iqH) systems are charged spin textures. Let us see how they arise and how their presence is shown experimentally.

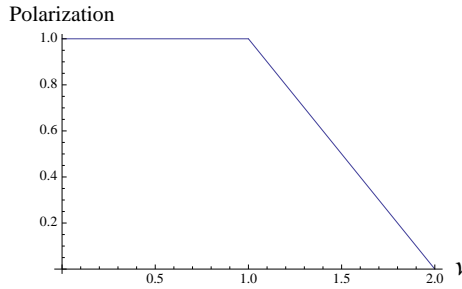


Figure 4.1: Polarization around $\nu = 1$ in the non-interacting picture.

Filling Landau levels near $\nu = 1$ Exactly at filling fraction $\nu = 1$, the lowest Landau level for electrons having their spin aligned with the magnetic field (we will call this spin up) is completely filled. Now suppose we want to move away from $\nu = 1$, in the direction of increased density. Let us start by adding

a single electron to the system. Clearly there are no states available for this electron in the LLL for up-electrons. Where will it go?

Two energy scales play a role in this problem if we neglect the electron-electron interactions, which we will do for now. In typical GaAs samples, the value of the single particle Zeeman splitting is a lot smaller than the Landau level splitting. This means that in our naive non-interacting picture, the electron will prefer to flip its spin antiparallel to the magnetic field, rather than stay aligned with it and jump to the next Landau level. One can repeat this logic all the way down to $\nu = 2$, where the LLL for both spin species is filled, leaving no net polarization.

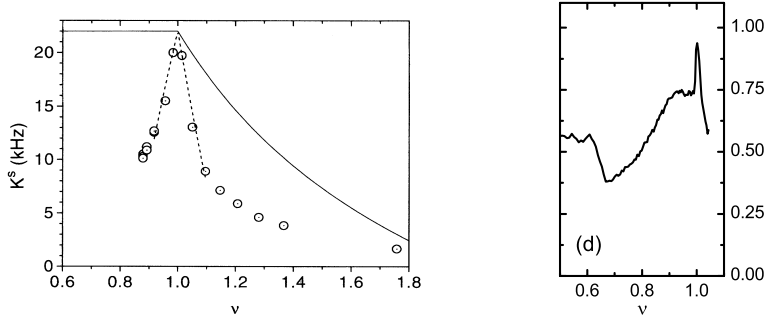
Decreasing the electron density below $\nu = 1$ amounts to removing spin-up electrons from the LLL, which does not change the polarization. A cartoon illustrating the above is given in Figure 4.1.

Skyrmions, failure of the single particle picture In Figure 4.2 results from two different experiments in which the polarization as a function of the filling fraction around $\nu = 1$ was measured is presented. Both the Nuclear Magnetic Resonance (NMR) and optical experiments agree with the picture that exactly at $\nu = 1$, the iqH system is (nearly) fully polarized. However, as one deviates slightly from filling fraction 1 the polarization drops very rapidly, much more quickly than the single particle picture illustrated in Figure 4.1 would predict. The slope of this drop is proportional to the amount of flipped spins and agrees with Hartree-Fock calculations [77, 78] that presume the formation of skyrmions. One also expects the size of skyrmions to grow as the g -factor in the GaAs material is tuned towards zero — something that can be achieved by changing the external pressure on the sample — and this effect has been observed in experiments [79, 80].

Skyrmion excitations are well described by wave functions of the form [81]

$$\psi_{\text{skyrmion}}^{(\lambda)} = \psi_{\text{B}}^{(\lambda)} \psi_{\text{iqH}},$$

where ψ_{iqH} is the ground state wave function for $\nu = 1$, see Eq. (4.3), and $\psi_{\text{B}}^{(\lambda)}$ is a wave function for bosons. These excitations are referred to as skyrmions because in an effective $O(3)$ - σ -model field theory approach (see Section 1.2, they correspond to field configurations carrying non-trivial topological charge. This is measured by the Pontryagin index [82], which is identified with the electric charge carried by the skyrmion. A typical spin profile (Pontryagin



(a) Knight shift as a function of filling fraction as measured by NMR experiments, taken from Ref. [75].

(b) Optical dichroism as a function of filling fraction as measured by optical absorption experiments, taken from Ref. [76].

Figure 4.2: Knight shift and optical dichroism, both measures for the spin polarization, around $\nu = 1$ as measured in experiments.

index $+1$, charge $+e$ skyrmion) reads

$$\mathbf{S}(r, \phi) = (\sqrt{1 - \sigma^2} \cos \phi, -\sqrt{1 - \sigma^2} \sin \phi, \sigma), \quad (4.14)$$

where $\sigma(r)$ is some function that smoothly goes from -1 at the origin to $+1$ at infinity.

CSTs in the MR state: numerics The paper [21], see also [83, 84], took up the study of spin-full excitations over the MR state, stressing that the results may shed light on some of the experimental findings regarding the spin-polarization at $\nu = 5/2$. A particular suggestion is that specific experimental probes aimed at detecting a spin-polarization at $\nu = 5/2$ [85] may excite spin-full excitations, thereby depolarizing the system. The authors of [21] report an extensive numerical study of up to $N = 20$ particles in spherical geometry, where angular momentum (L) and total spin (S) are good quantum numbers.

They identified low-lying states on the diagonal $L = S$ as well as spin-

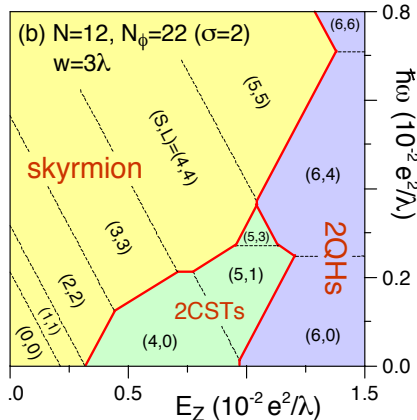


Figure 4.3: Phase diagram of exact diagonalization studies of the Coulomb Hamiltonian in a magnetic field for spinful electrons for one excess flux quantum above the $\nu = 5/2$ state. The horizontal (vertical) axis represents the Zeeman energy (lateral harmonic confinement energy). The lowest-energy state for each point in this plane is calculated and three different regimes have been identified: two polarized quasiholes, two Charged Spin Textures and one skyrmion. Figure taken from Ref. [21].

full ground states with $L = 0$ or $L = 1$. The $L = S$ states are associated with charge $2q = e/2$ skyrmions. The $L = S = 0$ state in particular is well described by a product state of the form $\psi_{\text{skyrmion}} = \psi_{\text{B}}^{(L=S=0)} \psi_{\text{MR}}$. The spin-full states with $L = 0(1)$ are naturally interpreted as being built from spatially separated charge q CSTs. The paper [21] presents a phase diagram, see Figure 4.3, specifying the nature of the spin-full excitations (skyrmions vs. separated CSTs) as a function of the Zeeman splitting and the lateral harmonic confinement strength, which is used to model disorder.

4.2.2 Construction of CST wave functions over the MR state

Here we follow a purely algebraic approach to obtain explicit expression for a variety of CSTs over the MR state. It rests on two observations. The first is explained above, culminating in Eq. (4.12), namely that the MR state can be written as a symmetrized product of two Laughlins. In the discussion

below we use the bosonic wave functions and denote the fundamental quasi-hole charge by q (the fermionic MR state would have $q = e/4$, the bosonic counterparts discussed here have $q = e/2$). The second observation [81] is that in the lowest Landau Level (LLL), the most general wavefunction for N spin-full fermions in $N + 1$ available 1-particle orbitals that vanishes when two particles are placed at the same position⁶ factorizes as $\psi_B \psi_{iqH}$, where ψ_B describes N spin-1/2 bosons in two orbitals. These orbitals can be viewed as the $L_z = \pm 1/2$ components of a $L = 1/2$ doublet of angular momentum. The combined orbital and spin angular momenta give rise to an $SU(4)$ symmetry, with the four 1-particle states ($L = S = 1/2$) corresponding to the fundamental (vector) representation, with Dynkin labels $[1\ 0\ 0]$ ⁷.

This $SU(4)$ algebra (for a similar problem containing an $SU(3)$ algebra, see Ref. [87]) is represented by operators of the form

$$T_{\alpha\beta} = \frac{1}{2} \{a_\alpha^\dagger, a_\beta\}, \quad \alpha, \beta \in \{\uparrow(+\frac{1}{2}), \uparrow(-\frac{1}{2}), \downarrow(+\frac{1}{2}), \downarrow(-\frac{1}{2})\},$$

which gives a total of $4 \times 4 = 16$ operators. They have commutation relations

$$[T_{\alpha\beta}, T_{\mu\nu}] = \delta_{\beta\mu} T_{\alpha\nu} - \delta_{\alpha\nu} T_{\mu\beta}.$$

The total number of bosons N in the four states is conserved, which means the operator

$$\sum_\alpha T_{\alpha\alpha} = \sum_\alpha (a_\alpha^\dagger a_\alpha + \frac{1}{2}) = N + 2$$

commutes with everything else and is, up to a constant shift, proportional to the quadratic Casimir operator. The fifteen remaining operators span the $SU(4)$ algebra. The number of ways one can put N bosons in four boxes,

$$\frac{(N+3)!}{N!3!} = \frac{(N+3)(N+2)(N+1)}{6},$$

⁶The Pauli principle only dictates that the wave function should vanish when two particles of identical spin are placed at the same position. The restriction to states that have the additional property that they vanish when two particles of opposite spin are placed at the same position makes the whole construction far more transparent. The price to pay is that not all possible states are reachable by this construction.

⁷For an excellent review on the theory of Lie groups, see [86]. This work also contains lists of irreducible representations of groups that arise in physical systems.

gives the dimensionality of the $[N 0 0]$ irrep of $SU(4)$. The partition sum for N such bosons becomes

$$\begin{aligned} Z_B &= SU(4) \text{ irrep } [N 0 0] \\ &= \sum_{K=0}^{N/2} (L = N/2 - K, S = N/2 - K). \end{aligned} \quad (4.15)$$

For large N the highest weight states (HW) of each of the $(L = S = N/2 - K)$ multiplets simplify to become

$$|\psi_B^K\rangle = \text{HW}(L = S = N/2 - K) \rightarrow |\downarrow_K, \uparrow_{N-K}\rangle,$$

with the left (right) position in the ket corresponding to the $L_z = -1/2 (+1/2)$ orbital.

The expression for a size- λ skyrmion in the disc geometry is then obtained as a weighted sum over these states [88, 81],

$$\begin{aligned} \left(\sum_K \lambda^K \psi_B^K \right) \psi_{\text{iqH}} &= \left(|0, \uparrow_N\rangle + \lambda |\downarrow, \uparrow_{N-1}\rangle + \cdots + \lambda^N |\downarrow_N, 0\rangle \right) \prod_{i < j} (z_i - z_j) \\ &= \prod_{i < j} (z_i - z_j) \prod_l (z_l |\uparrow\rangle_l + \lambda |\downarrow\rangle_l) e^{-\frac{|z_l|^2}{4}}, \end{aligned} \quad (4.16)$$

leading to the spin texture eq. (4.14).

The bosonic MR state is uniquely characterized as the highest density LLL state that is annihilated by the pairing Hamiltonian (see the discussion surrounding Eq. (4.11))

$$H_{\text{pair}} = \sum_{i < j < k} \delta(z_i - z_j) \delta(z_j - z_k).$$

We restrict ourselves to states that satisfy the very same MR pairing condition $H_{\text{pair}}\psi = 0$. For spin-1/2 bosons, the highest density state with this "MR pairing" property is the non-Abelian spin singlet (NASS) state [89] with filling fraction $\nu = 4/3$. In spherical geometry, the NASS state is realized for $N_\phi^{\text{NASS}} = 3/4N - 2$ flux quanta. The total space of paired states for N_ϕ in the vicinity of $N_\phi^{\text{MR}} = N - 2$ can be understood through counting formulas for

						$N_\phi=3$	$S=0$	$S=1$	$S=2$
$N_\phi=1$	$S=0$	$N_\phi=2$	$S=0$	$S=1$	$S=2$	$L=0$	1	0	1
$L=0$	1	$L=0$	1	0	1	$L=1$	0	2	0
		$L=1$	0	1	0	$L=2$	2	1	1
		$L=2$	1	0	0	$L=3$	0	1	0
						$L=4$	1	0	0

Table 4.1: Multiplicities of (L, S) multiplets in state space for $N = 4$ bosonic spin-1/2 particles on the sphere, subjected to MR pairing condition and in the presence of flux N_ϕ . The $L = S = 0$ state at $N_\phi = 1$ is the bosonic NASS state, the state with $L = 0, S = 2$ at $N_\phi = 2$ is the bosonic MR state.

spin-full quasiholes over the NASS state [90]. In table 4.1 we list the dimensions of each of the (L, S) subspaces for $N = 4$ particles for $N_\phi = N_\phi^{\text{NASS}} = 1$, $N_\phi = N_\phi^{\text{MR}} = 2$, $N_\phi = N_\phi^{\text{MR}} + 1 = 3$.

The idea is now to extend the trial states Eq. (4.12) to the spin-full case, by including factors of type ψ_B separately in both group *I* and group *II*. All states generated in this way satisfy the pairing property. They constitute a subset of all paired states at $N_\phi = N_\phi^{\text{MR}} + 1$ as listed in table 4.1.

We first analyze the symmetric product of the states ψ_B for groups *I* and *II*. In $SU(4)$ group theory

$$Z_B^{I,II} = [N/200] \otimes_{\text{sym}} [N/200] = \sum_{l=0}^{N/4} [N - 4l/2l0].$$

For $N = 4$, the $l = 0$ contribution has $(L, S) = (2, 2), (1, 1)$ and $(0, 0)$, totaling 35 states, while the $l = 1$ term comprises $(L, S) = (2, 0), (1, 1), (0, 2), (0, 0)$, totaling 20 states. For general N, l , the representation $[N - 4l/2l0]$ contains fully polarized states ($S = N/2$) at $L = N/2 - 2l$. Note that if we were to fully symmetrize over all N particle coordinates, only the $l = 0$ term would survive, reducing the construction to the states $|\psi_B^K\rangle$ describing the iqH skyrmion.

However we first perform what we call the Lowest-Landau-Level lift of ψ_B

$$\psi_B \rightarrow \psi_B(\{x_{i \in I \cup II}\}) \psi_I^L(\{x_{j \in I}\}) \psi_{II}^L(\{x_{k \in II}\}),$$

where the sets of coordinates $\{x_i\}$ contain both the up-spins z_i and down-spins w_i . The polynomial ψ_B is then symmetric with respect to exchanging z_i

and z_j if i, j are in the same group, and similarly for the down spin coordinates; we require no further symmetries. If we only then symmetrize over all N particles, we keep a much bigger set of spin-full states satisfying the pairing condition. In general, states obtained for 2 orbitals lift to independent states at $N_\phi = N - 1$. One exception is $(L, S) = (0, 0)$ at $N = 4$, where the LLL-lifts from the $l = 0, 1$ multiplets coincide.

We now argue that the states that survive after the symmetrization step with $l > 0$ can be viewed as charge $q (=e/2$ for these bosonic wave functions) CST separated by a distance set by l , where $l = N/4$ corresponds to the situation that two q CST sit on opposite poles of the sphere. This is most easily seen by focussing on the fully polarized ($S = N/2$) states, where the expressions can be compared to explicit formulas describing spin-less charge q quasiholes. The states (in disc geometry) for N paired, spin-polarized bosons at $N_\phi = N - 1$ are obtained by expanding the 2-quasihole wavefunction

$$\text{Symm}_{I, II} \prod_{i \in I} (\eta_1 - z_i) \prod_{i < j \in I} (z_i - z_j)^2 \prod_{k \in II} (\eta_2 - z_k) \prod_{k < l \in II} (z_k - z_l)^2$$

on a basis of symmetric polynomials in η_1, η_2 , where the powers of the η_s indicate the location of the two quasiholes. On the sphere, the resulting angular momenta are (for N a multiple of 4) $L = N/2, N/2 - 2, \dots, 0$. To leading order in $1/N$, the state at $L = 0$ corresponds to $\eta_1^{N/2} \eta_2^0 + \eta_1^0 \eta_2^{N/2}$ indicating that indeed the two quasiholes are on opposite sides of the sphere. For the spin-full case, one similarly finds that 2-CST states with $L \ll N/2$ correspond to well-separated CSTs.

For working towards explicit expressions, it is most convenient to perform the LLL lift and subsequent symmetrization in second quantization. Within each group, the LLL lift amounts to an embedding of a state defined on 2 orbitals to one on N orbitals, with coefficients set by the expansion of the corresponding Laughlin factor. It has the important property that both L and S quantum numbers are preserved. For the simple example of the 2-particle, polarized $\nu = 1/2$ Laughlin state (corresponding to one of the groups I, II for

$N = 4$ particles and $N_\phi = 3$ flux quanta) the LLL-lift takes the form

$$\begin{aligned} |\uparrow_2, 0\rangle &\rightarrow 2\sqrt{6}|\uparrow, 0, \uparrow, 0\rangle - 4|0, \uparrow_2, 0, 0\rangle \\ |\uparrow, \uparrow\rangle &\rightarrow 6|\uparrow, 0, 0, \uparrow\rangle - 2|0, \uparrow, \uparrow, 0\rangle \\ |0, \uparrow_2\rangle &\rightarrow 2\sqrt{6}|0, \uparrow, 0, \uparrow\rangle - 4|0, 0, \uparrow_2, 0\rangle. \end{aligned} \quad (4.17)$$

We will work out the second line above as an example. In first quantization this state corresponds to the lift of $(z_1 + z_2)$:

$$(z_1 + z_2)(z_1 - z_2)^2 = (z_1^3 + z_2^3) - (z_1 z_2^2 + z_1^2 z_2), \quad (4.18)$$

where we have expanded on a basis of symmetric monomials. When going from first to second quantization on the sphere, particles in orbital $l = 0, \dots, N_\phi$ obtain an additional factor $\sqrt{l!} \sqrt{(N_\phi - l)!}$, giving

$$\begin{aligned} (z_1^3 + z_2^3) &\rightarrow \sqrt{6}\sqrt{6}|\uparrow, 0, 0, \uparrow\rangle \\ (z_1 z_2^2 + z_1^2 z_2) &\rightarrow \sqrt{2}\sqrt{2}|0, \uparrow, \uparrow, 0\rangle, \end{aligned}$$

which leads to (4.17) after we plug in the relative coefficients found in the expansion (4.18). The symmetrization over groups I and II is easily done through the step

$$\begin{aligned} |\dots, m_I, \dots\rangle \times_s |\dots, m_{II}, \dots\rangle &\rightarrow \\ \sqrt{\frac{(m_I + m_{II})!}{m_I! m_{II}!}} |\dots, m_I + m_{II}, \dots\rangle, & \end{aligned} \quad (4.19)$$

where m_I, m_{II} indicate the occupation number of a given orbital (including its spin-label).

As an explicit example, we present the two $L = S = 1$ states for $N = 4$ particles with $N_\phi = 3$. In the first step we identify the $L = S = 1$ highest weight states within the two distinct $SU(4)$ multiplets with Dynkin labels $[400]$ and $[020]$,

$$\begin{aligned} \psi_B^{[400]} &\propto [\sqrt{2}|\uparrow, \uparrow\uparrow\downarrow\rangle + |\uparrow, \downarrow\uparrow_2\rangle - 3|\downarrow, \uparrow\uparrow_2\rangle] + [I \leftrightarrow II] \\ \psi_B^{[020]} &\propto [-\sqrt{2}|\uparrow, \uparrow\uparrow\downarrow\rangle + 2|\uparrow, \downarrow\uparrow_2\rangle] + [I \leftrightarrow II] \end{aligned} \quad (4.20)$$

where we use single (double) arrows for indicating the particles in group *I* (*II*). In the second step we perform the LLL-lift and then symmetrize, leading to

$$\begin{aligned}
\psi^{[400]} &\propto 5|0, \downarrow, \uparrow_3, 0\rangle - 3\sqrt{2}|0, \uparrow\downarrow, \uparrow, \uparrow\rangle \\
&\quad + 7|0, \uparrow_2, \downarrow, \uparrow\rangle - \frac{5}{3}\sqrt{3}|0, \uparrow, \uparrow_2\downarrow, 0\rangle - |0, \uparrow_2, \uparrow, \downarrow\rangle \\
&\quad - \sqrt{3}|\downarrow, 0, \uparrow_2, \uparrow\rangle + 3|\downarrow, \uparrow, 0, \uparrow_2\rangle - \sqrt{6}|\uparrow, 0, \uparrow\downarrow, \uparrow\rangle \\
&\quad + 3\sqrt{3}|\uparrow, 0, \uparrow_2, \downarrow\rangle + 3|\uparrow, \downarrow, 0, \uparrow_2\rangle - 3\sqrt{2}|\uparrow, \uparrow, 0, \uparrow\downarrow\rangle \\
\psi^{[020]} &\propto 4|0, \downarrow, \uparrow_3, 0\rangle - \frac{3}{2}\sqrt{2}|0, \uparrow\downarrow, \uparrow, \uparrow\rangle \\
&\quad + 2|0, \uparrow_2, \downarrow, \uparrow\rangle - \frac{4}{3}\sqrt{3}|0, \uparrow, \uparrow_2\downarrow, 0\rangle + |0, \uparrow_2, \uparrow, \downarrow\rangle \\
&\quad - 2\sqrt{3}|\downarrow, 0, \uparrow_2, \uparrow\rangle + 6|\downarrow, \uparrow, 0, \uparrow_2\rangle + \sqrt{6}|\uparrow, 0, \uparrow\downarrow, \uparrow\rangle \\
&\quad - 3|\uparrow, \downarrow, 0, \uparrow_2\rangle - \frac{3}{2}\sqrt{2}|\uparrow, \uparrow, 0, \uparrow\downarrow\rangle. \tag{4.21}
\end{aligned}$$

We remark, while the construction correctly reproduces two linearly independent paired states at $L = S = 1$, the algebraic structure is not very transparent. For one thing, the $SU(4)$ symmetry is lost in the LLL-lift. In addition, the two states eq. (4.21) are not orthogonal.

The (L, S) states constructed here can directly be compared to the numerical ground states found in Ref. [21]. In particular, where [21] finds $L = 0, 1$ groundstates for $N = 12$ at $S = 4, 5, 6$ we expect good overlaps with the states presented here.

The bosonic parts of the wavefunctions simplify considerably in the large- N limit: the leading polarized states of the $[N00]$ and $[0N/20]$ irreps are

$$\psi_{\text{B}}^{[N00]} \rightarrow |0, \uparrow_{N/2} \uparrow_{N/2}\rangle, \quad \psi_{\text{B}}^{[0N/20]} \rightarrow |\uparrow_{N/2}, \uparrow_{N/2}\rangle.$$

We can then consider states with K overturned spins as in eq. (4.16), separately in groups *I* and *II*. This leads to simple expressions for the situation where the spin-textures in groups *I*, *II* have sizes λ_I, λ_{II} . Starting from $\psi_{\text{B}}^{[0N/20]}$, with group *I*, *II* textures on opposite sides of the 2-orbital subspace, and then taking these expressions through the LLL lift and symmetrization,

leads to 2-CST configurations where the charge q CSTs sit on opposite sides of the sphere. This expression, expanded in powers of the sizes λ_I and λ_{II} , symbolically reads

$$\sum_{K_I, K_{II}} \lambda_I^{K_I} \lambda_{II}^{K_{II}} \left(\begin{array}{c} \text{Symm} \\ I, II \end{array} \right) (\text{LLL} - \text{lift}) |\uparrow_{N/2-K_I} \downarrow_{K_{II}}, \downarrow_{K_I} \uparrow_{N/2-K_{II}}\rangle. \quad (4.22)$$

From here on we will label our textures as $\text{CST}[w_I, w_{II}]$, where w_I, w_{II} are the winding numbers (with respect to a given location on the sphere) of the skyrmions that would appear in group I, II if the symmetrization step in our construction were not performed. The $SU(4)$ label $[N 0 0]$ corresponds to the $\text{CST}[1, 1]$ and $[0 N/2 0]$ gives a spatially separated $\text{CST}[1, 0]$ and $\text{CST}[0, 1]$.

4.2.3 Properties of CSTs over the MR state

For a given quantum Hall state we measure the components of the spin field by acting with

$$\mathbf{S}(z, \bar{z}) = \sum_{I, I'} \left(a_{I, \alpha}^\dagger \sigma_{\alpha\beta} a_{I', \beta} \right) \phi_I^\dagger(\bar{z}) \phi_{I'}(z)$$

where the $\phi_I(z)$ are the single particle wave functions, which depend on the geometry and our normalization is such that a polarized system has $S_z = 1$. In Figure 4.4 we plot the expectation value of the spin vector for a configuration with $N = 8$, $\lambda_I = 1.0$, $\lambda_{II} = 0.0$.

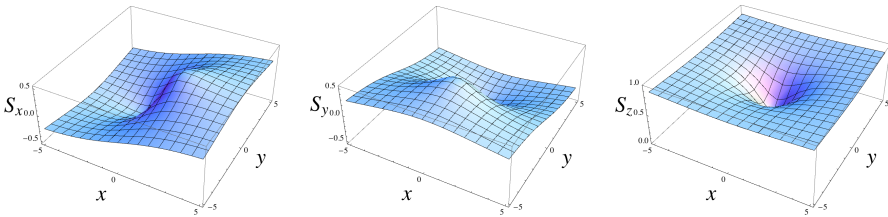


Figure 4.4: Spin components S_x , S_y and S_z for configuration with single $\text{CST}[1, 0]$ at the origin and a quasihole at infinity, after stereographic projection.

In a Conformal Field Theory (CFT) based description [59], the quasihole

operator comes with an Ising σ -field. For N even, a collection of these σ -fields will fuse to the identity operator, whereas they fuse to the ψ sector for N odd. This is due to the fact that the electron operator carries a ψ field, so performing the contractions of an odd number of electron operators within the CFT correlator will always leave one ψ field: this one has to pair with the fusion product of all the σ -fields in order for the total correlator to fuse to the identity.

It was shown in [91] that the density profile of the system on the sphere after the fusion of two charge q quasiholes to a charge $2q$ quasihole differs between the two cases: in the case N even the density drops to zero at the location of the $2q$ quasihole, whereas the density drop for N odd is wider and less deep.

This has consequences for the possible spin textures that may arise as a result of fusing elementary CST[1,0]. Our construction recovers the polarized quasihole states in the limit $\lambda \rightarrow 0$. This means we expect the density for up-particles to vanish in the core of the fusion product of two CST[1,0] for N even, but not for N odd.

This becomes rather obvious in the two-layer construction we have been using throughout this paper. For N even, the particles can be divided equally into two groups. The $K_I = K_{II} = 0$ term appearing in the expansion of two quasiholes analogous to (4.22), but now for both quasiholes at the same position is then

$$|0, \uparrow_{N/2}\rangle \text{ for group } I, \quad |0, \uparrow_{N/2}\rangle \text{ for group } II.$$

However for N odd we have to divide the particles unequally among the two groups. The division that requires the least amount of total flux is $(N+1)/2$, $(N-1)/2$. The N_ϕ is equal for both groups, and is at least $N-1$: this is the highest power for a single particle appearing in the expansion of Laughlin factor for the group containing $(N+1)/2$ particles⁸. Note that the $N_\phi^{\text{MR}} = N-2$, so that states with an odd number of particles will always have quasiholes present.

This extra flux in the system gives two extra orbitals to the particles in the smaller group, whereas the particles in the larger group have no additional

⁸Note one can also divide the particles unequally in the case N even. This leads to states with quasiholes: consider the division $N/2+1$, $N/2-1$. The particles in the first group require at least $N_\phi = N$, which means the particles in the second group have four excess fluxes.

orbitals. The first term in the expansion now becomes

$$|0, 0, \uparrow_{(N-1)/2}\rangle \text{ for group } I, \quad |\uparrow_{(N+1)/2}\rangle \text{ for group } II.$$

Even without performing the whole calculation one can already see that the density will not vanish since the particles in group *II* are spread homogeneously over the sphere. The natural texture

$$\sum_K \lambda^K \left(\begin{array}{c} \text{Symm} \\ I, II \end{array} \right) (\text{LLL} - \text{lift}) |\downarrow_K, 0, \uparrow_{(N-1)/2-K}\rangle |\uparrow_{(N+1)/2}\rangle, \quad (4.23)$$

has winding number 2 for group *I* and 0 for group *II*. Therefore we argue that the simplest possible charge $2q$ configuration has winding indices $[2, 0]$ for N odd.

We have studied three representative cases in detail: a skyrmion CST[1, 1] for $N = 8$, a separated CST[1, 0]/quasihole pair for $N = 8$ and a single CST[2, 0] for $N = 7$. The results are in Figure 4.5. We have chosen these cases for the following reasons. The CST[1, 0] is the fundamental charge q spin texture, associated with the σ -field in the Ising CFT. The skyrmion CST[1, 1] is given because it shows that our construction includes the results of earlier studies [81]. It is also the fusion product, following the discussion above, of two elementary CST[1, 0] in the trivial (N even) fusion channel. The CST[2, 0] is the fusion product of two CST[1, 0] when the overall fusion channel (in CFT language) is ψ or alternatively stated, when the number of particles N is odd.

Two observations about the behaviour of these textures are in place. First of all we see that the the CST[2, 0] has winding number 2 when the azimuthal angle runs from 0 to 2π . Furthermore, the (expectation value of the) length of the spin vector vanishes in the core of the CSTs of type [1, 0] and [2, 0]. For N large the latter effect seems to hold for all CST[n , 0]. This behavior closely mimicks that of the ‘‘polar core vortex’’ appearing in rotating spin-1 Bose-Einstein condensates [92]. The observation that the MR state carries an effective spin-1 field due to the pairing of the electrons has been made in earlier studies [93, 84]. The BEC polar core vortices have the following mean field spin vector expectation value

$$\mathbf{S}(r, \phi) = (\sqrt{2\rho(1-\rho)} \cos n\phi, -\sqrt{2\rho(1-\rho)} \sin n\phi, \rho),$$

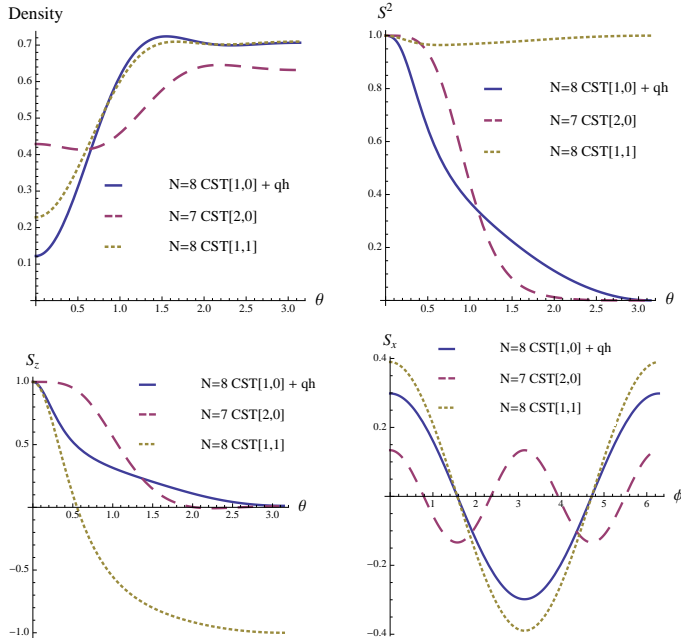


Figure 4.5: Density, S^2 and S_z of a $N = 8$ CST[1,0]/quasihole pair, an $N = 7$ CST[2,0] and an $N = 8$ skyrmion (CST[1,1]) at $\lambda = 2.0$ as a function of the polar angle θ at azimuthal angle $\phi = 0$ and S_x for the same systems as a function of ϕ at $\theta = \frac{\pi}{2}$. The spin textures are centered at $\theta = \pi$, for the $N = 8$ CST[1,0] there is a quasihole at $\theta = 0$.

with $\rho(r)$ equal to 0 at the origin and approaching 1 at infinity. The Pontryagin density in polar coordinates equals

$$\rho_{\text{top}}(r, \phi) = \frac{1}{4\pi} \frac{1}{r} \mathbf{S} \cdot (\partial_r \mathbf{S} \times \partial_\phi \mathbf{S}),$$

which for the texture (4.24) means that the integrated Pontryagin density

equals

$$\begin{aligned} Q_{\text{top}} &= \int d^2r \rho_{\text{top}} = \int_0^\infty dr 2\pi r \frac{1}{4\pi r} n \rho \partial_r \rho = \\ &= \frac{n}{2} \int_0^\infty dr \frac{d}{dr} \left(\frac{1}{2} \rho^2(r) \right) = \frac{n}{4}. \end{aligned}$$

Numerical values for our CST[1,0] textures approach $\frac{1}{4}$ for $\lambda \gg 1$. For a general texture CST[w_I, w_{II}] the integrated Pontryagin density is no longer a topological index in the usual sense (the target space manifold is \mathbb{R}^3 instead of S^2 , so the integral does not have to be an integer). Also, the relation between electric and topological charge densities, $\rho_{\text{elec}} = \nu e \rho_{\text{top}}$, valid in Abelian quantum Hall states, takes a different form in general non-Abelian states, of which the MR state is a prototypical example.

4.3 Spin texture read out of a qubit

In the absence of spin, the fundamental charge- q quasihole excitations over the MR state are known to behave as non-Abelions: the presence of n such excitations leads to a total of $2^{n/2-1}$ topologically different states, all degenerate as long as the excitations are sufficiently separated. In the formalism where the MR wavefunctions are obtained as conformal blocks in a conformal field theory (CFT), this degeneracy can be traced to fact that the $e/4$ quasiparticles carry a σ field, with Ising fusion rules $\sigma \times \sigma = 1 + \psi$. The topological distinction among the $2^{n/2-1}$ internal states of a collection of n quasiholes over the MR state makes them ideally suited to act as a (topologically protected) quantum register. Quantum gates can be implemented through particle braiding and readout is in principle possible by bringing the quasiparticles to one location and then probing the 1-particle density profile of the resulting composite excitation.

In this Section we consider the same process of readout through fusion, but now in the presence of the spin degree of freedom. We thus analyze the thought-experiment where a collection of n elementary charge q CST are brought to the same location and fuse into a composite excitation of charge nq . Focusing on the spin texture carried by the fused, composite excitation, we will establish a direct connection between the winding numbers characterizing

the texture and the fusion sector of the underlying non-Abelions. This in principle enables the readout of a MR quantum register through the detection of a characteristic spin texture.

Fusion of multiple MR quasiholes Excess flux ΔN_ϕ over a MR state leads to $n = 2\Delta N_\phi$ quasiholes. The fusion product of the corresponding σ fields can result in F ψ -quanta, with $0 \leq F \leq \Delta N_\phi$. These ψ quanta will be absorbed by F unpaired particles in the MR qH condensate. The number F provides information about the topological state of the system: a determination of F is equivalent to partially reading out the quantum register spanned by the fusion space of the quasiholes. If we now bring all quasiholes to the origin, the lowest surviving field product in the sector with F ψ 's is : $\psi(0)\partial\psi(0)\dots\partial^{F-1}\psi(0)$:, where the colons denote normal ordering. This leads to the following "big hole" wave function, expressed in the form of a CFT correlator

$$\Psi_{\text{big hole}}(z_1, \dots, z_N; \Delta N_\phi, F) = \prod_{i < j} (z_i - z_j) \dots \prod_k z_k^{\Delta N_\phi} \langle : \psi(0)\partial\psi(0)\dots\partial^{F-1}\psi(0) : \psi(z_1)\dots\psi(z_N) \rangle_{\text{CFT}}. \quad (4.24)$$

In [94] Read and Rezayi presented a general analysis of wavefunctions for quasiholes over the MR state, which they characterized by the same quantity F , the number of unpaired particles, and a set of integers $\{m_1, \dots, m_F\}$. They provide the following general expression for the $n = 2\Delta N_\phi$ quasihole states in the presence of ΔN_ϕ extra fluxes

$$\Psi_{m_1, \dots, m_F}(z_1, \dots, z_N; w_1, \dots, w_{2\Delta N_\phi}) = \frac{1}{2^{(N-F)/2} (N-F)/2!} \sum_{\sigma \in S_N} \text{sgn}\sigma \prod_{k=1}^F z_{\sigma(k)}^{m_k} \prod_{l=1}^{(N-F)/2} \frac{\Phi(z_{\sigma(F+2l-1)}, z_{\sigma(F+2l)}; w_1, \dots, w_{2\Delta N_\phi})}{(z_{\sigma(F+2l-1)} - z_{\sigma(F+2l)})} \prod_{i < j} (z_i - z_j),$$

where

$$\Phi(z_1, z_2; w_1, \dots, w_{2\Delta N_\phi}) = \frac{1}{\Delta N_\phi!^2} \sum_{\tau \in S_{2\Delta N_\phi}} \prod_{r=1}^{\Delta N_\phi} (z_1 - w_{\tau(2r-1)})(z_2 - w_{\tau(2r)}).$$

We recognize the equivalence of Eq. (4.24) and a special case of this expression, namely the one where the set m_k has been chosen such that the highest obtainable value of L_z is reached and all the quasihole coordinates are sent to the origin. This corresponds to the expression

$$\prod_{i < j} (z_i - z_j) \prod_k z_k^{\Delta N_\phi} \sum_{\sigma \in \mathcal{S}_N} \text{sgn} \sigma z_{\sigma(1)}^{-1} \cdots z_{\sigma(F)}^{-F} \cdots \frac{1}{z_{\sigma(F+1)} - z_{\sigma(F+2)}} \cdots \frac{1}{z_{\sigma(N-1)} - z_{\sigma(N)}}, \quad (4.25)$$

which is easily seen to be equivalent to Eq. (4.24).

In preparing for the introduction of the spin degree of freedom, we wish to rewrite this "big hole" wavefunction in yet another form by using the bosonization of the *Ising* CFT introduced in Section 4.1.3.

To extend the 'two group' formula to the 'big hole' wave function Eq. (4.24), we need to bosonize the normal ordered field product: $\psi(0)\partial\psi(0)\dots\partial^{F-1}\psi(0)$; , which we will do as follows. Let us locate the ψ fields at locations w_i and pull out all derivatives. The desired expression is then precisely the regular part of

$$\partial_{w_2} \partial_{w_3}^2 \dots \partial_{w_F}^{F-1} (e^{i\varphi} + e^{-i\varphi})(w_1) \dots (e^{i\varphi} + e^{-i\varphi})(w_F)$$

that survives after sending all the w_i to zero. Following a similar logic as in the evaluation of Eq. (4.13) we must determine which terms in the expansion of this product contribute. Only two terms contribute: one where we choose all the positive exponentials and one where we choose all the negative ones. The contribution of the positive exponentials

$$\partial_{w_2} \partial_{w_3}^2 \dots \partial_{w_F}^{F-1} \prod_{i < j} (w_i - w_j) e^{i \sum_k \varphi(w_k)},$$

has only one term that survives when all w_i are sent to zero, namely the one where all the derivatives act on the polynomial part (more precisely, the $w_1^0 w_2^1 \dots w_F^{F-1}$ term in its expansion). The same reasoning applies to the negative exponentials and one is left with the particularly simple identification

$$: \psi(0)\partial\psi(0)\dots\partial^{F-1}\psi(0) : \leftrightarrow (e^{iF\varphi} + e^{-iF\varphi})(0). \quad (4.26)$$

With this result, we can rewrite the wavefunction Eq. (4.24) in the following

way using the ‘two group’ construction. To maintain charge neutrality we put $\frac{N-F}{2}$ particles in group *I* and $\frac{N+F}{2}$ particles in group *II*. The resulting expression is

$$\text{Symm}_{I, II} \left[\prod_{i,j \in I} (z_i - z_j)^2 \prod_{i \in I} z_i^{\Delta N_\phi + F} \times \prod_{k,l \in II} (z_k - z_l)^2 \prod_{k \in II} z_k^{\Delta N_\phi - F} \right]. \quad (4.27)$$

One can interpret this result in a different way. Since the number of flux quanta required to accommodate the Laughlin wave function is different between groups *I* and *II*, the groups will have different excess flux. In spherical geometry, assuming $N_\phi = N - 2 + \Delta N_\phi$, the particles in group *I* have $\Delta N_\phi^I = \Delta N_\phi + F$ and those in group *II* have $\Delta N_\phi^{II} = \Delta N_\phi - F$. We shall now demonstrate that the number of excess flux quanta per group determines the shape of the possible spin textures.

Textures with higher winding numbers In Section 4.2.2 we explained that for iqH states the wave function for a skyrmion factorizes as [82, 77]

$$\Psi_{\text{Skyrmion}} = \Psi_B \times \Psi_{\text{iqH}}, \quad (4.28)$$

where Ψ_{iqH} is the ground state wavefunction for filling $\nu = 1$ and Ψ_B is a wavefunction for spinful bosons in two orbitals [81]. Recall that (see Eq. (4.16)) in second quantization Ψ_B is given by

$$|0, \uparrow_N\rangle + \lambda | \downarrow, \uparrow_{N-1} \rangle + \cdots + \lambda^N | \downarrow_N, 0 \rangle, \quad (4.29)$$

where λ determines the size of the texture, and the construction is such that in the limit $\lambda \rightarrow 0$ one is left with the quasihole wave function. The generalization to the paired MR state allowed us to write down separate boson wave functions (4.29) for both Laughlin factors in the two-group formulation of the MR wave function. The two single particle angular momentum states in this expression are due to one extra flux quantum being present. The skyrmion resulting from this wave function has Pontryagin index (or winding number) 1; higher topological charge textures can be built by adding extra flux quanta and repeating the procedure.

We have already alluded to what comes now in the discussion preceding Eq. (4.23), where for an odd number of particles the simplest CST had winding

numbers $[2, 0]$. For a texture with winding number w , one has to add w flux quanta to the ground state. This opens up $w + 1$ orbitals for the bosons and the superposition for a texture with winding number w is

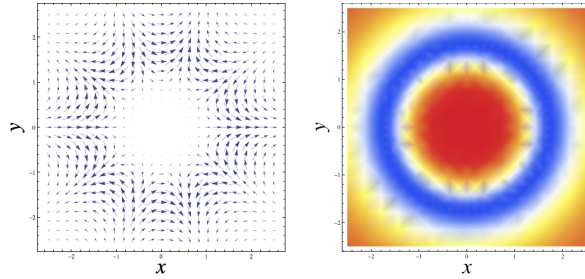
$$|0, \dots, \uparrow_N\rangle + \lambda |\downarrow, \dots, \uparrow_{N-1}\rangle + \dots + \lambda^N |\downarrow, \dots, 0\rangle. \quad (4.30)$$

We assume that the textures appearing in both groups will maximize their winding numbers separately, meaning that the particles will use all available orbitals to arrive at wave function superpositions such as (4.30). This will allow us to determine the number of unpaired fermions present in the system, as we shall show now.

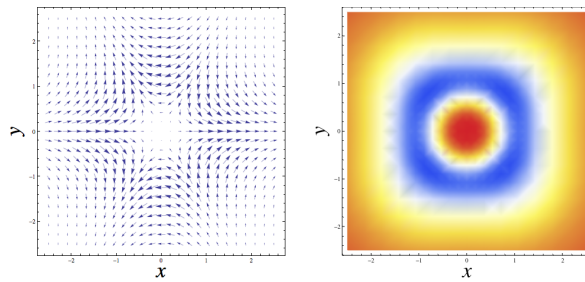
Fusion channel to spin texture locking Combining the results specified in the above we arrive at the following claim: the composite CST with winding numbers $[\Delta N_\phi + F, \Delta N_\phi - F]$ that is associated with the fusion product of $2\Delta N_\phi$ elementary CSTs over the MR state necessarily carries F unpaired fermions.

In general, the fusion channel label F satisfies $(-1)^F = (-1)^N$. Thus, the simplest situation for N odd is $F = 1$ and $\Delta N_\phi = 1$, leading to a CST labeled as $[2, 0]$.

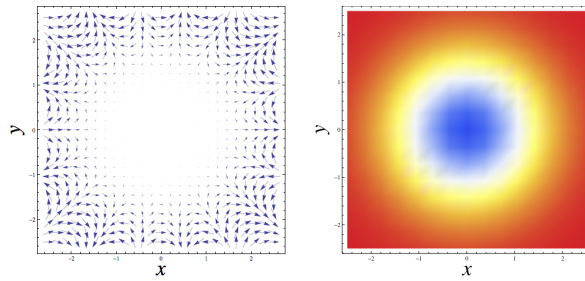
In Figures 4.6(a)–(c) we display the the spin textures for $N = 8$ particles in the presence of $\Delta N_\phi = 4$ excess flux quanta. Possible sectors are $F = 0$ with CST $[4, 4]$, $F = 2$ with CST $[6, 2]$ and $F = 4$ leading to CST $[8, 0]$.



(a) CST[4,4]



(b) CST[6,2]



(c) CST[8,0]

Figure 4.6: Stereographic projection of the (S_x, S_y) vector field (left) and the length of the spin vector S^2 (right) for spin textures CST[4,4], CST[6,2] and CST[8,0]. All CSTs have $\lambda_1 = \lambda_2 = 0.5$ and $N = 8$. In the S^2 plots, warmer colors correspond to a longer length of the spin vector. The normalization is such that $S^2 = 1$ far away from the core of the CST.

Spin texture readout In the fully polarized MR state the fingerprint left by the unpaired fermions takes the form of an altered density profile [91] and energy difference [95] with respect to the state without unpaired fermions. We find that, within the framework we used here, the textures formed by the electron spins are unique and in 1-1 correspondence with the number F characterizing the fusion sector of the non-Abelian CST. This provides a novel method to determine the number of unpaired fermions and thus to read out the (F -number of the) topological quantum register.

In the present work, we have circumvented the task of minimizing the realistic (Coulomb and Zeeman) interaction energies by working within the zero energy subspace of the pairing Hamiltonian (4.11). The rationale for this is the well-established fact that in the spin-polarized case the correlations found in systems with realistic interactions agree with those enforced by the pairing condition $H_{\text{pair}}\psi = 0$. In addition, we have relied on the ‘two group’ Ansatz and have assumed that the particles in each group I, II separately maximize their winding number.

It remains to be confirmed that our results capture the essence of what happens when realistic (Coulomb and Zeeman) interactions are used instead of the pairing condition. A numerical approach is possible in principle but very challenging in practice. The spin degree of freedom makes the use of exact diagonalization highly nontrivial due to the size of the Hilbert spaces involved in the problem. A Monte Carlo study is hindered by the fact that no simple first-quantized expressions have been found yet for the CST wave functions.

4.4 Summary

- We have constructed wave functions for Charged Spin Textures (CSTs) over the Moore-Read (M-R) fractional quantum Hall state. By using the “two-group” formalism for the M-R wave function, they satisfy the pairing condition by construction.
- These CSTs are labeled by two winding numbers $[w_I, w_{II}]$, one for each group of particles. They generalize the skyrmions; a charge n skyrmion equates to a $[n, n]$ CST.
- The fundamental CST carrying winding numbers $[1, 0]$ has the peculiar property that all three components of the spin vector vanish in its core. This is unique to the M-R state since it requires pairing of spin- $\frac{1}{2}$ electrons into a spin-1 vector field.
- The CST $[1, 0]$ reduces to a half flux-quantum quasihole in the limit where the size of the CST goes to zero. We therefore claim it carries the same non-Abelian statistics.
- The composite CST that results from the fusion of multiple elementary CSTs has winding numbers that correlate to the number of unpaired fermions in the system. Therefore this fusion process constitutes a readout of the quantum register spanned by the fusion space of the underlying non-Abelian particles.

CHAPTER 5

Conclusions and outlook

Two separate directions of original research have been presented in this thesis. We will first discuss these two subjects, after which we will propose directions for future research.

Lattice model for DGTs The first part, contained in Chapter 3, concerns a lattice model for a particular TQFT, a Discrete Gauge Theory. We have introduced a set of multiparameter actions for these theories that display a rich phase structure, and showed in particular that all the allowed condensates of pure magnetic flux are realized in certain well anticipated regions of coupling constant space. The set of open string operators that we defined form a set of order parameters that allowed us to determine the content of the condensate and to measure the topological symmetry breaking index q .

Once the condensate is identified, we have shown how to unambiguously reconstruct the S -matrix of the low-energy theory in a broken or unbroken phase by measurements of the complete set of braided loop operators, using the anyonic loop operators we proposed in earlier work [35]. Due to an auxiliary gauge symmetry these operators are particularly well suited to detect the nontrivial splittings of fields that correspond to fixed points under fusion with

the condensate. We found that as expected the excitations that are confined in a broken vacuum give rise to rows and columns of zeroes in the broken S -matrix. Our work clearly demonstrates that the euclidean approach allows for a very straightforward method to completely determine the nature of the broken phase.

fqH CSTs In the second part of this thesis, presented in Chapter 4, we construct wave functions for Charged Spin Textures (CSTs) over the Moore-Read quantum Hall state. Inspired by an algebraic construction for skyrmions over the integer quantum Hall state [81] and the colourful or two-component construction for the M-R state [73] and encouraged by numerical studies [21] and experiments [85] we found that it is possible to construct wave functions satisfying the M-R clustering condition which carry a spin texture around the elementary quasi hole.

These textures are a generalization of skyrmions: they carry a pair of winding numbers $[w_I, w_{II}]$ instead of just one. We identified the topological charge n skyrmion with an $[n, n]$ CST and found that the elementary CST, with winding number $[1, 0]$, has the peculiar property that the length of the spin vector vanishes in the CST core. This is reminiscent of the polar core vortices [92] appearing in spin-1 Bose-Einstein condensates, which in hindsight is not surprising: the M-R state can be interpreted as a condensate of paired spin- $\frac{1}{2}$ electrons in the spin-1 channel.

We also show that the pair of winding numbers is correlated to the number of unpaired fermions arising in the fusion of multiple elementary CSTs. This number gives insight as to which path was taken in the Bratelli diagram of the collection of σ fields that underlie the CSTs. Therefore determining the winding numbers of a composite CST equates to (partially) reading out the topologically protected quantum register spanned by the fusion space of those σ particles.

Future research Let us start by pointing out some obvious directions for future research directly connected to the work presented in this thesis. In our research on DGTs we showed that the reason the modular S -matrix changes in the broken phase is largely due to the contribution of the so-called vacuum exchange diagram. In an upcoming more theoretical paper [34] we will extend the approach used in this work, the use of observables and in particular the

S-matrix to determine the phase structure of a TQFT to a far wider range of theories, in particular the $SU(N)_k$ TQFT arising from Chern-Simons actions.

It would be interesting to study different models exhibiting different topological phases by somehow formulating them in the euclidean 3-dimensional framework, to our knowledge such an approach is unfortunately not yet available for Chern Simons theories. One expects that for Levin Wen models [96] our approach could be implemented though. Another path is to investigate the phase structure after adding dynamical matter fields that transform non-trivially. It is known that in such situations the Wilson type criteria break down as the strings can break, this necessitates the development of different diagnostic tools [43, 97].

Our work on CSTs in the M-R state still lacks a crucial component: the relation between the wave functions we propose and the states resulting from realistic Hamiltonians. Two different roads need to be travelled here. First of all, it needs to be determined whether realistic interactions — Coulomb and Zeeman — energetically favour the creation of an elementary CST with a finite size λ over the presence of a polarized quasi hole in a certain part of the phase diagram of the M-R state, which seems likely based on exact diagonalization studies [21]. The most natural means of studying this problem would be through a Monte Carlo simulation in which the energy is calculated for a given trial wave function. Once this machinery is in place, it can also be used to check whether the composite CSTs (having larger winding numbers) actually maximize both their winding numbers, as is presupposed in the mechanism for the read out of a quantum register we presented. A second check for these CST wave functions would consist of a comparison between those that we propose and those that follow from exact diagonalization [21] of realistic interactions, which we believe is under way [98].

If we take a broader perspective, several other interesting venues of research based on the work in this thesis come to mind. For example, it is known that the NASS [89] state shares many characteristics with the M-R state. More specifically, it is the wave function satisfying the same clustering condition but carries total spin zero. It would therefore seem quite natural that the two states are connected to each other by some sort of symmetry breaking, perhaps of the sort discussed in Chapter 2.

On a different note, the proposal that the BF theory is a good field-theoretical description of topological insulators (TIs) [99] in the same sense that Chern-Simons (CS) theory captures the essential physics of the (fractional) quantum

Hall effect is promising. The topological symmetry breaking formalism used in this thesis connects different TQFTs, such as DGTs and CS theories, by symmetry breaking through Bose condensation. It would be interesting to study whether something of the sort can be achieved for these BF theories.

Finally, two recent articles [100, 101] discuss the emergence of fractionalized Majorana fermions on domain walls in a system consisting of two fractional quantum Hall droplets of opposite spin coupled to superconductors and ferromagnets. Although these fractional Majoranas seem to obey a parafermionic algebra [102], they are not universal for quantum computation. This is in contrast to quantum Hall states based on parafermionic CFTs [103], and it seems as though only a subset of the spectrum is realized in these fractionalized Majorana proposals. Also it is unlikely that these fractional Majoranas form a braided tensor category, as the spectra of TQFTs do. Perhaps this can be understood within the framework of topological symmetry breaking, where the algebra of fields on the \mathcal{T} level is also not braided.

Bibliography

- [1] F. W. NIETZSCHE. *Die fröhliche Wissenschaft*. 1882.
- [2] E. A. ABBOTT. *Flatland*. 1884.
- [3] Bookworm arXiv. <http://arxiv.culturomics.org/>.
- [4] Y. AHARONOV AND D. BOHM. Significance of electromagnetic potentials in the quantum theory. *Phys.Rev.*, 115:485–491, 1959.
- [5] G. 'T HOOFT. Magnetic Monopoles in Unified Gauge Theories. *Nucl.Phys.*, B79:276–284, 1974.
- [6] A. M. POLYAKOV. Particle Spectrum in the Quantum Field Theory. *JETP Lett.*, 20:194–195, 1974.
- [7] E. WITTEN. Quantum Field Theory and the Jones Polynomial. *Commun.Math.Phys.*, 121:351, 1989.
- [8] D. J. THOULESS, M. KOHMOTO, M. P. NIGHTINGALE, AND M. DEN NIJS. Quantized Hall Conductance in a Two-Dimensional Periodic Potential. *Phys.Rev.Lett.*, 49:405–408, 1982.
- [9] A. KITAEV. Periodic table for topological insulators and superconductors. *AIP Conf.Proc.*, 1134:22–30, 2009, arXiv:0901.2686 [cond-mat.mes-hall].

- [10] S. RYU, A. P. SCHNYDER, A. FURUSAKI, AND A. W. W. LUDWIG. Topological insulators and superconductors: Tenfold way and dimensional hierarchy. *New J.Phys.*, 12:065010, 2010.
- [11] E. CARTAN. Sur une classe remarquable d’espaces de Riemann, I. *Bulletin de la Société Mathématique de France*, 54:214–216, 1926.
- [12] E. CARTAN. Sur une classe remarquable d’espaces de Riemann, II. *Bulletin de la Société Mathématique de France*, 55:114–134, 1927.
- [13] S. M. GIRVIN. The Quantum Hall Effect: Novel Excitations and Broken Symmetries. ArXiv:9907002, 1998.
- [14] T. H. R. SKYRME. A Unified Field Theory of Mesons and Baryons. *Nucl.Phys.*, 31:556–569, 1962.
- [15] BELAVIN, A. A. AND POLYAKOV, ALEXANDER M. AND SCHWARTZ, A. S. AND TYUPKIN, YU. S. Pseudoparticle Solutions of the Yang-Mills Equations. *Phys.Lett.*, B59:85–87, 1975.
- [16] ’T HOOFT, GERARD. Computation of the Quantum Effects Due to a Four-Dimensional Pseudoparticle. *Phys.Rev.*, D14:3432–3450, 1976.
- [17] F. A. BAIS. Flux metamorphosis. *Nucl. Phys.*, B170:32, 1980.
- [18] F. WILCZEK. Magnetic flux, angular momentum, and statistics. *Phys. Rev. Lett.*, 48:1144–1146, Apr 1982.
- [19] F. WILCZEK. Quantum mechanics of fractional-spin particles. *Phys. Rev. Lett.*, 49:957–959, Oct 1982.
- [20] A. Y. KITAEV. Fault-tolerant quantum computation by anyons. *Ann. Phys.*, 303:2–30, 2003, arXiv:quant-ph/9707021 [quant-ph].
- [21] A. WÓJS, G. MÖLLER, S. H. SIMON, AND N. R. COOPER. Skyrmions in the Moore-Read State at $\nu = \frac{5}{2}$. *Phys. Rev. Lett.*, 104:086801, Feb 2010, arXiv:0910.4176 [cond-mat.str-el].
- [22] S. AN, P. JIANG, H. CHOI, W. KANG, S. H. SIMON, L. N. PFEIFFER, K. W. WEST, AND K. W. BALDWIN. Braiding of Abelian and Non-Abelian Anyons in the Fractional Quantum Hall Effect. *eprint arXiv:1112.3400*, December 2011, arXiv:1112.3400 [cond-mat.mes-hall].

- [23] A. KITAEV AND J. PRESKILL. Topological Entanglement Entropy. *Phys. Rev. Lett.*, 96:110404, Mar 2006, arXiv:hep-th/0510092 [hep-th].
- [24] M. LEVIN AND X.-G. WEN. Detecting Topological Order in a Ground State Wave Function. *Phys. Rev. Lett.*, 96:110405, Mar 2006, arXiv:cond-mat/0510613 [cond-mat].
- [25] G. 'T HOOFT. On the Phase Transition Towards Permanent Quark Confinement. *Nucl.Phys.*, B138:1, 1978.
- [26] E. P. VERLINDE. Fusion Rules and Modular Transformations in 2D Conformal Field Theory. *Nucl. Phys.*, B300:360, 1988.
- [27] F. A. BAIS, B. J. SCHROERS, AND J. K. SLINGERLAND. Broken quantum symmetry and Confinement Phases in Planar Physics. *Phys. Rev. Lett.*, 89:181601, 2002, arXiv:hep-th/0205117 [hep-th].
- [28] F. A. BAIS, B. J. SCHROERS, AND J. K. SLINGERLAND. Hopf symmetry breaking and confinement in (2+1)-dimensional gauge theory. *JHEP*, 0305(068), 2003, arXiv:hep-th/0205114 [hep-th].
- [29] F. A. BAIS AND J. K. SLINGERLAND. Condensate-induced transitions between topologically ordered phases. *Phys. Rev.*, B79:045316, 2009, arXiv:0808.0627 [cond-mat.mes-hall].
- [30] F. A. BAIS, J. K. SLINGERLAND, AND S. M. HAAKER. Theory of Topological Edges and Domain Walls. *Phys. Rev. Lett.*, 102:220403, 2009, arXiv:0812.4596 [cond-mat.mes-hall].
- [31] F. A. BAIS AND J. K. SLINGERLAND. Topological entanglement entropy relations for multi phase systems with interfaces. June 2010, arXiv:1006.2017 [cond-mat.str-el].
- [32] E. B. DYNKIN. Semisimple subalgebras of semisimple Lie algebras. *Trans.Am.Math.Soc.*, 6:111, 1957.
- [33] P. H. BONDERSON. Non-abelian anyons and interferometry. *Thesis (Cal-Tech)*, 2007.
- [34] F. A. BAIS, S. ELIËNS, AND J. C. ROMERS. Topological symmetry breaking and tensor categories. (in preparation), 2012.

- [35] F. A. BAIS AND J. C. ROMERS. Anyonic order parameters for discrete gauge theories on the lattice. *Ann. Phys. (N.Y.)*, 324:1168–1175, 2009, arXiv:0812.2256 [cond-mat.mes-hall].
- [36] F. A. BAIS AND J. C. ROMERS. The modular S-matrix as order parameter for topological phase transitions. *New J.Phys.*, 14:035024, 2012, arXiv:1108.0683 [cond-mat.mes-hall].
- [37] M. DE WILD PROPITIUS AND F. A. BAIS. Discrete gauge theories. 1995, arXiv:hep-th/9511201 [hep-th]. Published in *Particles and Fields*. (CRM Series in Math. Physics), pp. 353-440.
- [38] D. HORN, M. WEINSTEIN, AND S. YANKIELOWICZ. Hamiltonian approach to \mathbb{Z}_N lattice gauge theories. *Phys. Rev. D*, 19:3715–3731, Jun 1979.
- [39] M. B. HASTINGS AND X.-G. WEN. Quasiadiabatic continuation of quantum states: The stability of topological ground-state degeneracy and emergent gauge invariance. *Phys. Rev.*, B72:045141, Jul 2005, arXiv:cond-mat/0503554 [cond-mat].
- [40] S. TREBST, P. WERNER, M. TROYER, K. SHTENDEL, AND C. NAYAK. Breakdown of a topological phase: Quantum phase transition in a loop gas model with tension. *Phys.Rev.Lett.*, 98:070602, 2007, arXiv:cond-mat/0609048 [cond-mat.stat-mech].
- [41] I. S. TUPITSYN, A. KITAEV, N. V. PROKOF'EV, AND P. C. E. STAMP. Topological multicritical point in the Toric Code and 3D gauge Higgs Models. *Phys.Rev.*, B82:085114, 2010, arXiv:0804.3175 [cond-mat.stat-mech].
- [42] R. BALIAN, J. M. DROUFFE, AND C. ITZYKSON. Gauge fields on a lattice. II. Gauge-invariant Ising model. *Phys. Rev.*, D11:2098–2103, Apr 1975.
- [43] K. GREGOR, D. A. HUSE, R. MOESSNER, AND S. L. SONDHI. Diagnosing deconfinement and topological order. *New Journal of Physics*, 13(2):025009, 2011, arXiv:1011.4187 [cond-mat.str-el].
- [44] V. G. DRINFELD. Quantum groups. *J. Sov. Math.*, 41:898–915, 1988.
- [45] F. A. BAIS, P. VAN DRIEL, AND M. DE WILD PROPITIUS. Quantum symmetries in discrete gauge theories. *Phys. Lett.*, B280:63–70, 1992, arXiv:hep-th/9203046 [hep-th].

- [46] P. ROCHE, V. PASQUIER, AND R. DIJKGRAAF. QuasiHopf algebras, group cohomology and orbifold models. *Nucl. Phys. Proc. Suppl.*, 18B:60–72, 1990.
- [47] K. G. WILSON. Confinement of Quarks. *Phys. Rev.*, D10:2445–2459, 1974.
- [48] M. G. ALFORD AND J. MARCH-RUSSELL. New order parameters for non-Abelian gauge theories. *Nucl.Phys.*, B369:276–298, 1992.
- [49] J. PRESKILL. Lecture Notes for Physics 219: Quantum Computation. Chapter 9: Topological quantum computation, 2004.
- [50] G. BHANOT AND M. CREUTZ. Phase diagram of \mathbb{Z}_N and U(1) gauge theories in three dimensions. *Phys. Rev. D*, 21:2892–2902, May 1980.
- [51] K. HUKUSHIMA AND K. NEMOTO. Exchange Monte Carlo Method and Application to Spin Glass Simulations. *J. Phys. Soc. Jpn.*, 65(6):1604–1608, 1996, arXiv:cond-mat/9512035 [cond-mat].
- [52] H. A. KRAMERS AND G. H. WANNIER. Statistics of the Two-Dimensional Ferromagnet. Part I. *Phys.Rev.*, 60:252–262, 1941.
- [53] H. A. KRAMERS AND G. H. WANNIER. Statistics of the Two-Dimensional Ferromagnet. Part II. *Phys.Rev.*, 60:263–276, 1941.
- [54] J. C. ROMERS, L. HUIJSE, AND K. SCHOUTENS. Charged spin textures over the Moore-Read quantum Hall state. *New Journal of Physics*, 13(4):045013, 2011, arXiv:1010.0897 [cond-mat].
- [55] J. C. ROMERS AND K. SCHOUTENS. Spin texture readout of a Moore-Read topological quantum register. *Phys. Rev. Lett.*, 2012, arXiv:1111.6032 [cond-mat].
- [56] K. v. KLITZING, G. DORDA, AND M. PEPPER. New Method for High-Accuracy Determination of the Fine-Structure Constant Based on Quantized Hall Resistance. *Phys. Rev. Lett.*, 45:494–497, Aug 1980.
- [57] D. C. TSUI, H. L. STÖRMER, AND A. C. GOSSARD. Two-Dimensional Magnetotransport in the Extreme Quantum Limit. *Phys. Rev. Lett.*, 48:1559, 1982.

- [58] R. B. LAUGHLIN. Anomalous quantum Hall effect: an Incompressible Quantum Fluid with Fractionally Charged Excitations. *Phys. Rev. Lett.*, 50:1395, 1983.
- [59] G. MOORE AND N. READ. Nonabelions in the fractional quantum Hall effect. *Nuclear Physics B*, 360:362, 1991.
- [60] N. K. WILKIN, J. M. F. GUNN, AND R. A. SMITH. Do Attractive Bosons Condense? *Phys. Rev. Lett.*, 80:2265–2268, Mar 1998.
- [61] N. K. WILKIN AND J. M. F. GUNN. Condensation of “Composite Bosons” in a Rotating BEC. *Phys. Rev. Lett.*, 84:6–9, Jan 2000.
- [62] J. W. REIJNDERS, F. J. M. VAN LANKVELT, K. SCHOUTENS, AND N. READ. Quantum Hall States and Boson Triplet Condensate for Rotating Spin-1 Bosons. *Phys. Rev. Lett.*, 89:120401, Aug 2002.
- [63] F. D. M. HALDANE. Fractional quantization of the Hall effect: a Hierarchy of incompressible quantum fluid states. *Phys. Rev. Lett.*, 51:605, 1983.
- [64] J. K. JAIN. Composite-fermion approach for the fractional quantum Hall effect. *Phys. Rev. Lett.*, 63:199–202, Jul 1989.
- [65] M. LEVIN, B. I. HALPERIN, AND B. ROSENOW. Particle-Hole Symmetry and the Pfaffian State. *Phys. Rev. Lett.*, 99:236806, Dec 2007.
- [66] S.-S. LEE, S. RYU, C. NAYAK, AND M. P. A. FISHER. Particle-Hole Symmetry and the $\nu = \frac{5}{2}$ Quantum Hall State. *Phys. Rev. Lett.*, 99:236807, Dec 2007.
- [67] E. H. REZAYI AND S. H. SIMON. Breaking of Particle-Hole Symmetry by Landau Level Mixing in the $\nu = 5/2$ Quantized Hall State. *Phys. Rev. Lett.*, 106:116801, Mar 2011.
- [68] S. M. GIRVIN. Particle-hole symmetry in the anomalous quantum Hall effect. *Phys. Rev. B*, 29:6012–6014, May 1984.
- [69] N. READ. Non-Abelian adiabatic statistics and Hall viscosity in quantum Hall states and $p_x + ip_y$ paired superfluids. *Phys. Rev. B*, 79:045308, Jan 2009.

- [70] S. H. SIMON, E. H. REZAYI, N. R. COOPER, AND I. BERDNIKOV. Construction of a paired wave function for spinless electrons at filling fraction $\nu = 25$. *Phys. Rev. B*, 75:075317, Feb 2007.
- [71] P. BONDERSON, V. GURARIE, AND C. NAYAK. Plasma analogy and non-Abelian statistics for Ising-type quantum Hall states. *Phys. Rev. B*, 83:075303, Feb 2011.
- [72] J. M. CAILLOL, D. LEVESQUE, J. J. WEIS, AND J. P. HANSEN. A Monte Carlo study of the classical two-dimensional one-component plasma. *Journal of Statistical Physics*, 28:325–349, 1982. 10.1007/BF01012609.
- [73] A. CAPPELLI, L. S. GEORGIEV, AND I. T. TODOROV. Parafermion hall states from coset projections of abelian conformal theories. *Nuclear Physics B*, 599(3):499 – 530, 2001, arXiv:hep-th/0009229 [hep-th].
- [74] K. SCHOUTENS, E. ARDONNE, AND F. J. M. VAN LANKVELT. Paired and clustered quantum Hall states. In A. Cappelli and G. Mussardo, editors, *Proceedings of the NATO Advanced Research Workshop “Statistical Field Theories” Como (Italy), June 18-23 2001*, pages 305–316, 2002, arXiv:cond-mat/0112379 [cond-mat].
- [75] S. E. BARRETT, G. DABBAGH, L. N. PFEIFFER, K. W. WEST, AND R. TYCKO. Optically Pumped NMR Evidence for Finite-Size Skyrmions in GaAs Quantum Wells near Landau Level Filling $\nu = 1$. *Phys. Rev. Lett.*, 74:5112–5115, Jun 1995.
- [76] P. PLOCHOCKA, J. M. SCHNEIDER, D. K. MAUDE, M. POTEMSKI, M. RAPAPORT, V. UMANSKY, I. BAR-JOSEPH, J. G. GROSHAUS, Y. GALLAIS, AND A. PINCZUK. Optical Absorption to Probe the Quantum Hall Ferromagnet at Filling Factor $\nu = 1$. *Phys. Rev. Lett.*, 102:126806, Mar 2009.
- [77] H. A. FERTIG, L. BREY, R. CÔTÉ, AND A. H. MACDONALD. Charged spin-texture excitations and the Hartree-Fock approximation in the quantum Hall effect. *Phys. Rev. B*, 50:11018–11021, Oct 1994.
- [78] H. A. FERTIG, L. BREY, R. CÔTÉ, A. H. MACDONALD, A. KARLHEDE, AND S. L. SONDHI. Hartree-Fock theory of Skyrmions in quantum Hall ferromagnets. *Phys. Rev. B*, 55:10671–10680, Apr 1997.

- [79] D. K. MAUDE, M. POTEMSKI, J. C. PORTAL, M. HENINI, L. EAVES, G. HILL, AND M. A. PATE. Spin Excitations of a Two-Dimensional Electron Gas in the Limit of Vanishing Landé g Factor. *Phys. Rev. Lett.*, 77:4604–4607, Nov 1996.
- [80] D. R. LEADLEY, R. J. NICHOLAS, D. K. MAUDE, A. N. UTJUZH, J. C. PORTAL, J. J. HARRIS, AND C. T. FOXON. Fractional Quantum Hall Effect Measurements at Zero g Factor. *Phys. Rev. Lett.*, 79:4246–4249, Nov 1997.
- [81] A. H. MACDONALD, H. A. FERTIG, AND L. BREY. Skyrmions without Sigma Models in Quantum Hall Ferromagnets. *Phys. Rev. Lett.*, 76:2153–2156, 1996, arXiv:cond-mat/9510080 [cond-mat].
- [82] S. L. SONDHI, A. KARLHEDE, S. A. KIVELSON, AND E. H. REZAYI. Skyrmions and the crossover from the integer to fractional quantum Hall effect at small Zeeman energies. *Phys. Rev. B*, 47:16419–16426, Jun 1993.
- [83] A. E. FEIGUIN, E. REZAYI, K. YANG, C. NAYAK, AND S. DAS SARMA. Spin polarization of the $\nu = 5/2$ quantum Hall state. *Phys. Rev. B*, 79:115322, Mar 2009.
- [84] I. DIMOV, B. I. HALPERIN, AND C. NAYAK. Spin Order in Paired Quantum Hall States. *Phys. Rev. Lett.*, 100:126804, Mar 2008, arXiv:0710.1921 [cond-mat].
- [85] M. STERN, P. PLOCHOCKA, V. UMANSKY, D. K. MAUDE, M. POTEMSKI, AND I. BAR-JOSEPH. Optical Probing of the Spin Polarization of the $\nu = \frac{5}{2}$ Quantum Hall State. *Phys. Rev. Lett.*, 105:096801, Aug 2010.
- [86] R. SLANSKY. Group theory for unified model building. *Physics Reports*, 79(1):1 – 128, 1981.
- [87] T. G. HASKELL AND B. G. WYBOURNE. A Dynamical Group for the Harmonic Oscillator. *Proceedings of the Royal Society of London. Series A, Mathematical and Physical Sciences*, 334(1599):pp. 541–551, 1973.
- [88] K. MOON, H. MORI, K. YANG, S. M. GIRVIN, A. H. MACDONALD, L. ZHENG, D. YOSHIOKA, AND S.-C. ZHANG. Spontaneous interlayer coherence in double-layer quantum Hall systems: Charged vortices and

- Kosterlitz-Thouless phase transitions. *Phys. Rev. B*, 51:5138–5170, Feb 1995, arXiv:cond-mat/9407031 [cond-mat].
- [89] E. ARDONNE AND K. SCHOUTENS. New class of non-Abelian spin-singlet quantum Hall states. *Phys. Rev. Lett.*, 82:5096, 1999, arXiv:cond-mat/9811352 [cond-mat].
- [90] E. ARDONNE, N. READ, E. REZAYI, AND K. SCHOUTENS. Non-abelian spin-singlet quantum Hall states: wave functions and quasihole state counting. *Nuclear Physics B*, 607(3):549 – 576, 2001, arXiv:cond-mat/0104250 [cond-mat].
- [91] E. PRODAN AND F. D. M. HALDANE. Mapping the braiding properties of the Moore-Read state. *Phys. Rev. B*, 80:115121, Sep 2009, arXiv:1001.1930 [cond-mat.str-el].
- [92] T. MIZUSHIMA, N. KOBAYASHI, AND K. MACHIDA. Coreless and singular vortex lattices in rotating spinor Bose-Einstein condensates. *Phys. Rev. A*, 70:043613, Oct 2004, arXiv:cond-mat/0407684 [cond-mat].
- [93] K. YANG AND E. H. REZAYI. Magnetization and Spin Excitations of Non-Abelian Quantum Hall States. *Phys. Rev. Lett.*, 101:216808, Nov 2008, arXiv:0805.4034 [cond-mat].
- [94] N. READ AND E. REZAYI. Quasiholes and fermionic zero modes of paired fractional quantum Hall states: The mechanism for non-Abelian statistics. *Phys. Rev. B*, 54:16864–16887, Dec 1996, arXiv:cond-mat/9609079 [cond-mat].
- [95] G. MÖLLER, A. WÓJS, AND N. R. COOPER. Neutral Fermion Excitations in the Moore-Read State at Filling Factor $\nu = 5/2$. *Phys. Rev. Lett.*, 107:036803, Jul 2011, arXiv:1009.4956 [cond-mat].
- [96] M. LEVIN AND X.-G. WEN. Fermions, strings, and gauge fields in lattice spin models. *Phys. Rev.*, B67:245316, 2003.
- [97] K. FREDENHAGEN AND M. MARCU. Confinement criterion for QCD with dynamical quarks. *Phys. Rev. Lett.*, 56:223–224, Jan 1986.
- [98] MÖLLER, GUNNAR. Private communication.

- [99] G. CHO AND J. MOORE. Topological BF field theory description of topological insulators. *Annals Phys.*, 326:1515–1535, 2011, arXiv:1011.3485 [cond-mat.str-el].
- [100] D. J. CLARKE, J. ALICEA, AND K. SHTENDEL. Exotic non-Abelian anyons from conventional fractional quantum Hall states. *ArXiv e-prints*, April 2012, arXiv:1204.5479 [cond-mat.str-el].
- [101] N. H. LINDNER, E. BERG, G. REFAEL, AND A. STERN. Fractionalizing Majorana fermions: non-abelian statistics on the edges of abelian quantum Hall states. *ArXiv e-prints*, April 2012, arXiv:1204.5733 [cond-mat.mes-hall].
- [102] E. FRADKIN AND L. P. KADANOFF. Disorder variables and para-fermions in two-dimensional statistical mechanics. *Nuclear Physics B*, 170(1):1 – 15, 1980.
- [103] N. READ AND E. REZAYI. Beyond paired quantum Hall states: Parafermions and incompressible states in the first excited Landau level. *Phys. Rev. B*, 59:8084, 1999, arXiv:cond-mat/9809384 [cond-mat].